Tu-PM-G7

STRUCTURAL CHANGES INDUCED BY TEMPERATURE IN CYTOCHROME *C* OXIDASE FROM MITOCHONDRIA AND BACTERIA STUDIED BY INFRARED SPECTROSCOPY [(J.L.R. Arrondo, I. Echabe and F.M. Goñi)] Dpto. Bioquímica. Univ.Pais Vasco. P.O.Box 644. 48080 Bilbao. Spain.

Cytochrome *c* oxidase is ubiquitous to all aerobic cells. In prokaryotes is a plasma membrane enzyme whereas in eukaryotes is localized into the mitochondrial inner membrane. In eukaryotes, three subunits are encoded in the mitochondrial DNA and the rest of the subunits in the nucleus. The mitochondrially coded proteins have homologous counterparts in the bacterial enzyme. We have studied the enzymes from mitochondria, *P. denitrificans* and a mutant from this bacteria lacking subunit III. The thermal behaviour of the three proteins is different. Thus, the mitochondrial protein conforms to a two-state denaturation in the range 45-60 °C, with a different behaviour for the band corresponding to α-helix (57 °C) or ß-sheet (48 °C). The *P. denitrificans* enzyme denaturation is accomplished in two steps (43.5 and 54 °C) similarly to the observation made by DSC. Thermal behaviour of the mutant differs from the other proteins. The denaturation temperature of the α-helix and ß-sheet components is alike in the mitochondrial enzyme if the heating is in multiple steps. The presence of detergents or urea also changes the thermal behaviour of the enzyme. The results indicate that inter-subunit interactions play an important role in the denaturation pattern.

Tu-PM-G8

INVESTIGATING THE MECHANISM OF ELECTRON TRANSFER IN SMALL COPPER BINDING PROTEINS: X-ray Crystallographic and Spectroscopic Studies of the Holo and Apoazurin from *Ps. fluorescens*.

((*T. E. S. Dahms, *M. J. Kaminski, ¶J. D. Biesterfeldt, *S. J. Evans, ¶A. G. Szabo & ‡X. Lee)) *University of Ottawa, Ottawa, Ontario, CA K1H 8M5 ¶University of Windsor, Windsor, Ontario, CA N9B 3P4 ‡Cleveland Clinic Foundation, Cleveland, Ohio, USA 44195.

Pseudomonas fluorescens (*Pfl*) azurin is classified as a small "blue copper protein" (λ_{max} = 280 nm, 600-625 nm) which complexes with cytochromes *c*, its redox partner, *in vivo*. Although the "blue copper proteins" have been studied extensively by various biochemical and physical techniques, the complete mechanism of electron transfer is not clear.

X-ray crystallographic data of the *Pfl* holoazurin ($P2_12_12_1$; a = 31.95 Å, b = 43.78 Å, c = 78.81 Å; Z = 1) at 2.05 Å resolution provides a three dimensional structure with the following unique features; a main chain "flip" at His35 and direct involvement of the His35 patch in the contact between symmetrically related molecules. These observations support a structural basis for the electron transfer through the His46-His35 channel to the next molecule which can be used as an approximate model for electron transfer between azurin and cytochrome *c*. Small apoazurin crystals were found to diffract to 2.5 Å resolution, providing sufficient data for the investigation of copper-induced conformational changes.

The structures of the *Pfl* holo and apoazurins will be discussed in detail, highlighting copper ligand geometry and electron transfer. An attempt will be made to grow crystals of the nickel and cobalt derivatives of azurin and the azurin-cytochrome complex. Structural information from these systems would facilitate a comparison of X-ray crystallographic data with that obtained by fluorescence (Hutnik & Szabo (1989) *Biochemistry*, **28**, 3935.), and further define the contact area between *Pfl* holoazurin and cytochrome C. Taken together, this data would more clearly define the electron transfer process *in vivo*.

CONTRACTILITY, LOCOMOTION, MOTILITY: MYOSIN

Tu-Pos1

DETECTION OF REPETITIVE TITIN EPITOPES DEPENDS ON THE LABELLING TECHNIQUE. ((K. Trombitás*, M.L. Greaser^ and G.H. Pollack+)) *Central EM Lab., Univ Med. School of Pecs, Hungary; ^Muscle Biology Lab. Univ. Wisconsin, Medison WI 53706; +Center for Bioengineering, Univ. of Washington, Seattle WA 98195.

A number of monoclonal antibodies against titin have been prepared in several laboratories which label the sarcomere at various positions from M-line to Z-line. Some of the antibodies recognize only a single epitope, but several label repetitive epitopes. Only one known monoclonal antibody (T30) binds to five epitopes with 42 nm spacing in the C-protein zone. Here, we describe work with monoclonal antibody H4 (Fassel and Greaser, 1995) which labels numerous epitopes depending on the labelling technique. This antibody showed two bands per sarcomere with the immunofluorescence method. Using indirect immuno-electron microscopy (anti-mouse IgG as secondary antibody), we found four repetitive epitopes 42 nm apart in each half sarcomere. When the secondary antibody was anti mouse IgG Fab' fragments conjugated with 1.4 nm gold particles, followed by silver enhancement (Nanoprobe Inc.), we could identify seven epitopes. The same four epitopes were accompanied by a fifth epitope 42 nm from the epitope nearest the M-line. Then, about 84 nm closer to the M-line, there appeared two additional epitopes spaced 42 nm apart. The first five epitopes correspond to the epitopes of the T30 antibody, the two additional to the epitopes of the T31 antibody (Fürst et al., 1989), which means that the H4 antibody covers seven epitopes of the nine striations associated with C protein and the 86K protein. Since the labelling showed a steeply decreasing gradient from the periphery towards the core of the fiber, the properly chosen antibody concentration is important for full identification of epitope positions—as is the new supersensitive labelling technique.

Tu-Pos2

A DIRECT DETERMINATION OF THE STEP-SIZE DISTANCE FOR ATP SPLITTING IN ACTIVELY CONTRACTING MUSCLE.

((C.R.Worthington and G.F.Elliott)) Carnegie Mellon Univ., Pittsburgh, PA 15213 and Oxford Research Unit, Open Univ., Oxford OX1 5HR UK.

The rate of energy consumption in muscle contraction and the velocity of shortening as a function of load have long been known from the pioneering work of A.V.Hill. Since those days information has accumulated about the structure of striated muscle and about the enthalpy supplied by each ATP molecule in the contractile process. In principle all this information can be combined to give the distance travelled in contracting muscle by one actin filament past one myosin filament as a result of the hydrolysis of one ATP molecule. This definition of the step-size distance in muscle is independent of any particular model of the physical-chemical process of muscle contraction since it depends only on experimentally determined quantities. We have carried out this calculation and report that the step-size distance on our definition is 1.7 nm at maximum shortening velocity. It decreases with load becoming zero when the force is isometric. The analysis supposes that muscle contracts as a result of a series of impulsive forces and it gives a physical meaning to Hill's constants a & b in Hill's force-velocity equation. Hill's constant b is related to the impulse-time and an estimate of 0.5 msec is obtained. Hill's constant a is related to the inertia of the system and to the viscous-like frictional resistance experienced by the filaments as the muscle shortens. We note however that a recent model for muscle (Elliott & Worthington Bioch. Biophys. Acta 1200, 109 [1994]) fits admirably within the frame-work of the present treatment. Some properties of this electrical model will be described.

Tu-Pos3

ISOLATION OF THE CIRCULAR DICHROISM (CD) SIGNAL FROM TRP510 IN MYOSIN SUBFRAGMENT 1 BY USE OF FLUORESCENCE DETECTED CD (FDCD) ((Sungjo Park, Katalin Ajtai, and Thomas P. Burghardt)) Department of Biochemistry and Molecular Biology, Mayo Foundation, Rochester, MN 55905.

FDCD was used to detect the CD signal from the five tryptophan residues in α-chymotryptic S1. FDCD was detected from native S1, and S1 after specific modification of the fast reacting thiol (SH1) with the fluorescent probe 5'iodoacetamidofluorescein (5'IAF). 5'IAF modifying S1 (5'F-S1) closely interacts with Trp510 of S1 totally quenching the emission from this tryptophan. Other tryptophans in S1 are not affected by 5'IAF[1]. The difference FDCD spectrum between the S1 and 5'F-S1 originates solely from the native structure of Trp510. Calculation of the tryptophan CD signal combined with the α-carbon structure of S1[2] indicates possible native conformation of the residue.
Supported by NIH (AR 39288), American Heart Association (GIA 930 06610), and Mayo Foundation.

1. Ajtai & Burghardt, 1995, Biochemistry, in press.
2. Rayment et al., 1993, Science 261, 50-58.

Tu-Pos4

DISTANCE BETWEEN THE ALKALI LIGHT CHAINS OF MYOSIN SUBFRAGMENT-1 BOUND TO F-ACTIN MEASURED USING FLUORESCENCE SPECTROSCOPY. ((L. Brown & B. Hambly)) Pathology Dept., Sydney University, NSW 2006 Australia.

Fluorescence resonance energy transfer (FRET) spectroscopy was used to measure the distance between a fluorescent donor probe bound to the alkali light chain (ALC) of myosin subfragment-1 (S-1) and an acceptor probe bound to the ALC of an adjacent S-1, when a mixture of these two labeled S-1 molecules was bound to filamentous actin (F-actin) in rigor buffer. No fluorescence quench occurred between this fluorescence probe pair. We calculated the apparent distance between these two fluorophores to be greater than 8.0 nm). Both the donor (N[[(iodoacetyl) amino]ethyl]-5-naphthylamine-1-sulphonic acid [IAEDANS]) and acceptor (5-iodoacetamide fluorescein [5-IAF]) fluorecent probes were bound stoichiometric-ally to the Cys 177 of separate samples of ALC-1 of rabbit skeletal muscle myosin and exchanged onto the α-chymotryptic S-1 fragment of myosin. The extent of labeling of the donor S-1 was 0.93 and the acceptor S-1 was 1.00. Two ratios of donor to acceptor S-1 samples were prepared: (i) 0.2 donor S-1:0.6 acceptor S-1:1 F-actin; (ii) 0.5 donor S-1:0.5 acceptor S-1:1 F-actin. No quenching of fluorescence was seen in either case. Sedimentation binding studies of the fluorescence samples showed that greater than 95% of S-1 had bound the F-actin. The distance between S-1 molecules bound to F-actin that can be predicted from the helical repeat of the F-actin filament is 6 nm. These results will be discussed in relation to the apparent flexibility between the motor domain and the light chain domain of the myosin head, when bound to F-actin in the rigor complex. Supported by the NH&MRC of Australia.

Tu-Pos5

CONTRACTION STUDIES WITH NON-NUCLEOTIDE ATP ANALOGS: SEARCH FOR THE WORLD'S SMALLEST ATP. ((D. Wang*, E. Pate‡, R. Cooke†, J. C. Grammer*, and R. G. Yount*)) *Dept. Biochemistry and Biophysics, and ‡Dept. Mathematics, Washington State University, Pullman, WA 99164, and †Dept. Biochemistry and Biophysics, University of California, San Francisco, CA.

Previous studies (Wang et al. *1993*, **J. Muscle Res. Cell Motil.** *14*, 484-97) have shown ATP analogs in which the adenine ring is replaced with a 2-nitrophenyl group and the ribose ring with an aminoethyl grouping (Fig 1, X=NH) elicits normal chemomechanical behavior

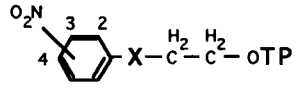

Fig. 1

from skinned muscle fibers. To define better the minimal structural requirements of substrates for contraction we have prepared the 3- and 4-nitrophenyl analogs. These analogs in contrast to the 2-nitrophenyl analog fail to support active tension (<3% ATP) or shortening of fibers. Methylation of the NH group (X=N-CH_3) of the 2-nitrophenyl analog dropped active tension and velocity of shortening to zero suggesting a critical hydrogen bond between the NH and the 2-nitro group would explain the ineffectiveness of the 3- and 4-nitro analogs. However, replacing the NH group of the 2-nitrophenyl analog with oxygen (X=O) yielded an analog able to support active tension and velocity of shortening 35-40% of the values given by ATP. This smallest ATP analog shows that the 2-nitrophenyl group need only to be spaced the appropriate distance from the triphosphate tail to be effective. The crystal structure of subfragment 1 with the bound 2,4-dinitrophenyl analog (I. Rayment, personal communication) should help decide why there is a stringent requirement for a 2-nitrophenyl grouping and why ethyl-bridging analogs work but propyl-bridging analogs (Wang et al., loc cit) do not. Supported by MDA (R.Y. and R.C.) and NIH, R.Y. (DK05795), E.P. (AR39643) and R.C. (AR42895).

Tu-Pos6

BINDING OF S1(A1) AND S1(A2) TO F-ACTIN. ((M. Xiao, A. Tartakowski, O.A. Andreev and J. Borejdo)) Baylor Res. Inst. 3812 Elm, Dallas, TX 75226 and Department of Oral Biology, Hebrew University, Jerusalem 91-010, Israel.

The binding curve of myosin subfragment-1 (S1) to F-actin is not a simple hyperbola (Andreev & Borejdo, J. Muscle Res. Cell Mot., 13, 523-533, 1992). This anomalous behavior may result either from the heterogeneity of S1 in regard to light chain isoforms or from the cooperativity between S1's. To distinguish between these possibilities we measured the affinity (K_a) and the orientation (Θ) of S1 isomers with respect to F-actin. Both K_a and Θ depended on the relative concentration of S1 isomer and actin: when actin filament was saturated with S1 each isomer bound F-actin with an $K_a=2x10^6$ M^{-1} and $\Theta=73°$. When filament was unsaturated with S1 each isomer bound F-actin with $K_a=1.2x10^7$ M^{-1} and $\Theta=65°$. S1(A1) and S1(A2) labeled on the light chain had different Θ when bound to unsaturated, but the same Θ when bound to saturated filaments. These results excluded heterogeneity as a reason for anomalous binding and suggested that binding occurred with negative cooperativity. We think that the negative cooperativity occurs when saturation of actin filaments leads to the lack of vacant adjacent sites on a filament and a consequent prevention of S1 binding to two actin protomers.

Tu-Pos7

MYOSIN HEADS BIND TO TWO ACTIN PROTOMERS IN THIN FILAMENTS OF RABBIT MUSCLE. ((J. Borejdo & M. Xiao)) Baylor Res. Inst., 3812 Elm St., Dallas, TX 75226.

Cis-parinaric acid (PA) binds specifically to myosin subfragment-1 (S1) of skeletal myofibrils through alkali light chain 1 (A1). Tests carried out in solution confirm earlier results showing that binding is specific, rapid, strong and rigid (Borejdo, Biochemistry 22, 1182, 1983). Scatchard plots of binding of S1(A1*PA) to F-actin were concave downwards confirming our earlier claim that binding occurred with the negative cooperativity (Andreev et al, Biochemistry 32, 12046, 1993). To discover orientation of heads in native muscle, we compared polarizations of fluorescence of PA (p_x) in the following three systems: (i) S1(A1*PA) added to a muscle fiber in concentrations saturating thin filaments, (ii) S1(A1*PA) added to a muscle fiber in concentrations non-saturating thin filaments, and (iii) PA added to a native muscle fiber. The p_x measured in (ii) and (iii) were the same and both were different from the p_x of (i). Since in (i) S1 binds to a single actin protomer and in (ii) to two protomers, we conclude that in rigor rabbit psoas muscle each myosin head binds to two actin monomers in a thin filament, and that this binding is different than binding of S1 to equimolar concentration of actin in solution.

Tu-Pos8

CONFORMATIONAL CHANGE ON MYOSIN HEAD INDUCED BY BINDING OF ATP ANALOGUE WHICH HAS "SYN" CONFORMATION AT N-GLYCOSIDE BOND ((Shinsaku Maruta, Takashi Ohki)) Department of Bioengineering, Soka University, Hachioji , Tokyo 192 JAPAN. (Spon. by T. Mitsui)

We have shown previously that ATP analgue 3'(2')-O-[N-methylanthraniloyl]-8-azido-ATP (Mant-8-N_3-ATP) which have "Syn" conformation at N-glycoside bond was incorporated into the region which contains Lys 681 of skeletal muscle myosin by photo irradiation [Maruta et al. (1989) Eur. J. Biochem. 184, 213-221]. Indeed, the loop contains Lys 681 was found in the part of the active site of crystal structure of skeletal muscle myosin reported by Rayment. Interactions of "Syn" conformation ATP analogues such as Mant-8-N_3-ATP, 8-Br-ATP with myosin head were studied. These analogues were hydrolyzed 30 times faster than regular ATP in the presence of Mg^{2+}. Trp fluorescence enhancement induced by 8-Br-ATP was just 5% when regular ATP was 15%. Ca^{2+}-ATP also worked as same as "Syn" ATP analogue. Acrylamide quenching of trapped ε-8-Br-ADP into active site by BeFx showed that the ATP binding pocket is open. Although acto S-1 was dissociated, super precipitation was not induced by these analogues. These results may suggest that binding of these ATP analogues to myosin mimic M• ATP state such as PPi and hydrolyze without proceeding to further step of transition state (M** • ADP • Pi) along the contractile cycle. Reactivity of RLR and SH1, SH2 in the presence of these analogues were also studied. The results of these analogues were compared with ternary complexes of Myosin • ADP • AlF_4^- (BeFn or Vi) which may mimic transition state (M** • ADP • Pi). Conformation at N-glycoside bond of ATP in the active site may be important to form transition state (M** • ADP • Pi).

Tu-Pos9

THE MOBILITY OF ESSENTIAL LIGHT CHAINS (ELC) IN MYOSIN FILAMENTS. EFFECTS OF IONIC STRENGTH, PH, AND PHOSPHORYLATION. ((Bishow Adhikari, Joshua Somerset, Kalman Hideg* and Piotr G. Fajer)) Inst. of Mol. Biophysics and NHMFL, FSU, Tallahassee. *U. of Pecs, Pecs, Hungary.

The relative geometry of the catalytic domain of myosin head with respect to the filament backbone is a function of pH, ionic strength (μ), and the regulatory light chain (RLC) phosphorylation [1,2]. Since the mobility of the catalytic domain is decoupled from that of regulatory domain [3], we now examine whether the two domains behave in the same way. ELC was labeled with InVSL at the cys-residue and exchanged into myosin. ST-EPR was used to determine protein mobility.
Increasing μ or decreasing pH both resulted in an increase of myosin head mobility. At pH 7.0, the effective rotational correlation times (τ_R) at μ = 45, 125, and 200 mM were 30-35, 15-20, and 8-12 μs, respectively. When pH was changed from 7.0 to 8.2 at μ = 125 mM, τ_R increased from 15-20 μs to 24-28 μs. In the presence of 10 mM $MgCl_2$, a marked increase (τ_R = 3-4 μs) in head mobility was observed. These trends follow those reported for the catalytic domain [2]. Thus the dynamic response of the head to the above modulators encompasses both domains.
The RLC was phosphorylated enzymatically using MLCK (*gift of Dr J. Stull*) and CaM. 2D gels showed that most of the RLC was phosphorylated under these conditions. Phosphorylated myosin filaments in the presence of Mg^{2+}, τ_R = 4.5±0.5 μs, were more mobile than the unphosphorylated myosin under identical conditions, τ_R = 7±0.5 μs. Therefore, the displacement of the phosphorylated heads observed by EM [1] is accompanied by the increased mobility.
[1] Levine et al., 1995. *Biophys. J.* 68:224s
[2] Ludescher et al., 1988. *J. Mol. Biol.* 200:69-99
[3] Adhikari et al., 1995. *Biophys. J.* 68:A67

Tu-Pos10

TEMPERATURE AND PHOSPHATE EFFECTS ON THE ELEMENTARY STEPS OF THE CROSS-BRIDGE CYCLE IN RABBIT SOLEUS SLOW-TWITCH MUSCLE FIBERS. ((Gang Wang and Masataka Kawai)) Dept. of Anatomy, University of Iowa, Iowa City, IA 52242

The force generation and phosphate release steps of the cross-bridge cycle are investigated with sinusoidal analysis in skinned rabbit soleus slow-twitch fibers at varying temperatures (15-30°C). The fibers are activated at pCa 4.40, ionic strength 180 mM, and the effects of phosphate (P) concentrations on four exponential processes (*A,B,C,D*) are studied. The results are consistent with the following partial cross-bridge scheme:

$$\mathrm{AMDP} \underset{k_{-4}}{\overset{k_4}{\rightleftharpoons}} \mathrm{AM^*DP} \overset{P}{\underset{K_5}{\rightleftharpoons}} \mathrm{AM^*D}$$

where A=actin, M=myosin, D=MgADP, and P=phosphate. We find that the equilibrium constant of force generation step K_4 increases significantly with temperature, and this step accompanies a large enthalpy increase (117 kJ/mol), indicating that the force generation step consists of an endothermic reaction. This step also accompanies a large entropy increase corresponding to 395 J/mol/deg. These observations are consistent with the hypothesis that the hydrophobic interaction between residues of actin and myosin underlies the mechanism of force generation. Changes in enthalpy and entropy of the force generation step are similar to those of fast-twitch rabbit psoas fibers, indicating the mechanism of force generation is similar in these two different fiber types. Unlike rabbit psoas, the phosphate association constant (K_5) increases with temperature in soleus slow-twitch fibers, which may explain the isometric tension saturation when temperature is elevated from 20°C to 35°C.

Tu-Pos11

AMINO TERMINAL PEPTIDE OF MYOSIN A1 LIGHT CHAIN BINDS ACTIN. ((T. Miyanishi, E. Yajima & T. Maita)) Biochemistry, Nagasaki Univ. Schl. Med., Nagasaki 85200, JAPAN.

We previously showed that the native amino-terminal peptide could bind actin (Hayashibara & Miyanishi (1994)). We synthesized the amino terminal peptide of myosin A1 light chain. The 14 residue peptide (SA) contains an N-trimethylated alanine residue at the amino-terminus and a cysteine residue at its carboxy-terminus replacing the ordnary alanine residue. SA formed dimer by disulfide bond between two molecules (SA-dimer). SA-dimer induced a significant increase of light scattering of f-actin solution that was observed as paracrystal like structure of actin filaments to be distinct from actin bundle induced by S-1 (A1) by electron microscopy. β mercaptoethanol treatment of SA retarded this induction, suggesting that SA dimer has two actin binding sites. SA was modified with iodoacetamidofluorescein to make the peptide fluorescent (SAF). SAF did not induce such paracrystal-like structure of actin filaments. In muscle fiber, SAF was found to bind actin band to make a fluorescent cross-striation. SAF could be cross-linked to actin molecule by a water-soluble carbodiimide. Fluorescent BrCN fragments from SAF crosslinked actin were isolated to sequence. This work was supported in part by the Ministry of Science, Culture and Education of Japan.

Tu-Pos12

ROTATIONAL DYNAMICS OF THE REGULATORY LIGHT CHAIN IN SCALLOP AND RABBIT MYOFIBRILS IN THE PRESENCE OF NUCLEOTIDE ANALOGS ((Sampath Ramachandran, Andrew J. H. Mattson and David Thomas)) University of Minnesota, Minneapolis, MN 55455

Crystallographic studies of myosin suggest that the the light-chain-binding domain undergoes a conformational change with respect to the catalytic domain during muscle contraction. In order to test this hypothesis, we used time-resolved phosphorescence anisotropy (TPA) to monitor the rotational motion of erythrosin-labeled gizzard regulatory light chain (ErIA-GRLC) in scallop and rabbit myofibrils in the presence of the substrate analogs ATP-γ-S and AMPPNP. In the presence of AMPPNP, both scallop and rabbit myofibrils gave anisotropy decays similar to rigor, **indicating that most myosin heads remain rigidly bound to actin.** In the presence of ATP-γ-S, substantial decay was seen, **indicating large-amplitude microsecond rotational motions.** These results agree with spectroscopic data from SH1 probes, which suggest that heads with ATP-γ-S and AMPPNP bound represent weak- and strong-binding intermediates, respectively, in the contraction cycle. These data support an earlier hypothesis that the **myosin head undergoes a disorder-to-order transition** during muscle contraction.

Tu-Pos13

SIMULTANEOUS ELECTRON PARAMAGNETIC RESONANCE AND FORCE OF A SINGLE SPIN-LABELED MUSCLE FIBER: CORRELATING MUSCLE MECHANICS WITH STRUCTURAL TRANSITIONS IN THE CATALYTIC DOMAIN OF MYOSIN. (Josh E. Baker, Nicholas J. Meyer, and David D. Thomas)
Dept. of Biochemistry, University of Minnesota Medical School, Minneapolis, MN 55455.

We have obtained electron paramagnetic resonance (EPR) signals from a single muscle fiber, specifically labeled with iodoacetamide spin label (IASL) at Cys 707 (SH1) in the catalytic domain of myosin, using a loop gap resonator (LGR) to maximize sensitivity. While monitoring the EPR signal at a single field position, we simultaneously recorded force with a force transducer mounted to the bottom plate of the LGR. Changes in force were correlated directly with EPR-detected transitions among three spectroscopically resolved structural states of the myosin catalytic domain, in response to changes in the concentration of ATP, calcium, and other ligands. This instrumentation permits a direct correlation of muscle mechanics and molecular dynamics in single muscle fibers under physiological conditions.

Tu-Pos14

MUSCLE CROSS-BRIDGE MICROSECOND ROTATIONAL DYNAMICS: COMPUTATIONAL SIMULATIONS OF TIME-RESOLVED OPTICAL ANISOTROPY ((David W. Hayden, Vincent A. Voelz and David D. Thomas)) Dept. of Biochemistry, University of Minnesota Medical School, Minneapolis, MN 55455.

Optical anisotropy of dyes covalently attached to myosin yields information about the amplitudes and rates of rotational motion of the myosin head in muscle fibers. We used the symmetry of the muscle fiber to simplify the simultaneous simulations of transient phosphorescence anisotropy (TPA) and fluorescence polarization (FP). The simulation of FP at the same time as TPA helps constrain the problem of dye orientation on the myosin head. We have simulated several models of myosin head rotation, including wobble in a cone and other diffusional models. These simulations provide insight into the possible motions of the myosin head and show clearly that some popular models are incompatible with the spectroscopic data.

Tu-Pos15

SPIN PROBES ON NOVEL SITES IN THE NECK REGION OF SKELETAL MUSCLE MYOSIN. ((J. Gollub, H. L. Sweeney, and R. Cooke)) Grad. Group in Biophysics, UCSF; Dept. Physiology, U. Penn.; Dept. Biochem. and Biophys. & CVRI, UCSF.

Using electron paramagnetic resonance (EPR), we have examined the orientation and mobility of probes on novel sites in the neck region of skeletal muscle myosin. A mutant of rabbit skeletal myosin regulatory light chain was constructed with the native cysteines removed and a novel cysteine in the c-terminal lobe (Y150C, C125S, C154S). This site was chosen to be buried in the structure, in the hope of providing better probe immobilization. The cysteine was nonreactive in native light chain and reactive in light chain denatured with 6M urea, showing that it was in fact buried. EPR spectra of a spin probe (methylmethane-thiosulfonate spin label) attached to this novel cysteine in the S1 proteolytic fragment of myosin indicate that the neck region of S1 is ordered in rigor fibers, presumably by the acto-myosin bond. We also chemically protected the more reactive cysteine (cys-125) of native rabbit skeletal muscle myosin regulatory light chain, allowing specific labeling of the presumably buried cys-154 with a spin label (4-maleimido-tempo spin label) subsequent to denaturation with 6M urea. EPR spectra of psoas fibers with the labeled light chain indicate that the neck region of myosin is at least partially ordered in rigor. These results corroborate previous results with probes on cys-125 and chicken gizzard light chain, indicating that the neck region of myosin is ordered in rigor. Supported by USPHS grant AR42895.

Tu-Pos16

MOLECULAR MODELING OF ACTOMYOSIN CROSSBRIDGE CYCLE. II. THE TRANSITION BETWEEN WEAK AND STRONG CROSSBRIDGES. ((J. Shi and P. Dreizen)) Physiology & Biophysics, SUNY Brooklyn, Brooklyn, NY.

We here relate conformational variants determined for S1 flexible loop 627-646 to the conventional model of the acto-S1 crossbridge cycle. We assume $A{\cdot}S1^{*}{\cdot}ADP{\cdot}P_i \longleftrightarrow A{\cdot}S1{\cdot}ADP{\cdot}P_i \longleftrightarrow A{\cdot}S1{\cdot}ADP$, taken as weak, activated weak, and strong crossbridges, respectively. In weak crossbridges, the 627-646 loop is found in an extended conformation, interacting with N-terminal actin via charge pairs lys640-glu4 and lys641-glu2, and no close interactions between actin and S1 otherwise. The transition to activated weak state is modeled as lateral sliding of S1 head in azimuthal plane, bringing the S1 627-646 loop close to the base of actin loop 1-28. There are charge pairs lys640-asp25 (weak) and lys641-glu4, and A·S1 interactions are limited to loop regions. The transition to strong crossbridge is modeled as an inward movement of S1 head toward the filament axis, with massive folding of 627-646 loop. The S1 loop-actin interaction shifts to charge pairs lys640-asp1 and lys641-glu4, and other secondary interactions between S1 loop and the base of actin 1-28 loop. The overall structure is now the same as the Rayment 1993 model of A·S1 complex, with addition of 627-646 loop. The present model neglects conformational changes in S1 head away from the 627-646 loop, which may of course drive transitions between weak and strong crossbridges and within strong cross-bridges. This seems an acceptable first approximation since weak crossbridges involve flexible regions of S1 predominantly and the Rayment model corresponds to early phase of strong crossbridges.

Tu-Pos17

MOLECULAR MODELING OF ACTOMYOSIN CROSSBRIDGE CYCLE. I. FLEXIBLE LOOP REGIONS IN WEAK AND STRONG CROSSBRIDGES. ((J. Shi and P. Dreizen)) Physiology & Biophysics, SUNY Brooklyn, Brooklyn, NY.

Initial formation of acto-S1 crossbridges appears to involve electrostatic interactions between actin 1-4 and S1 heavy chain in 20kD-50kD junction (near 640-642) or 50kD lower domain (near 572-574). These sites can be identified as 170 and 180kD bands, respectively, on SDS electrophoresis following EDC zero-length crosslinking. The 2 S1 sites are in flexible regions having no structure in the Rayment model of myosin S1. We have modeled these flexible S1 loops by means of homologous loop searches, molecular dynamics, and energy minimization in distant-dependent dielectric, keeping constant the atomic coordinates for actin and the rest of S1 Cα structure. The 627-646 loop generates 3 major conformational classes, readily identified with weak crossbridges, strong crossbridges, and a space-filling but biologically uninteresting form. The loop is extended in weak crossbridges, and folded in strong crossbridges. Crossbridge construct calculations show weak crossbridge is stabilized by favorable electrostatic interactions between actin and loop, with secondary interactions balancing minor structural distortion in the loop. The strong crossbridge is more stable, with favorable electrostatic and van der Waals energies from actin-loop and the loop itself. The flexible loop 571-575 also generates multiple conformations which can be used to construct S1 states in weak and strong crossbridges. Again, the strong crossbridge is more favorable, with greater electrostatic and van der Waals energies for the actin-loop interaction.

Tu-Pos18

KINETIC CHARACTERISATION OF DIFFERENT LENGTH FRAGMENTS OF THE MYOSIN HEAD EXPRESSED IN *DICTYOSTELIUM DISCOIDEUM*. ((Michael Geeves, Susanne Kurzawa, Deborah Hunt & Dietmar Manstein)). MPI für Molekulare Physiologie, 44139 Dortmund, Germany & NIMR, Mill Hill,London NW7 1AA, U.K.

We have previously described the isolation and characterisation of two fragments of *D. discoideum* myosin: A full length head including both native light chains (M864 or MHF) and a short catalytic domain-like fragment, lacking the light chain binding region (LCBR), M754. These studies suggested that nucleotide binding and the communication between the nucleotide site and the actin site were disrupted in M754. Here we describe the pre-steady-state kinetics for two slightly longer head fragments M761, lacking the complete LCBR, and M781, truncated at residue 13 of the first IQ repeat. Both proteins were over produced in *D. discoideum* carrying either an N-terminal (M781) or C-terminal (M761) His-tag and purified by Ni2+-chelate affinity chromatography.

For each head fragment we examined the rates of ATP binding and hydrolysis by the isolated fragment; the rates of actin binding to the fragment; the rates of ATP induced dissociation of actin from the actin.head-fragment complex and the competition between ATP and ADP binding to actin.head-fragment.

This data suggests that, for these single headed myosin fragments, the light chain binding domain is not essential for the interaction with actin, the binding or hydrolysis of ATP or the communication between the actin and nucleotide sites. Loss of the 755-761 peptide results in altered nucleotide binding and communication between the two sites, while actin binding itself is little affected. The addition of an N-terminal affinity tag, consisting of seven His residues, has no detectable effect on the kinetic behaviour of the myosin head.

Tu-Pos19

ANALYSIS OF CONFORMATIONAL CHANGE OF SMOOTH MUSCLE MYOSIN REGULATORY LIGHT CHAIN ACCOMPANIED WITH PHOSPHORYLATION USING ^{19}F-NMR. ((Shinsaku Maruta, Nobutaka Saeki, Kohji Banno, Stéphane M. Gagné*, Mitsuo Ikebe#, and Brian D. Sykes*)) Department of Bioengineering Soka University, Hachioji, Tokyo 192 JAPAN, *Department of Biochemistry University of Alberta, Edmonton, Alberta T6G 2H7 CANADA, #Department of Physiology & Biophysics, Case Western Reserve University, Cleveland, Ohio.

To study the conformational change of smooth muscle myosin regulatory light chain (LC20) induced by phosphorylation using ^{19}F-NMR, ^{19}F-labelled LC20 mutant (5-F-Trp substituted for Phe 22) was prepared. The cDNA clone encoding the open reading frame of mutant LC20 (Phe 22 → Trp) was subcloned into the polylinker of pT7-7 vector and it was transformed into E.coli BL21 tryptophan auxotroph strain. The recombinant LC20 (Phe 22 → Trp) was expressed in the presence of 5-Fluoro-Trp. The mutant was purified by the column chromatography of DEAE-Sephacel and Sephacryl S-200. ^{19}F-NMR spectra of the dephosphorylated mutant showed two signals at -49.0 ppm and -49.6 ppm which have different chemical shift from free F-Trp. These two signals were equilibrium relation each other. Phosphorylation of this mutant reduced the -49.0 ppm signal and increase the -49.6 ppm signals concomitantly. Equilibrium go to -49.6 ppm by adding of 25mM detergent CHAPS or increasing temperature to 35°C from 5°C. Small angle X-ray scattering experiment showed that LC20 exists as dimer. Sedimentation equilibrium experiment using analytical ultra centrifugation also indicated that monomer-dimer equilibrium. These results may suggest that signal at -49.0 ppm and -49.6 assign to dimer and monomer respectively. Phosphorylation may induce conformational change to prevent LC20 from forming dimer.

Tu-Pos20

EFFECTS OF METABOLIC INHIBITION ON MYOSIN LIGHT CHAIN PHOSPHORYLATION AND FORCE PRODUCTION OF ISOLATED RAT MYOMETRIUM. ((M.J. Taggart*, C.B. Menice, S. Wray* and K.G. Morgan)) Physiological Laboratory, University of Liverpool, United Kingdom* and Boston Biomedical Research Institute, Boston, MA 02114.

Metabolic inhibition of uterine smooth muscle with cyanide results in a fall in force accompanied by significant intracellular metabolite changes including decreased [ATP] and [PCr]. Consequently, the phosphorylation potential of the tissue may have declined. We, therefore, studied the extent of myosin light chain (MLC) phosphorylation, a major regulated determinant of smooth muscle contractility, and force production of metabolically inhibited myometria isolated from adult virgin rats.

Tissues were equilibrated in oxygenated HEPES-buffered Krebs at 37°C and stimulated in 40mM K^+-Krebs with or without cyanide (2mM). Samples were frozen for MLC phosphorylation determination by two-dimensional gel electrophoresis. Resting phosphorylation levels were 9.2%±2.2 (n=5). High K^+-stimulation rapidly increased force which remained at near-maximal levels (86%±8.5 (5)) after 10 mins. MLC phosphorylation increased to a peak at 1 minute (58%±6.3 (5)) declining to supra-basal levels at 10 mins (31%±4.5 (5)). High K^+-stimulation in the presence of cyanide significantly reduced force at all time points (force was 25% ± 5.5 (4) of maximum at 10 mins). Phosphorylation levels, however, were not significantly altered (30%±11 (4) at 10 mins). These results suggest that myometrial metabolic inhibition impairs contractile activity without a concomitant reduction of MLC phosphorylation.
Supported by NIH grant HL31704 and The Wellcome Trust (U.K.).

Tu-Pos21

ALTERNATIVE SPLICING OF SMOOTH MUSCLE MYOSIN HEAVY CHAINS AND ITS FUNCTIONAL CONSEQUENCES ((H. Haase, and I. Morano)) Max Delbrück Center for Molecular Medicine, 13122 Berlin, Germany.

The aim of our study was to determine the relation between alternatively spliced myosin heavy chain (MHC) isoforms and contractility of smooth muscle. The relative amount of MHC with an alternatively spliced insert in the 5´- (amino terminal) domain was determined on the protein level using a peptide-directed antibody (a25K/50K) raised against the inserted sequence (QGPSFAY). Smooth muscle MHC isoforms of both bladder and myometrium but not non-muscle MHC reacted with a25/50K. Using a quantitative Western-blot approach the amount of 5´-inserted MHC in rat bladder was detected to be about 8-fold higher than in normal rat myometrium. The amount of heavy chain with insert was found to be decreased by about 50% in the myometrium of pregnant rats. Although bladder contained significantly more 5´-inserted MHC than myometrium, apparent maximal shortening velocities (Vmax) were comparable being 0.138 ± 0.012 and 0.114 ± 0.023 muscle length per second (ML/s) of skinned bladder and normal myometrium fibers, respectively. The decreased expression of 5'-inserted MHC during pregnancy was associated with increased Vmax being 0.210 ± 0.025 ML/s in the late pregnant state. Phosphorylation of myosin light chain 20 induced by maximal Ca^{2+}/calmodulin activation were the same in bladder and myometrial fibers. These results suggest that the amount of 5'-inserted MHC is not necessarily associated with Vmax of smooth muscle.

Tu-Pos22

OVEREXPRESSION OF CALPONIN IN SMOOTH MUSCLE CELLS AND 3T3 FIBROBLASTS INHIBITS CELL PROLIFERATION. ((Z. Jiang, R.W. Grange, M.P. Walsh* and K.E. Kamm)) Dept. Physiol., U.T. Southwestern, Dallas, TX 75235 and *Dept. Med. Biochem., U. Calgary, Alberta, Canada T2N 4N1.

Calponin (CaP; basic isoform) is an actin-binding protein that inhibits actomyosin MgATPase activity and is expressed in differentiated smooth muscle. Cultured bovine tracheal (BT) smooth muscle cells (pass 1 or 2) expressed a small fraction (0.02±0.01, n=8) the amount of CaP in tissues, while NIH 3T3 cells expressed none, when determined by western blot. Our hypothesis is that expression of CaP in BT and 3T3 cells will inhibit actomyosin-dependent processes. CaP expression in 3T3 cells transfected with a pACsk.2CMV5 vector containing cDNA for avian CaP was assessed by immunofluorescence which revealed two patterns of distribution. The majority of staining cells had normal morphology with CaP localized along stress fibers, while a minor population of cells had elongated processes with CaP localized at the cell margins. In order to achieve high efficiency expression, an adenovirus encoding the CMV-CaP construct (AdV-CaP) was generated by homologous recombination in 293 cells. BT and 3T3 cells infected with AdV-CaP expressed amounts of CaP similar to smooth muscle tissues, 0.039 and 0.015 µg/µg total protein, respectively, with >90% of cells expressing. To evaluate the effects of CaP expression on cell function, BT and 3T3 cells were infected with AdV-CaP for 48 hr, then replated at low density. Cell proliferation rates for AdV-CaP-infected cells were inhibited 11-fold for BT cells and 4-fold for 3T3 cells compared to control. These results show that overexpressed CaP 1) targets to actin-containing structures in cells and 2) acts to modify cellular proliferation. Future experiments will evaluate mechanisms by which expressed CaP affects cell motile functions.

Tu-Pos23

MYOSIN BINDING SITES CONTROL ACTIN FLEXIBILITY.
((E.Prochniewicz, and D.D.Thomas)) University of Minnesota.

Rigor binding of myosin heads (S1) significantly decreases the microsecond flexibility of actin. To explain the mechanism of these changes, we used two other methods to perturb myosin binding sites on actin and examined the effects on microsecond flexibility, measured by time-resolved phosphorescence anisotropy (TPA) of erythrosin-iodoacetamide (ErIA) labeled actin. (1) Monomers were crosslinked with EDC, which is known to react with the myosin-binding region in the N-terminus of actin, then copolymerized with uncrosslinked ErIA-labeled actin monomers at a 1:1 molar ratio. This treatment greatly reduced actin flexibility; TPA of the copolymer became similar to that of acto-S1. Subsequent binding of S1 to the copolymer had only a very slight effect. (2) ErIA F-actin was treated with Fab against residues 1-7, also resulting in a substantial decrease in flexibility, so that the TPA decay became similar to that of acto-S1. Both perturbations were accompanied by inhibition of actin motility without abolishing interaction with myosin. These observations imply that **(a) the effect of myosin on the flexibility of actin results from structural changes in the myosin binding sites on actin, and (b) the changes in rigidity play a regulatory role in the process of contractility.**

Tu-Pos24

CRYSTALLOGRAPHIC ANALYSIS OF PROFILIN I FROM *ACANTHAMOEBA*.
((K.A. Magnus*, S. Liu*, A.A. Federov§, T.D. Pollard¶, E.E. Lattman¥ and S.C. Almo§)) *Dept. Biochem., Case Western Reserve Univ., Cleveland, OH 44106. §Dept. Biochem., Albert Einstein Coll. of Medicine, Bronx, NY 10461. ¶Dept. Cell Biol. & Anat. and ¥Dept. Biophys. & Physiol. Chem., Johns Hopkins Univ. Sch. of Medicine, Baltimore, MD 21205

Profilin I from *Acanthamoeba castellanii* is an actin cytoskeletal protein implicated in phosphoinositol based signaling. The protein (12 kDa) has been crystallized in two different forms. One of these forms proved amenable to 3D structural determination using heavy atom isomorphous methods and was used as a test molecule in molecular replacement to determine the second structure. The differences between the profilin I crystal structures are in their respective lattice contacts as anticipated, but there are also significant variations in the actin binding helical region and in the loop preceding this helix. Analysis of the heavy atom derivative modifications that lead to an uninterpretable electron density map for the native profilin I structure shows large numbers of sites for two of the derivatives. A third heavy atom derivative, K_2HgI_4, had fewer sites but they are sufficiently asymmetric so as to be unrefinable using an isotropic model.

Tu-Pos25

LOCALIZATION OF ACTIN-BINDING AND ACTOMYOSIN ATPase INHIBITORY DOMAINS IN THE C-TERMINUS OF SMOOTH MUSCLE CALDESMON.
((Ze Wang and Samuel Chacko)) Department of Pathobiology, University of Pennsylvania, Philadelphia, PA 19104.

We systematically designed a series of mutants of chicken gizzard caldesmon (CaD) by COOH-terminal truncations and internal deletions using both PCR-related cloning strategy and site-directed mutagenesis. These CaD mutants were expressed in Sf9 cells using a baculovirus expression system, and the precise locations of the actin-binding domain and the region responsible for the CaD-induced inhibition of actin-activated Mg-ATPase activity of smooth muscle myosin were determined. Our results reveal a strong actin-binding motif in the region between residues 718 and 737. Further analysis showed that the high affinity actin-binding domain consists of 6 amino acid residues from Lys^{718} to Glu^{723}. This six amino acid-region also represents the core sequence responsible for the CaD-induced inhibition of actin activation of Mg-ATPase of smooth muscle myosin, although the maximal inhibition of ATPase by CaD also requires the sequence between residues 728 and 731. Interestingly, the latter region is not responsible for actin binding. These data provide the first direct evidence for a relationship between the binding of CaD to a specific actin binding domain and the inhibition of actomyosin ATPase activity. Furthermore, experiments using CaD mutants with internal deletions of 28 amino acids also confirms our previous observation that the region between 690 and 717 is responsible for the weak inhibition of actomyosin ATPase. These inhibitory determinants are located in the region between either Asn^{690} and Gly^{717} or Lys^{718} and Ala^{731}, and they function independently. Supported by NIH Grants DK39740 & DK47514.

Tu-Pos26

FLEXURAL RIGIDITY OF ACTIN FILAMENTS STUDIED IN THE LASER LIGHT TRAP
((Donald E. Dupuis, William H. Guilford, and David M. Warshaw)) Mol. Physiol. & Biophys., Univ. of Vermont, Burlington, VT 05405.

Biological processes from cell division to muscular contraction depend upon the mechanical properties of actin filaments. Two such properties are axial stiffness (related to the elastic modulus, E) and resistance to bending (flexural rigidity, EI). Kojima et al. (1994) have estimated the axial stiffness of actin to be 44 pN/nm for a 1 μm filament. Other groups treating the actin filament as a flexible polymer that undergoes thermal bending, have estimated actin filament's EI (range: $4\text{-}73\times10^3$ $pNnm^2$) based on measurements of the filament's persistence length. To estimate EI, we attached the ends of a fluorescently labeled actin filament to two microsphere "handles" captured in independent laser light traps. The light traps were manipulated to apply a range of tensions (0-6 pN) to a filament via the microsphere handles. With increasing filament tension, the displacement of the microspheres, as measured by a photodiode detector, was inconsistent with a bead-actin filament system that is rigid and static. This inconsistency is due to the beads rotating in the trap and the filaments bending near their attachments to accommodate this rotation. We modeled how bead rotation and bending of the actin filament might occur based on beam theory. Fitting this model to the experimental data resulted in an estimated EI of $\approx10\times10^3$ $pNnm^2$, a value within the range of previously reported results, albeit using a novel method. In addition, these data support the idea that actin filaments are more compliant than previously assumed.

Tu-Pos27

STEADY-STATE FLUORESCENCE POLARIZATION ANALYSIS OF RHODAMINE-PHALLOIDIN BINDING TO MUSCLE.
((V. Zhukarev, J.W. Sanger, J.M. Sanger, Y.E. Goldman, H. Shuman)) Pennsylvania Muscle Institute, U. of Penn. Sch. of Med., Philadelphia, PA 19104 (Spon. by L.W. Tu)

Phalloidin probes have been used to measure orientation changes of thin filaments during muscle contraction (Prochniewicz et al., *JCB*, 97:1663, 1983). Several groups found, however, that phalloidin binds nonuniformly to thin filaments in skeletal muscle (Bukatina et al., *Histochem.*, **81**:301, 1984; Szchestna et al., *JMRCM*, **14**:594, 1993). We used steady-state fluorescence polarization microscopy to measure the local intensity and orientation of rhodamine-labeled phalloidin in skeletal myofibrils from fibers extracted in glycerol for 14 days. Fluorescence is 1.5-4.5 fold higher at both ends of the thin filaments than it is in between (Intensity in Fig.). In deblurred images, 50% of the total labeling is in the Z lines and at the pointed ends of the thin filaments (arrows). At the Z lines and the pointed ends, the fluorescence polarization ratio measured parallel to the myofibril axis ($P_\parallel$) is equal to the fluorescence polarization ratio measured perpendicular ($P_\perp$) suggesting that the probe is randomly oriented in these regions. In the middle of the thin filaments $P_\parallel$ = 0.263 ± 0.023 and $P_\perp = 0.046 \pm 0.039$ (means ± SD, n=12) suggesting that the probe is parallel to the thin filaments. These data suggest either non-specific binding of phalloidin at the ends of the filaments or inhibition of phalloidin binding in the middle. Supported by NIH grant HL-15835 to the PMI.

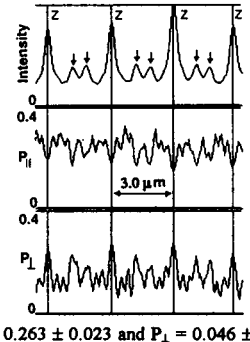

Tu-Pos28

ELASTIC PROPERTIES OF SINGLE TITIN MOLECULES MADE VISIBLE THROUGH FLUORESCENT F-ACTIN BINDING
((Miklós S.Z. Kellermayer and Henk L. Granzier)) VCAPP, WSU, Pullman, WA 99164-6520. (Spon. by K. Trombitás)

We have previously shown that both cloned titin fragments and native titin are able to bind F-actin (Li *et al, Biophys.J.* **69**, 1508, 1995; Kellermayer and Granzier, submitted). In the present work we use the actin-binding property of titin to study its elastic characteristics.

A nitrocellulose-coated coverslip was covered with anti-titin antibody (9D10). Non-specific binding sites on the surface were blocked, followed by the addition of native titin (purified according to Soteriou *et al, J.Cell Sci.* **104**, 119, 1993). Subsequently, fluorescent actin filaments were added. Filaments were then observed using fluorescence video microscopy.

Fluorescent actin filaments were found tethered to the coverslip surface. Filaments were pivoting around a single point of attachment, indicating that they bound to single titin molecules. Maximal angular distribution of the pivoting actin filament was ±467° around the mean position. By attaching a glass microneedle to the actin filament and moving the microscope stage, it was possible to stretch titin. After a maximum displacement of 7.75 μm, the actin filament was observed to break loose from the microneedle and, driven by titin's elastic recoil, snap back to its original position. The initial, resolvable (33 ms resolution) velocity of recoil was 150 μm/s. Velocity decayed with a calculated $t_{1/2}$ of 25 ms.

The actin-binding property of titin allowed us to study the elastic characteristics of single titin molecules. The method revealed that titin possesses a high degree of torsional and longitudinal flexibility. Attachment of fluorescent actin filaments to titin provides a useful tool to further probe titin's molecular properties.

Tu-Pos29

CALCIUM-DEPENDENT INHIBITION OF *IN VITRO* THIN-FILAMENT MOTILITY BY NATIVE TITIN ((Miklós S.Z. Kellermayer and Henk L. Granzier)) VCAPP, WSU, Pullman, WA 99164

Titin is a giant filamentous protein that spans the distance between the Z- and M-lines of the vertebrate muscle sarcomere and plays a fundamental role in the generation of passive tension. Titin has been shown to bind strongly to myosin, making it tightly associated to the thick filament in the sarcomere. Recent observations have suggested the possibility that titin also interacts with actin, implying further functions of titin in muscle contraction. We show—using *in vitro* motility and binding assays—that native titin interacts with both filamentous actin and reconstituted thin filaments.

Addition of native titin in the *in vitro* acto- or thin filament-HMM motility assays resulted in a decrease in velocity of the moving filaments and in an increase in the number of the immobile ones. The decrease in velocity increased with increasing molar ratio of titin to HMM. The inhibition of thin-filament motility was Ca-dependent: inhibition became more pronounced upon increasing [Ca]. In *in vitro* binding assays, both actin and reconstituted thin filaments bound to titin attached to nitrocellulose-coated surface. Binding of thin filaments to titin was Ca-dependent: larger quantities of thin filaments bound to titin at increased [Ca].

Our observations indicate that native titin is able to bind both actin and reconstituted thin filaments. This binding results in the inhibition of the motility of actin or thin filaments over HMM, possibly by tethering the filaments to the nitrocellulose surface. The Ca-dependent *in vitro* motility and binding assays point to an increased affinity of thin filaments to titin at high [Ca]. Our results suggest that titin's role may extend beyond the generation of passive tension, to a possible regulatory role in muscle contraction and cell motility.

CARDIAC E-C COUPLING

Tu-Pos30

TEMPERATURE AFFECTS TWITCH AMPLITUDE DIFFERENTLY IN CAT AND RABBIT CARDIAC VENTRICULAR MYOCYTES. ((J.L. Puglisi, K.S. Ginsburg, J.W.M. Bassani and D.M. Bers)) Loyola University Chicago, Maywood, IL 60153.

In our previous study of temperature effects on Ca transport during relaxation in cardiac ventricular myocytes (*BJ* 68:A135, 1995), we noted that the cat showed an unusual increase of twitch amplitude with warming (from 25 to 35°C), opposite to that in rabbits and other mammals. This was also unique to the twitch *vs* caffeine-induced contractures. We further explored this issue. After treatment with 10 μM thapsigargin (TG), to prevent SR function, twitches were smaller and slower. However the cat myocytes still showed an increase and the rabbits a decrease in twitch amplitude at 35°C. Thus, this difference does not seem to be attributable to differences in SR function or myofilament Ca sensitivity. At 35°C rabbit action potential duration (APD) was reduced to 67±3% (n=5) compared to 89±7% (n=5) in the cat. Thus, the longer cat APD, higher I_{Ca} and, therefore, prolonged active state at 35°C may allow relatively more Ca entry to occur during the AP and more time for myofilament activation (compared to rabbit). The greater Ca influx and APD at 35°C in the cat may offset the acceleration of Ca removal (which would decrease twitch amplitude). In rabbit faster Ca removal at 35°C may dominate, to reduce twitch amplitude.

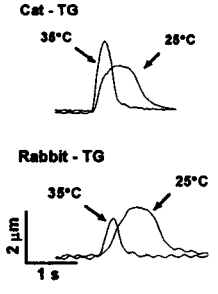

Tu-Pos31

SARCOPLASMIC RETICULUM Ca CONTENT IN INTACT FERRET VENTRICULAR MYOCYTES. ((K.S. Ginsburg and D. M. Bers)) Dept of Physiology, Loyola Univ Chicago, Maywood, IL 60153.

We evaluated the SR Ca content in ferret ventricular myocytes using the perforated patch voltage clamp technique (with indo-1 to monitor Ca_i transients). Cells were Ca loaded by several different voltage clamp protocols at 0.5 Hz in the presence and absence of isoproterenol to obtain a range of SR Ca contents. The total Ca influx at the last of each train of conditioning pulses was measured by integration to obtain the Ca influx per steady state pulse. The SR Ca content was quantified by rapid application of 10 mM caffeine at $E_m = -70$ and integration of the induced inward Na/Ca exchange current ($I_{Na/Ca}$). The $\int I_{Na/Ca}$ was normalized for cell capacitance. Using surface to volume measurements in ferret ventricular myocytes (7.96 pF/pL non-mitochondrial water, Satoh *et al.*, *AJP* in press) these current integrals were converted to cellular Ca content of the SR in units of μmol/l non-mitochondrial water (μM). These values are also corrected for the amount of Ca removed by systems other than Na/Ca exchange during the decline of $[Ca]_i$ at a caffeine-induced contracture in ferret myocytes (25%; *J Physiol* 476:295-308,1994). The figure show that the SR Ca content appears to saturate at 193 μM (K_m ~2 μM, curve fit). Notably, the SR content is almost maximal when Ca influx was 10 μM which corresponds to typical Ca influx attributable to I_{Ca} activated by a 200 ms pulse to 0 mV. Thus the SR Ca content may be nearly maximal under normal conditions and some changes previously attributed to progressive SR loading might be due more to increased fractional SR Ca release.

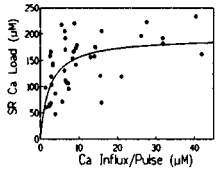

Tu-Pos32

REGULATION OF CARDIAC SR CA^{2+} RELEASE CHANNEL BY LUMENAL AND CYTOSOLIC CA^{2+} AND pH ((Le Xu, Geoffrey Mann and Gerhard Meissner)) Department of Biochemistry and Biophysics, University of North Carolina, Chapel Hill, NC 27599-7260

In cardiac muscle, the influx of Ca^{2+} during an action potential triggers the massive release of Ca^{2+} by opening the SR Ca^{2+} release channel. The effects of a changing intracellular ionic environment on cardiac Ca^{2+} release channel activity were examined. Single cardiac Ca^{2+} release channels were half-maximally activated by ~3 μM cytosolic Ca^{2+} and halfmaximally inhibited by ~5 mM cytosolic Ca^{2+}. Regulation of channel activity by cytosolic Ca^{2+} and the kinetics of channel gating were modulated by membrane potential, SR lumenal Ca^{2+}, and cytosolic MgATP. Ca^{2+} release channel acitivity was highly dependent on cytosolic pH and less on lumenal pH. [^{3}H]Ryanodine binding to SR vesicles showed a strong dependence on Ca^{2+} concentration and pH. In the absence of Mg^{2+} and AMPPCP, [^{3}H]ryanodine binding was decreased without an appreciable change of the Ca^{2+} dependence of binding, whereas in the presence of MgAMPPCP the free Ca^{2+} concentration for half-maximal binding was increased from ~5 μM at pH 7.3 to ~100 μM at pH 6.2. These results show that regulation of SR Ca^{2+} release channel activity by cytosolic Ca^{2+} is affected by SR lumenal Ca^{2+}, cytosolic and lumenal pH, Mg^{2+}, and adenine nucleotides. Accordingly, changes in intracellular ionic environment such as those occuring during ischemia can be expected to have profound effects on SR Ca^{2+} release. Supported by NIH.

Tu-Pos33

LUMINAL SR DIVALENT CATION INFLUENCES Ca^{2+}-INDUCED RELEASE IN CARDIAC MUSCLE. ((C.I. Spencer, R.J. Barsotti and J.R. Berlin)) Bockus Research Institute, Graduate Hospital, Philadelphia, PA 19146.

Triggered release of SR Ca^{2+} or Sr^{2+} was compared in saponin-permeabilized rat ventricular trabeculae to determine if the luminal divalent cation affects the release mechanism. After maximal SR loading in solutions with pCa or pSr 6.2, the peak of the transient isometric contraction induced by caffeine (10 mM) was 70 +/- 9 % and 88 +/- 8 % (SEM, $p<0.05$, n=4) of maximal tension at pCa 4.5 and pSr 4.5. SR release was also triggered by laser flash photolysis of caged Ca^{2+} under conditions producing no direct myofilament activation (NP-EGTA, 100 μM; 50 μM total Ca^{2+}). Tension due to photolysis of NP-EGTA was 82 +/- 12 % of that induced by caffeine in Ca^{2+} loaded trabeculae but only 30 +/- 2% of caffeine-induced tension in Sr^{2+} loaded trabeculae ($p<0.05$, see Fig.). This difference is not due to different myofilament sensitivity to Ca^{2+} and Sr^{2+}. Caffeine-induced release was unaffected by the cation species in the SR while Ca^{2+}-induced release of Sr^{2+} occurred less readily than Ca^{2+}-induced Ca^{2+} release. These results are consistent with those from voltage clamped single myoyctes in which Ca^{2+} currents failed to release Sr^{2+} from the SR and suggest that the SR luminal divalent cation affects Ca^{2+}-induced SR release in cardiac muscle.

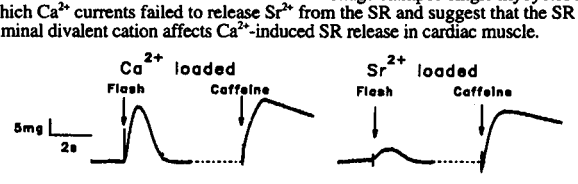

Tu-Pos34

EFFECT OF PROPOFOL ON SARCOPLASMIC RETICULUM Ca^{2+} CONTENT IN SINGLE RAT CARDIAC MYOCYTES (I.A. Kudryashova, Ph.D. and T.J.J. Blanck, MD, Ph.D.) Department of Anesthesiology, Hospital for Special Surgery, Cornell University Medical College, New York, 10021.

Propofol is a short acting intravenous induction agent that induces cardiovascular depression. Little is known, concerning its mechanism of action. Because of the importance of intracellular Ca^{2+} mobilization during the performance of cardiac contractility, sarcolemmal Ca^{2+} influx and sarcoplasmic reticulum (SR) Ca^{2+} content can be potential sites, at which Propofol exerts its cardiac depressant effect.

In single rat cardiac myocytes, continuously perfused at 37°C and loaded with fura-2/AM, the effect of Propofol on the intracellular Ca^{2+} transient produced by 10 mM Caffeine or KCl-membrane depolarization was studied with a fluorescent microscope. We found that after 5 minutes exposure to Propofol in concentrations 50, 70, 100 μM the peak of Caffeine-induced Ca^{2+} release was decreased. The anesthetic effect was dose-dependent. The peak of the fluorescent response to Caffeine significantly decreased upon pre-incubation of the myocytes with Propofol at 50, 70, 100 μM to 35.9, 45.3, 59.2%, respectively ($P < 0.05$). Propofol at 30 μM did not effect the SR Ca^{2+} content during the application of Caffeine. The acute addition of Propofol in a concentration range 30-100 μM to perfusion solution caused no transient change in the cytoplasmic Ca^{2+} concentration and the resting $[Ca^{2+}]_i$ was also unaffected by Propofol. Studying the time dependence of Propofol's effect on the SR Ca^{2+} release induced by Caffeine, we found that the effect of Propofol appears immediate. On the other hand, we found that incubation of myocytes with 100 μM Propofol depressed the Ca^{2+} transient activated by 30 mM KCl up to 20 or 30%. Nitrendipine (1 μM) inhibited up to 80% of the initial net Ca^{2+} influx during this membrane depolarization.

We suggest that the cardiac effect of Propofol could be related to modification of SR Ca^{2+} uptake or release and/or with the inhibition of sarcolemmal L-type Ca^{2+} influx.

Tu-Pos35

Ca^{2+}-LOADED CANINE VENTRICULAR MYOCYTES GENERATE DOUBLE $[Ca^{2+}]_i$ TRANSIENTS AND DOUBLE CONTRACTIONS WHEN ACTION POTENTIALS ARE PROLONGED.

(Bela Szabo, T. Banyasz, A. Kulcsar and R. Lazzara) Univ. of Oklahoma Hlth. Sci. Ctr. and VA Med. Ctr.

It has been demonstrated that the gain of CICR in cardiac cells depends on membrane voltage and on SR Ca^{2+} content during voltage clamp. We examined the effects of intracellular Ca^{2+} load and long depolarization on $[Ca^{2+}]_i$ transients in fura-2 loaded myocytes and on contractions in the absence of fura-2. Ca^{2+} load was induced by increasing $[Ca^{2+}]_o$ from 1.8 to 3.6mM. Action potentials were prolonged by Cs^+ (4.0 mM) at low $[K^+]_o$ (2.0 mM). Under these conditions the $[Ca^{2+}]_i$ transient and contraction were accompanied by a slow $[Ca^{2+}]_i$ transient and contraction before their relaxation was complete. Slow contractions were also observed during constant current pulses to depolarize the sarcolemma to 0 - +50 mV between 50 - 800 msec following the upstroke of the action potential. A blockade of DHP receptors with D600 (3.0 μM) did not inhibit the slow contraction although it abolished CICR. Slow contractions were accompanied by a transient depolarization of the sarcolemma. The observations suggest that in Ca^{2+}-loaded myocytes a Ca^{2+} release occurs from intracellular stores during long depolarizations independently of I_{Ca}.

Tu-Pos36

TWO COMPONENTS OF CA^{2+} RELEASE FROM SARCOPLASMIC RETICULUM IN HUMAN ATRIAL MYOCYTES (Stéphane N. Hatem, Agnès Bénardeau, Jean-Jacques Mercadier). CNRS URA-1159, Hôpital Marie Lannelongue, Le Plessis Robinson, France

Ca^{2+} signaling in cardiac myocytes depends on the ultrastructural organization of the sarcoplasmic reticulum (SR). We examined Ca^{2+} signaling in human atrial myocytes isolated from 19 samples of atrial appendages obtained during surgery (patients aged 39±6 yrs). Patch-clamped myocytes were dialysed with an internal solution containing (in mM): KAsp 115, KCl 15, MgATP 3, HEPES 10, glucose 10, $MgCl_2$ 2, NaCl 5, pH 7.3 and 0.1 Indo-K salt (used as the Ca-dye). Following the activation of ICa (by 150 msec test pulses from -60 to 0 mV), two types of Cai-transients (C) were observed: a short triangular-shaped C (C1) (in 25 cells) with a time to peak (tp) of 58±3 ms and a duration (time for half decrease, t1/2) of 352±14 ms, and a prolonged dome-shaped C (C2) (in 21 cells) (tp: 109±14 ms; t1/2: 633±23 ms). C1 and C2 were observed independently of cell size and disease, and both were caused by the SR Ca^{2+} release as they were suppressed by caffeine (5 mM, n=7) or ryanodine (100 μM, n=5). In myocytes exhibiting C2, subthreshold ICa (by test pulses from -60 to-30 mV), activated an initial slowly rising component of C, followed by a large component. In myocytes exhibiting C1, 1 μM isoproterenol induced C2 (n=8). During wash-out of caffeine, the recovery of C1 preceded that of C2. Both results indicate that the activation of C2 depends on Ca^{2+} loading of the SR. In 35% of myocytes, a train of pulses (-60 to 0mV) at 0.1 Hz resulted in an alternation of C1 and C2. We conclude that two components of SR Ca^{2+} release are present in human atrial myocytes, and could reflect a poorly developed t-tubule and junctional SR network.

Tu-Pos37

CALCIUM SIGNALING IN CARDIAC MYOCYTES OF TRANSGENIC MICE OVEREXPRESSING NA^+-CA^{2+} EXCHANGER. ((S. Adachi-Akahane*, K Philipson*, and M. Morad*)) *Dept Physiol, UCLA; *Dept Pharmacol & Institute Cardiovascular Sciences, Georgetown Univ. Med. Ctr., Washington, DC 20007.

In rat ventricular myocytes, Na^+-Ca^{2+} exchanger appears to be excluded from Ca^{2+} microdomains surrounding the DHP/ryanodine receptor complex (Adachi-Akahane, et al., Biophys. J. 1995). To probe whether the failure of the exchanger to trigger Ca^{2+} release results from insufficient activity of the exchangers, we examined calcium signaling in ventricular myocytes of mice overexpressing Na^+-Ca^{2+} exchanger (Li, et al., Biophys. J. 1994). Simultaneous recordings of membrane currents and Fura-2 signal were conducted in mouse ventricular myocytes dialyzed with 10mM Na^+. In transgenic, but not in control myocytes dialyzed with 0.1-0.2mM Fura-2, activation of I_{Ca} was followed by large "hump" and "tail" of inward current representing $I_{Na\text{-}Ca}$. These currents were abolished by caffeine- or thapsigargin-induced depletion of Ca^{2+} from the SR. Ca^{2+} release caused by rapid (<50ms) application of caffeine activated (≈7pA/pF) $I_{Na\text{-}Ca}$ in transgenic vs. 1.5pA/pF in control mice. In transgenic but not in control myocytes, inward Ca^{2+} flux via the exchanger at +80mV caused a slow rise in $[Ca^{2+}]_i$ triggering large $Ca^{2+}{}_i$-transients. In SR-depleted transgenic and control myocytes, depolarization to +80mV caused a 500 vs. 100nM rise in $[Ca^{2+}]_i$, respectively. In 2mM Fura-2 dialyzed myocytes, $I_{Na\text{-}Ca}$ failed to activate in transgenic and control myocytes. We conclude that despite 5-10 fold higher exchanger activity in transgenics, the exchanger remains functionally excluded from the DHP/ryanodine receptor Ca^{2+}-signaling microdomains. Supported by NIH HL16152 (MM) and HL48509 (KP).

Tu-Pos38

H_2O_2-STIMULATION OF Ca^{2+}-SIGNALING IN INTACT CARDIAC MYOCYTES. ((Y. J. Suzuki, J. Monterubio, L. Cleemann, D. R. Abernethy, and M. Morad)) Department of Pharmacology, Georgetown University Medical Center, Washington, DC 20007.

In cardiac muscle, intracellular amplification of Ca^{2+}-signal by the Ca^{2+}-induced Ca^{2+} release mechanism is controlled by cross signaling between L-type Ca^{2+} channel and ryanodine-receptor, while Na^+-Ca^{2+} exchanger is the major extrusion mechanism for Ca^{2+}. Since redox reactions appear to serve as biological signal transduction mechanisms, we searched for components of Ca^{2+}-signaling in cardiac myocytes that may be affected by micromolar concentrations of H_2O_2. In freshly isolated whole cell clamped rat and guinea-pig ventricular myocytes dialyzed with 0.2 mM Fura-2, I_{Ca}, Na^+-Ca^{2+} exchange current, and intracellular Ca^{2+}-transients were simultaneously measured. Rapid (<50 ms) exposure of cells to H_2O_2 (50-100 μM) resulted in suppression of I_{Ca}, but enhancement of voltage-dependent Ca^{2+} release transients, suggesting increased efficiency of Ca^{2+}-induced Ca^{2+} release transients mechanism. H_2O_2 also enhanced the initial rate of caffeine-induced Ca^{2+} release transients and the accompanying Na^+-Ca^{2+} exchange current. Our results show that effects of H_2O_2 at micromolar levels are significantly different than the reported, general suppressive effects of H_2O_2 on ionic channels at millimolar (toxic) concentrations. Stimulation of signal transduction components by low levels of H_2O_2 suggests possible oxidative regulation of Ca^{2+}-signaling events. Supported by NIH HL16152.

Tu-Pos39

SUBENDOCARDIAL MYOCYTES FROM HEARTS WITH LEFT VENTRICULAR DYSFUNCTION HAVE ABNORMALLY LONG Ca^{2+} TRANSIENTS. ((G.L. Smith, M.A. McIntosh & S. Currie)) Institute of Biomedical Life Sciences, West Medical Building, Glasgow University, Glasgow G12 8QQ.

We examined the time course of the intracellular Ca^{2+} transient in myocytes isolated from the sub-endocardial region of the left ventricle. Rabbits with LVD, indicated by reduced cardiac output response to a volume challenge, raised LV end-diastolic pressure and reduced ejection fraction, were sacrificed 8 weeks after ligation of the marginal branch of the left coronary artery. LV sub-endocardial myocytes were isolated by enzymatic dispersion of sub-endocardial regions removed from Langendorf perfused hearts after an initial collagenase digestion. Myocytes were incubated with 1μM Fura-AM for 5 min. Fura-2 fluorescence transients in response to field stimulation at 0.33Hz were measured in myocytes perfused with HEPES buffered Tyrode's solution at 36-37°C. The average duration (50% rise time to 50% decay time) of Ca^{2+} transients measured in LV sub-endocardial myocytes from 3 normal hearts were 246ms ±12ms, 239ms ±13 and 231ms ±9. Cells from hearts with LVD had durations of 294ms ±21ms, 348ms ±45ms and 665ms ±132ms. 8 -13 cells from each heart were studied. Some myocytes isolated from hearts with LVD had Ca^{2+} transients with a normal time course. However, at least half of the cells had Ca^{2+} transients with significantly prolonged decays. These latter transients exhibited a distinct plateau phase which in some transients lasted for more than 1s. The differences between hearts from the LVD group may represent marked intercellular differences: a greater degree of heterogeneity may be associated with more severe LVD.

Tu-Pos40

FURA-2 CALCIUM TRANSIENTS DURING SARCOMERE ISOMETRIC TWITCHES IN RAT CARDIAC TRABECULAE. ((Paul M.L. Janssen and Pieter P. de Tombe)). Bowman-Gray School of Medicine, Winston-Salem, NC 27157.

Studies on isolated myocardium are hampered by uncontrolled sarcomere length (SL) shortening in the central segment due to damaged end-compliance. The impact of SL shortening on the intracellular calcium transient is unknown. Accordingly, we developed a method to measure the intracellular calcium transient in rat cardiac trabeculae during sarcomere isometric twitches. SL was measured by laser diffraction techniques, force (F) was measured by a silicon strain gauge, muscle length (ML) was controlled by a servo motor. Intracellular calcium was measured by fluorescence of FURA-2 that was loaded exclusively into the cytosol via iontophoresis of the free salt during impalement of a single myocyte with a micro-pipette. An iterative computer algorithm was used to "clamp" SL in the central segment of the muscle preparation every 6th twitch. Next, the laser diffraction system was switched off, while the computer continued to control ML of the trabecula so as to maintain constant SL. Low intensity FURA-2 fluorescence at 510 nm was then recorded at 340 nm and 380 nm UV light excitation, after which SL was again monitored by laser diffraction to confirm steady state. The figure shows a typical recording of 3 averaged twitches in which SL was kept constant at 1.9 µm (data smoothed by 50 ms running average filter). We conclude that this system can be used to measure intracellular calcium during sarcomere length controlled twitches in isolated cardiac trabeculae.

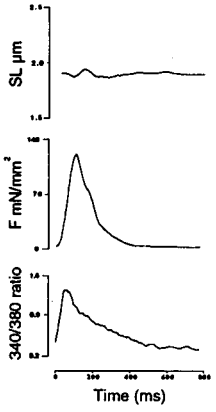

Tu-Pos41

DIRECT EVIDENCE THAT Na CURRENTS ENHANCE TRIGGERED CONTRACTIONS IN HEART: NEED FOR A FUZZY SPACE. ((A. Morani and J.H.B.Bridge)) C.V.R.T.I, Bldg. 500, University of Utah, Salt Lake City, UT 84112.

We investigated the hypothesis that Na current can augment triggered contractions by stimulating reverse Na-Ca exchange. We voltage clamped Guinea pig ventricular cells (30°C) with single suction microelectrodes containing 10 mM Na. Cells were held at -80 mV in a superfusing solution containing 145 mM Na and 2.7mM Ca. This solution was abruptly changed (100 msecs) for one containing either 50 or 20 mM Na and 100 nM Ca. We then depolarized cells every 70 msecs from -80 to -40 mV for 20 msecs between 1 and 9 times. When the superfusing Na was 50 mM this activated 20 nA uncontrolled Na currents and when the superfusing Na was 20 mM the 5 nA Na currents could be controlled. With 100 nM extracellular Ca we did not expect to activate any reverse Na-Ca exchange or Ca current after activating the Na currents even under circumstances where we lost control of the membrane potential. The Normal superfusing solution was then rapidly returned to the cell which was then held at -40 mV. We next depolarized the cell to +50 mV to activate a triggered contraction. The size of the triggered contraction was significantly enhanced and depended upon the number of Na currents that preceded it (Fig). Between each trial the cell was paced to steady state to ensure uniform loading of the SR. Integration of Na currents suggest that if they were to have enhanced triggered contractions they must have done so by accumulating in a small fraction of the cell's volume (fuzzy space).

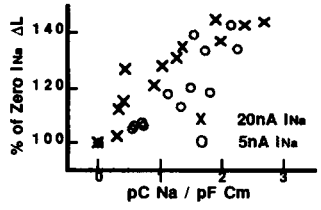

Tu-Pos42

EFFECT ON THE INDO-1 TRANSIENT OF APPLYING Ca CHANNEL BLOCKER FOR A SINGLE BEAT IN VOLTAGE-CLAMPED GUINEA-PIG MYOCYTES. ((A. J. Levi, J Li, K.W. Spitzer, and J.H.B.Bridge)) Dept. Physiology, University of Bristol, U.K., C.V.R.T.I, University of Utah, Salt Lake City, UT 84112.

We used a rapid solution switcher technique to investigate the mechanisms which trigger Ca release from the sarcoplasmic reticulum (SR) in guinea-pig ventricular myocytes. We patch clamped myocytes at 36°C, Indo-1 was used to monitor intracellular Ca, and we established a standard level of SR Ca load before each test pulse by applying a train of conditioning pulses. Rapid application of nifedipine (32µM; $I_{Ca,L}$ blocker) 8 seconds before a test pulse, together with a ramp depolarization to pre-block Ca channels, inhibitied $I_{Ca,L}$ elicited by the following test pulse (98-99% inhibition). In cells dialyzed internally with 10mM Na-containing solution, nifedipine application before a +10mV test pulse blocked between 67-76% of the phasic Ca_i transient. This suggests that in the absence of $I_{Ca,L}$, another trigger mechanism for SR release exists which is able to trigger between 33-24% of the Ca_i transient (in cells dialyzed with 10mN Na, and pulsed to +10mV). For a given dialyzing Na level, the fraction of the Ca_i transient which remained during nifedipine increased as test potential became more positive. For a given test potential, the fraction of the phasic Ca_i transient which remained during nifedipine increased as the dialyzing Na level was increased. In cells dialyzed with Na-free solution and pulsed to +10mV, between 9-12% of the Ca_i transient remained with nifedipine. In contrast, in cells dialyzed with 20mM Na and pulsed to +10mV, between 43-53% of the Ca_i transient remained during nifedipine. The results are consistent with the hypothesis that both $I_{Ca,L}$ and a second mechanism are able to trigger SR release and the resulting Ca_i transient. Since, in the absence of $I_{Ca,L}$, the fraction of the remaining Ca_i transient increased with more positive test potential and higher internal Na, this is consistent with the possibility that the second trigger mechanism may be Ca entry by reverse Na/Ca exchange elicited by a step depolarization.

Tu-Pos43

EXCITATION-CONTRACTION COUPLING IS DEPRESSED IN A RAT MODEL OF HYPERTROPHY. ((E. McCall & D.M. Bers)) Loyola Univ. Chicago, Maywood, IL 60153.

We studied whether E-C coupling was altered in a rat model of hypertrophy (abdominal aortic banding, 16 wk). Heart weight increased from 1.77±0.07g (sham, n=10)) to 2.28±0.08g (banded, n=12, p<0.001). We determined the efficacy of different trigger Ca currents (I_{Ca}) to elicit contractions in patch-clamped ventricular myocytes from both groups. With 1 mM $[Ca]_o$ the effectiveness of a given I_{Ca} to induce contraction was similar in sham and banded animals, under conditions where SR Ca loading is expected to be equivalent. With 0.5 mM $[Ca]_o$ the contractions elicited for a given I_{Ca} were smaller in myocytes from banded animals (Fig). This modification occurred throughout the range of currents elicited, shifting the I_{Ca}-contraction relationship downward (Fig). The underlying mechanism is not yet known but could be reduced responsiveness of Ca-induced Ca release in hypertrophied myocytes at low $[Ca]_o$.

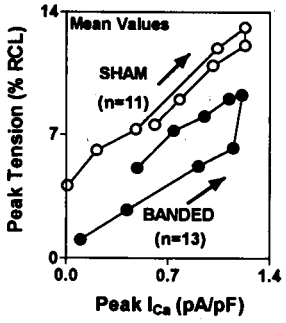

Tu-Pos44

PRESENCE OF A HUMP DURING THE INACTIVATION PHASE OF THE L-TYPE CALCIUM CURRENT OF GUINEA-PIG VENTRICULAR CARDIOMYOCYTES. ((Lacampagne A., Brette F. and Le Guennec J-Y.)) Laboratoire de Physiologie Animale, Fac. des Sciences, 37200 TOURS (France) (Spon. By J.A. Argibay)

To correctly analyse the physical properties of ion channels and the actions of drugs upon them, it is important that the membrane conducts only ionic species believed permeant. Thus, Cs+ is often used to replace K+ to study calcium current (ICa). However it is known that Cs+ may be responsible of a transient outward current which distorts measurement in guinea-pig ventricular myocytes[1].

In conditions where intra- and extracellular Na+ ions were replaced by Cs+ and K+ by Cs+, we observed the presence of a notch in the inactivation phase of ICa. This hump was more obvious at negative voltages. It was not due to a known transient outward current since 2 mM 9-AC or 4-AP did not supress it. After blockade of ICa by 200 µM Cd2+ or in nominally free extracellular calcium, no transient outward current was observed. When Ba2+ was used as the charge carrier, the hump disappeared. From these results, we concluded that this notch was not consecutive to a contaminant current[1] but was linked to the entry of calcium through L-type calcium channels, probably by the calcium-dependent inactivation pathway of the current.

[1]Christé G., De La Chapelle B., Lemtiri-Chlieh F. And Ojeda C., J. Physiology. (1989) 418, 169P.

Tu-Pos45

CHANGES IN THE L-TYPE Ca^{2+} CURRENT DURING CARDIAC DEVELOPMENT. ((S. Moreno, M. Mayorga-Luna, J. Ramos-Franco and R. Mejía-Alvarez)) Department of Physiology. National Institute of Cardiology "Ignacio Chávez". Mexico City, Mexico.

Several lines of evidence indicate that there is an increase of L-type Ca^{2+} current (I_{Ca}) density during postnatal development of the cardiomyocyte. This phenomenon leads to a puzzling question: how an immature myocyte with low density of these channels is able to sustain functional contractility which, at neonatal stage, directly depends on the magnitude of extracellular Ca^{2+} entry?. A possible answer is that the voltage dependence of the channel changes during development. To address this issue, we recorded I_{Ca} with the whole-cell configuration of the patch clamp technique in single ventricular myocytes from adult and new born rats. Our results indicate that in fact I_{Ca} density increases with development, from 3.0 ± 0.7 pA/pF (n = 6) in new born, to 11 ± 2 pA/pF (n = 13) in adult. In addition, the steady-state voltage dependence is different between these stages. In adult, the inactivation curve (f_∞) is centered (V_h) at -39 mV with a slope (k) of 5 mV (n=8), while in new born V_h = -20 mV and k = 7 mV (n=3). Similarly, the activation curve (d_∞) in adult has a V_h = -24 mV and k = 6 mV (n = 13), and in new born V_h = -11 mV and k = 8 mV (n = 6). Therefore, in adult the fraction of functional channels that remain active under steady-state conditions (f_∞ x d_∞) has a maximum of 4%, at -31.5 mV, while in new born such a fraction has a maximum of 12%, at -17.5 mV. These results support the hypothesis that even though the ventricular myocyte in new born rat has a lower density of functional L-type Ca^{2+} channels, they operate with higher steady-state activity in the plateau voltage range. This functional property allows the myocyte to have larger extracellular Ca^{2+} entry during the plateau phase of the action potential, which is direct responsible for the activation of the contraction. This work was supported by CONACYT 3547-M to RMA, and by NIH-Fogarty TW00077-02 to RMA.

Tu-Pos46

INTRACELLULAR FREE-Zn^{2+} IN VENTRICULAR CARDIAC MYOCYTES: OXIDANT-INDUCED ALTERATION AND EFFECT ON I_{Ca}. ((B. Turan, H. Fliss* and M. Désilets*)) Dept. of Biophysics, University of Ankara, Ankara, Turkey and *Dept. of Physiology, University of Ottawa, Ottawa, Canada K1H 8M5.

The important intracellular role of Zn^{2+} is now well recognized but only partly understood. Furthermore, little is known regarding free-Zn^{2+} homeostasis although alteration of protein redox status may well constitute an important regulatory mechanism. This study was aimed at determining: 1) the possible changes of intracellular free-Zn^{2+} concentration ($[Zn^{2+}]_i$) induced by HOCl and Na_2SeO_3, two oxidants known to strongly react with protein thiols, and 2) the effect of intracellular Zn^{2+} on ion currents. $[Zn^{2+}]_i$ was measured at 37°C in rabbit ventricular myocytes iontophoretically injected with fura-2 from small patch electrodes, and was calculated from the fluorescence shifts induced by the membrane-permeant Zn^{2+} chelator TPEN. Measured resting $[Zn^{2+}]_i$ was equal to 0.23±0.03 nM (n=16). HOCl (0.1 mM) and Na_2SeO_3 (1 mM) caused a rapid rise of $[Zn^{2+}]_i$ which reached steady-state levels within 5 min; the average values being equal to 7.7±1.7 (n=13) and 6.1±1.7 nM (n=5), respectively. These changes were independent of the presence of external Ca^{2+}. Ion currents, elicited by 300-ms pulses from -50 to 0 mV, were not significantly affected by the oxidants during the 5 min exposure. However, a large inhibition of I_{Ca} was observed when TPEN was added after the oxidants (72±6% inhibition, n=18), an effect significantly greater than that observed in the presence of TPEN alone (34±7%, n=6). Furthermore, exposure to 1 µM of the Zn^{2+} ionophore Zn-pyrithione also caused an inhibition of I_{Ca} (21±3%, n=12). These results are interpreted as an inhibitory effect of intracellular Zn^{2+} of I_{Ca}, with TPEN acting as a shuttle that facilitates diffusion of Zn^{2+} towards the membrane surface.

Tu-Pos47

NERVE STIMULATION DOES NOT PLAY A ROLE IN TRIGGERED PROPAGATED CONTRACTIONS IN CARDIAC TRABECULAE. ((Yingming Zhang, Henk E.D.J. ter Keurs)) University of Calgary, AB, Canada.

Cardiac arrhythmias can be induced by triggered propagated contractions (TPCs). TPCs can be elicited in the damaged end regions of cardiac trabeculae. This local contraction can subsequently propagate through the trabecula. The propagation velocity (Vp) is in the range of 70-200 µm/s in skinned fibers, but 0.1-15 mm/s in intact trabeculae. The high velocities in intact trabeculae may result from accelerated propagation of TPCs by neurotransmitters released due to activation of nerve endings by electrical stimulation of the muscle. Hence, we investigated the effects of cholinergic and adrenergic agonists and antagonists. Specifically, we studied whether acetylcholine (Ach) and α or ß-adrenergic blockade reduced Vp. Trabeculae from rat right ventricle were mounted between a motor and a force transducer. A silicon strain gauge and laser diffraction techniques were used to measure force and sarcomere length at two sites along the trabecula. TPCs were induced by trains of 15 stimuli at 2Hz with 15 second intervals. Neither Ach (1µM), atropine (1µM) nor α blockade by phentolamine (1µM) affected twitch force (Ft) or Vp. ß blockade by 1 µM propranolol decreased Ft slightly (~10%), but had no effect on TPCs. Adrenergic stimulation by phenylephrine (0.1-100µM) and isoproterenol (1-100nM) increased Vp corresponding to an increase of Ft, similar to the effect of varied external $[Ca^{2+}]$. The effects of α and ß agonists are consistent with an increased Ca^{2+} content of the sarcoplasmic reticulum. Our observations suggest that nerve stimulation does not play a role in TPCs in isolated cardiac trabeculae.

Tu-Pos48

Ca-DEPENDENCE OF ISOMETRIC FORCE KINETICS IN RAT SINGLE SKINNED CARDIOMYOCYTES. ((C. Vannier, H. Chevassus and G. Vassort)) U-390 INSERM, CHU Arnaud de Villeneuve, 34295 Montpellier Cedex 5, France.

The contractile force of cardiac muscle determined by myosin actin interactions is under the control of Ca ions. Force can be modulated by mechanisms that cause changes either in the cytosolic Ca transient during an action potential or in the sensitivity to Ca ions of the contractile proteins.

In single skinned cells, Ca sensitivity was investigated at different sarcomere lengths (1.8, 2.1, 2.7 and 3.3 µm). Maximal force was recorded at 2.1 µm and was decreased below 10% at 3.3 µm sarcomere length. With increasing sarcomere length, the tension-pCa relationships were shifted towards lower Ca concentrations and their slope decreased.

Crossbridge kinetics were investigated at different pCa_s by analyzing tension redevelopment after a brief slack release/reextension of the sarcomere length during Ca activation of the skinned cell.

The rate of tension redevelopment k_{tr} increased with increasing Ca concentrations up to 5.19 ±0.37 s^{-1} at maximal activation (pCa 4.5). The relation k_{tr} versus pCa was sigmoïdal and could be fitted by the Hill equation with pCa_{50} = 5.67±0.21 and n_H=2.21±0.29. The relation between relative k_{tr} and relative force was curvilear.

These results demonstrated that in cardiac muscle, like in skeletal muscle, Ca ion is a modulator of both the extent and kinetics of force generating crossbridges.

Tu-Pos49

ONE WEEK CAPTOPRIL TREATMENT DOES NOT AFFECT TWITCH TENSION, TIME COURSE AND STROPHANTIDIN SENSITIVITY IN RABBIT RIGHT VENTRICULAR MUSCLE. ((S. Baudet and J. Noireaud)) Cardiol. Lab., Laënnec Hosp., Nantes, France

Angiotensin-converting enzyme inhibitors are increasingly used in the treatment of heart failure because of their potential effect on the intracardiac renin-angiotensin system (IRAS). The role of IRAS in healthy hearts is not clearly defined although Hool et al. (1995, AJP, 268, C366) recently reported that one week oral captopril treatment (8 mg/kg) halved the intracellular Na activity in rabbit right ventricular muscle. The resulting increased transsarcolemmal Na gradient should decrease the sarcoplasmic reticulum (SR) Ca load (and hence, isometric contraction) and accelerate relaxation, both effects being mediated by the Na/Ca exchanger. It should also increase the concentration range for positive inotropic effects of cardiac glycosides. These different parameters were studied using similar conditions and preparations than Hool et al. (1995). At 0.5 Hz and 37°C, twitch tension was similar in control (C, n = 18) and captopril-treated (T, n = 20) muscles (8 ± 1 *vs* 9 ± 2 $mN.mm^{-2}$, n.s.) as were time to peak tension (164 ± 8 *vs* 156 ± 5 ms) and time to half-relaxation ($t_{1/2}$: 109 ± 7 *vs* 99 ± 4 ms). In a subset of muscles (C: n = 10; T: n = 12), there was no significant difference for the amplitude (12 ± 2 *vs* 9 ± 2 $mN.mm^{-2}$) of the rapid cooling contracture (RCC) - an indirect index of SR Ca load - and $t_{1/2}$ of the tension transient following rewarming of the muscle (312 ± 17 *vs* 318 ± 18 ms). When muscles were left quiescent for various time periods after steady stimulation, the amplitude of the first post-rest RCC decreased with time in C and T. Despite a trend for a faster post-rest decay in T muscles, it was not significant (resting time *vs* group interaction: n.s.). The cardiotonic glycoside strophantidin increased twitch tension in both C and T muscles within a narrow range (1 and 7 µM) before occurrence of toxicity signs (biphasic relaxation, aftercontractions and/or contracture). There was no differential effect of the glycoside on twitch tension depending on the group (no significant interaction). These data suggest that, despite the expected increased Ca efflux through the Na/Ca exchanger, other mechanisms such as a decreased expression of the Na/Ca exchanger and/or higher SR Ca uptake capacities may compensate for the increased transsarcolemmal Na gradient.

Tu-Pos50

ARRHYTHMIC CONTRACTIONS INDUCED BY ACTIVATION OF PURINERGIC RECEPTORS IN SINGLE VENTRICULAR MYOCYTES. ((Bin-Xian Zhang and Meredith Bond)) Department of Molecular Cardiology, Research Institute, Cleveland Clinic Foundation and Department of Physiology and Biophysics, Case Western Reserve University, Cleveland, OH.

The concentration of extracellular ATP in the heart increases under various physiological and pathological conditions, e.g. during myocardial ischemia; ATP activation of myocardial purinergic receptors may thus play an important role in regulation of myocardial contraction. We have investigated the effect of activation of purinergic receptors on the contraction of electrically stimulated adult rat ventricular myocytes. 2-methyl-thio-ATP (2-M-S-ATP) (0.1–25 µM) was superfused over electrically stimulated (0.2–0.3 Hz, 29°C) myocytes and cell shortening was recorded by video-edge detection. 2-M-S-ATP increased the amplitude of the electrically stimulated contractions in a biphasic manner with a maximal 70% increase in amplitude of the contractions at 5 µM 2-M-S-ATP and smaller increases at higher 2-M-S-ATP concentrations. This effect was independent of stimulation frequency and was not reversible with wash-out of 2-M-S-ATP. 2-M-S-ATP superfusion also resulted in arrhythmic contractions which decreased in frequency with increased stimulation frequency from 0.2 to 0.3 Hz. This effect was reversed by removal of 2-M-S-ATP. These two effects of 2-M-S-ATP superfusion thus demonstrate differential modulation by frequency of electrical stimulation and different responses to agonist washout. We therefore propose that multiple intracellular signalling pathways may mediate purinergic activation of contraction in the heart.

Tu-Pos51

PHENAMIL-INDUCED POSITIVE INOTROPY IS PRODUCED BY A VOLTAGE-MEDIATED INDIRECT EFFECT ON SODIUM-CALCIUM EXCHANGE. (A. Guia, D. Bose and R. Bose) Dept. of Pharmacology, Univ. of Manitoba, Winnipeg, Manitoba, Canada, R3E 0W3.

Phenamil is an amiloride derivative that inhibits epithelial-type Na channels and cardiac inwardly rectifying potassium channels (I_{K1}) at concentrations that produce positive inotropy in canine ventricular tissue (EC50=59µM, Guia *et al*, *Biophys. J.*, **59**:422a, 1991). Phenamil inhibits I_{K1} and prolongs phase 3 of the action potential (AP) without affecting L-type calcium channels or outwardly rectifying potassium channels (Guia *et al*, *J. Pharmacol. Exper. Ther.*, **274**:649, 1995). The goal of this study was to determine the mechanism by which cytosolic Ca is increased by phenamil to produce positive inotropy. The sarcoplasmic reticulum was not required for the production of positive inotropy since cyclopiazonic acid (100µM) or ryanodine (100nM) did not reduce the inotropic effects of phenamil. Cytosolic pH, measured with BCECF, was unaffected by phenamil. Phenamil did not directly affect Na-Ca exchange as assessed by two successive rapid cooling contractures produced in unstimulated tissues. Since Na-Ca exchange is dependent on the repolarization phase of the AP for its electrochemical driving force, the prolongation of this phase reduces the driving force for the exchanger resulting in reduced removal of cytosolic Ca by the exchanger and in positive inotropy. (Supported by MRC and HSFC)

Tu-Pos52

DIFFERENTIAL BASAL AND GLUCOCORTICOID-INDUCED EXPRESSION OF L-TYPE Ca^{2+} CHANNEL mRNAs IN RAT CARDIOVASCULAR TISSUES. ((K. Takimoto, A.F. Fomina, J.M. Nerbonne and E.S. Levitan)) Dept. of Pharmacology, Univ. of Pittsburgh, Pittsburgh, PA 15261.

Dihydropyridine-sensitive voltage-gated (L-type) Ca^{2+} channels play a central role in cardiac and smooth muscle excitation-contraction coupling. Expression of the α_{1C} and α_{1D} gene transcripts that encode pore-forming subunits of L-type channels was separately measured with RNase protection assays. Rat α_{1D} mRNA is found in lung, aorta and atrium, but not in ventricle, while α_{1C} mRNA is seen in all of these tissues. Expression of α_{1C} mRNA, but not α_{1D} mRNA, is up-regulated by glucocorticoid hormones in atrium and ventricle. This up-regulation of channel mRNA is also observed in GH_3 pituitary cells, and is blocked by the glucocorticoid antagonist RU 38486. In contrast, α_{1C} mRNA levels were glucocorticoid-insensitive in lung and aorta. Finally, RT-PCR analysis of α_{1D} transcript suggests that atrial channel mRNA may be tissue-specifically spliced. Thus, expression of the two L-type Ca^{2+} channel α_1 subunit mRNAs is tissue-specific and is differentially controlled by glucocorticoids.

Tu-Pos53

DISTRIBUTIONS OF "CA^{2+} SPARKS" IN RAT VENTRICULAR CARDIOMYOCYTES RECORDED WITH RAPID CONFOCAL MICROSCOPY. ((L. Cleemann, G. DiMassa, and M. Morad)) Inst. Cardiovascular Sci. and Dept. Pharmacol., Georgetown Univ. Med. Ctr, Washington, DC 20007.

"Ca^{2+}-sparks" in cardiomyocytes, implied based on confocal microscopy performed in the line scan mode, are thought to represent local, quantal Ca^{2+} releases by single or clustered DHP-/ryanodine-receptor complexes. The local build up of Ca^{2+} in "μ-domains" is supported also by the finding that Ca^{2+} signaling remains intact when global intracellular $[Ca^{2+}]$ is strongly buffered (Adachi-Akahane, Biophys. J., present issue). To examine the "Ca^{2+} sparks" in greater detail we used an acousto-optically steered, confocal laser microscope (Noran Instruments) to measure two dimensional Ca^{2+} distribution (fluo-3AM) at rates up to 480 frames per second. The myocytes were activated by zero or high K^+, high Ca^{2+} or caffeine and were studied also during spontaneously occurring Ca^{2+} overload. The patterns of activation included: a) synchronous activation throughout the cell, b) regularly repeated propagated wave fronts originating from single or multiple foci, c) aborted waves and d) irregular waves propagated in complicated patterns without interruption. Localized, brief Ca^{2+} transients, identified as "Ca^{2+} sparks," were seen especially in cells during Ca^{2+} overload. "Ca^{2+} sparks" increased in frequency prior to appearance of propagated waves and were absent following the wave, suggesting they are produced only when the SR is fully loaded with Ca^{2+}. These results show that rapid, two-dimensional recording of "Ca^{2+} sparks" is feasible and can be quantified to provide critical mechanistic information about signaling of Ca^{2+} release. Supported by NIH HL16152.

Tu-Pos54

VISUALIZATION OF CALCIUM SPARKS IN RAT CARDIAC CELLS BY VIDEO FLUORESCENCE MICROSCOPY. ((I. Parker and W.G. Wier)) University of Maryland at Baltimore, 655 W. Baltimore St. Baltimore, MD 21201.

Calcium sparks are localized calcium transients occurring at rest and during depolarization in cardiac muscle cells. Sparks are usually observed with line-scan confocal microscopy, but we show here that wide-field video fluorescence microscopy can also provide good resolution of sparks and has the major advantage of permitting rapid sampling throughout a large fraction of the cell (as opposed to 10^{-12}liter, as typical in confocal line-scanning). Myocytes were loaded with fluo-3 by incubation with 10 μM fluo-3/AM for 1 hour, and fluorescence images were recorded using an intensified CCD camera fitted to an inverted microscope equipped with a 60X oil immersion objective (NA 1.4, Nikon). A high proportion of cells showed spontaneous sparks, at frequencies from <1 /cell/s to >10 /cell/s, and localized flurries of sparks sometimes gave rise to abortive or propagating calcium waves. Sparks appeared both as bright, sharply localized signals and also as fainter, more diffuse fluorescence signals. To characterize the sparks, average fluorescence intensity within a 1μm^2 area of the image was measured. The sharply resolved sparks were about 10% of the amplitude of stimulated $[Ca^{2+}]_i$-transients, rose to a peak within 1 video frame and decayed with half-times of 30-200 ms. Following spontaneous waves and evoked action potentials the frequency of sparks as strongly reduced for several seconds but their mean amplitude was only depressed slightly. Support: HL29743 (W.G.W.) and GM48071 (I.P.).

Tu-Pos55

DIFFUSION AND SR Ca TRANSPORT BOTH CONTRIBUTE TO THE DECLINE OF $[Ca]_i$ DURING Ca SPARKS. *((A.M. Gómez, H. Cheng, W.J. Lederer and D.M. Bers)) Depts of Physiol, Univ Maryland, Baltimore and Loyola Univ Chicago*

The time-course of decay of local $[Ca^{2+}]_i$ elevations (Ca^{2+} sparks) is faster than the global decline of $[Ca^{2+}]_i$ during a normal depolarization-activated $[Ca^{2+}]_i$ transient. While the decay rate of the later is due primarily to cytosolic Ca^{2+} removal by the SR Ca-ATPase and Na^+/Ca^{2+} exchanger, the decay of local $[Ca^{2+}]_i$ during the Ca^{2+} spark may also involve diffusion. The aim of this study was to evaluate the contribution of the SR Ca^{2+}-pump to the kinetics of Ca^{2+} decline during Ca^{2+}-sparks. Experiments were carried out in isolated cardiac rat myocytes, using the fluorescent Ca^{2+} indicator fluo-3 and a laser scanning confocal microscope. Ca^{2+}-sparks before and after the blockade of the SR Ca^{2+} ATPase by 5μM thapsigargin (TG) were examined in 0 Na^+, 0 Ca^{2+} to block the Na^+/Ca^{2+} exchanger. The spark frequency was diminished up to a 28% of the control level. The amplitude of the calcium spark (peak florescence normalized to the base fluorescence) was not modified ((mean±SEM) control: 1.7±0.1, n=20, and after TG: 1.6±0.1, n=10, p=N.S.). But, the time constant of $[Ca^{2+}]_i$ decay was slowed ((mean±SEM) control: 20.6±1.7 ms, n=20; after TG: 33.3±5.7 ms, n=10, p<0.02), while remaining much faster than the decay of the global $[Ca^{2+}]_i$ transient. The figure shows representative traces of the decay of $[Ca^{2+}]_i$ transients due to Ca^{2+}-sparks before and after TG and the decline of the depolarization -activated global $[Ca^{2+}]_i$ transient. We conclude that while Ca^{2+}-diffusion is the main process in the decline of the local $[Ca^{2+}]_i$ during the spark, Ca^{2+} transport by the SR makes a significant contribution.

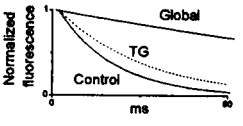

Tu-Pos56

Calcium gradients underlying excitation-contraction coupling in atrial myocytes

((J. Hüser, S. L. Lipsius and L. A. Blatter)) Loyola University Chicago, Stritch School of Medicine, Department of Physiology, Maywood, IL 60153, USA

Ca^{2+} release from the sarcoplasmic reticulum (SR) via the Ca^{2+}-induced Ca^{2+} release (CICR) mechanism is a crucial step in e-c coupling in cardiac cells. Ultrastructural and immunohistochemical studies suggest that in mammalian atrial cells, which lack a transverse-tubular network, the SR is in close proximity to the surface membrane. Besides these 'peripheral couplings' there is evidence for additional SR subcompartments not in contact with the sarcolemmal membrane ('corbular SR'). However, the presence of ryanodine receptors in corbular SR suggests that these stores are capable of participating in CICR. Using confocal imaging in combination with the Ca^{2+}-sensitive fluorescent probe fluo-3 we studied the spatial properties of electrically evoked $[Ca^{2+}]_i$ transients in cat atrial myocytes. In response to electrical stimulation Ca^{2+} release was detected first in the cell periphery. Subsequently, the elevation of $[Ca^{2+}]_i$ propagated towards the cell center probably by CICR from release sites located in central regions of the myocyte. Blocking SR Ca^{2+} release by preincubation of cells with ryanodine (50 μM) unmasked spatial $[Ca^{2+}]_i$ gradients associated with Ca^{2+} influx alone. $[Ca^{2+}]_i$ increased faster and to higher levels at the cell periphery than in the center. Under conditions known to induce Ca^{2+} overload ($[Ca^{2+}]_o$ = 10 mM), we observed localized $[Ca^{2+}]_i$ transients characteristic of Ca^{2+} sparks. The frequency of these Ca^{2+} sparks was higher at the periphery than in the center. In contrast, when the overall Ca^{2+} load was low, Ca^{2+} release was restricted to the subsarcolemmal space without further propagation toward the cell center. Progressive loading of the SR during a positive staircase led to increased subsarcolemmal release and increased propagation of release towards the cell center. It is concluded that in atrial myocytes there are two functionally different populations of Ca^{2+} stores which exhibit properties proposed for 'peripheral coupling SR' and 'corbular SR'. These stores differ with respect to the Ca^{2+} release mechanism as well as the kinetics of Ca^{2+} loading and are responsible for the local $[Ca^{2+}]_i$ gradients during e-c coupling in atrial myocytes.

Tu-Pos57

CALCIUM SPARK FREQUENCY IS AFFECTED BY $[Ca]_i$, SR Ca LOAD AND REST IN VENTRICULAR MYOCYTES. ((H. Satoh, L.A. Blatter, and D.M. Bers)) Department of Physiology, Loyola University Chicago, Maywood, IL 60153

Post-rest potentiation of twitches in rat and rabbit ventricular myocytes can be observed without a measurable change in the SR Ca content or trigger Ca. It was suggested that the availability of the SR Ca release channel is transiently depressed after a twitch and gradually recovers over several sec. Here we explore this issue at the microscopic level using confocal fluorescence microscopy, isolated rat and rabbit ventricular myocyte and the Ca indicator fluo-3 to measure local spontaneous increases of $[Ca]_i$ attributed to SR Ca release (Ca sparks). After an electrically evoked twitch in rat myocytes the frequency of Ca sparks increases over several sec to reach a steady state ($t_{1/2}$ ~8s). This increase in spark frequency in rat was converted to a rest-dependent decrease in spark frequency by enhancing Ca extrusion via Na/Ca exchange in Ca-free solution (which slowly depletes SR Ca). A similar rest-dependent decrease in spark frequency and SR Ca load was observed in rabbit myocytes under control conditions. When this rest decay of SR Ca in rabbit was prevented by Na-free, Ca-free solution (to block Na/Ca exchange) an increase in resting spark frequency as in control rat was observed. Since $[Ca]_i$ did not increase during the rest, this increase in spark frequency cannot be attributed to Ca_i-dependent activation. The increase in spark frequency could be due to either a slow (and undetectable) increase in SR Ca or a slow recovery of the SR Ca release channel from inactivation or adaptation. The decrease in spark frequency as SR Ca content declines can be seen even at times when $[Ca]_i$ is not changing, suggesting that spark frequency is also affected by intra-SR Ca load. Thus resting Ca spark frequency can be increased by increases in either $[Ca]_i$, SR Ca load or rest period after a twitch.

Tu-Pos58

MODULATION OF SPATIAL AND TEMPORAL CHARACTERISTICS OF CALCIUM SPARKS: EFFECTS OF BAYK 8644, CAFFEINE AND RYANODINE. ((H. Satoh, D.M. Bers, and L.A. Blatter)) Department of Physiology, Loyola University Chicago, Maywood, IL 60153

The L-type Ca channel agonist BayK 8644 (BayK) has been shown to increase Ca leak from the SR at rest. The visualization of local increase in cytosolic Ca concentration ($[Ca]_i$) called "Ca sparks" has enabled us to investigate the elementary events of Ca leak from the SR. In this study, the effects of BayK, caffeine and ryanodine on the frequency and the spatial and temporal properties of individual Ca sparks were investigated in ferret ventricular myocytes with laser scanning confocal microscopy and the fluorescent Ca indicator fluo-3. The frequency of Ca sparks was studied during the 20 sec interval of rest following interruption of electrical stimulation. BayK (0.1 μM) increased the spark frequency approximately threefold but did not change the spatial and temporal characteristics of individual sparks. The increase in spark frequency by BayK was suppressed by the addition of nifedipine (10 μM), but was not affected by the perfusion with Ca-free solution (10 mM EGTA), suggesting that BayK acts at sarcolemmal Ca channels but the effect is not mediated by increased Ca influx. Low concentration of caffeine (0.5 mM) increased both the frequency and the duration of individual sparks. Ryanodine (0.1 μM) produced long-lasting localized increases of $[Ca]_i$, reflecting the continuous opening of SR Ca release channels. These data suggest that BayK may activate Ca leak from the SR at rest through a putative functional linkage between the sarcolemmal and the SR Ca channels while caffeine and ryanodine act directly on the SR release channels.

Tu-Pos59

THE PROBABILITY OF Ca^{2+} SPARK OCCURRENCE IN HEART MUSCLE DEPENDS ON THE SQUARE OF THE UNITARY L-TYPE Ca^{2+} CHANNEL CURRENT. ((L.F. Santana, A. M. Gómez, Heping Cheng, Mark B. Cannell, and W.J. Lederer)) Dept. of Physiology, School of Medicine, Univ. of Maryland at Baltimore. (Spon. by L.F. Santana)

We performed experiments to determine how sarcoplasmic reticulum (SR) Ca^{2+}-release channels are recruited by sarcolemmal L-type Ca^{2+} channels during excitation-contraction (EC) coupling in rat ventricular myocytes. Changes in cytosolic $[Ca^{2+}]$ were monitored in fluo-3-loaded myocytes using a confocal microscope with whole-cell voltage clamp. This approach allowed us to simultaneously record single SR Ca^{2+} release events (Ca^{2+} sparks) and membrane currents. In order to quantify Ca^{2+} sparks during incremental 10 mV steps between -40 and 50 mV the Ca^{2+} channel blocker nifedipine (1μM) was used. To assure a constant level of nifedipine blockade and SR Ca^{2+} load, four conditioning pulses to 0 mV were applied prior to each test pulse. The voltage dependence of I_{Ca} and of Ca^{2+} sparks had the archetypal bell-shape curve but differed in their position in the voltage axis. We found that over this voltage range the ratio of the probability of spark occurrence (P_s) to the whole cell I_{Ca} (P_s/I_{Ca}) is virtually identical to the voltage dependence of ion permeation through a single L-type Ca^{2+} channel, thus suggesting that P_s depends on $(i_{Ca})^2$. We designed an additional series of experiments intended to investigate the relationship between the activation of L-type Ca^{2+} channels and the subsequent recruitment of Ca^{2+} sparks without the intervention of nifedipine. We applied 2 mV steps in the range of -48 to -28 mV. Our results show that for cells with normal SR Ca^{2+} load, P_s and I_{Ca} have an e-fold increase every 7.15 ± 0.15 mV and 7.31 ± 0.15 mV (n=16) respectively. The similarity between these slopes suggest that when a single SR Ca^{2+} release unit is activated by depolarization, a single L-type Ca^{2+} channel is responsible for the activating Ca^{2+} influx.

Tu-Pos60

FACTORS SHAPING THE CONFOCAL IMAGE OF THE CALCIUM SPARK IN CARDIAC MUSCLE CELLS ((V. R. Pratusevich, C. W. Balke, and W. G. Wier)) University of Maryland at Baltimore, MD 21201

Local calcium transients (LCTs, or calcium sparks) are fundamental events in cardiac excitation-contraction coupling, and are typically evaluated by confocal microscopic imaging of fluorescent Ca^{2+} -indicators (fluo-3). To characterize correctly the spatio-temporal features of calcium sparks, as derived from confocal line-scans, we have developed a theoretical model combining simulation of the release (from SR), diffusion, binding and uptake of Ca^{2+}, with simulation of image formation in our confocal microscope. An appropriate (i.e. inside a living cell) 3D point-spread function (PSF) was measured by imaging fluorescent beads (0.1 μm in diameter) which had been phagocytized by an alveolar macrophage. Convolution of the bound fluo-3 (to Ca^{2+}) with the PSF produced hypothetical 3-D calcium sparks. Frequency distributions were calculated for the spark image parameters (peak amplitude, time-constants of rise and fall) in two cases: 1) when the position of the scan-line was fixed, and sparks arose at other sites in the cell, and 2) when one spark was imaged from all the possible scan lines. In general, these frequency distributions are not normal (Gaussian) because of the contributions of a large number of 'out-of-focus' calcium sparks, and because sparks arise only at the t-tubule SR junctions (rather than from all possible spatial locations). Blurring by the confocal microscope and diffusion of Ca^{2+} thus results in a substantial uncertainty in the estimation of characteristics of calcium sparks. HL29473.

Tu-Pos61

THE ROLE OF LOCAL EVENTS AND DIFFUSION IN CARDIAC EC-COUPLING ((C. Amstutz, A. Michailova, E. Niggli)) Dept. of Physiology, University of Bern, Switzerland.

Our aim is to model and understand the control of Ca release from the sarcoplasmic reticulum as well as the subcellular diffusion of Ca in cardiac muscle. Mathematical models of Ca diffusion in the subsarcolemmal space and in the cytosol were developed. On the molecular level, we simulate the interactions of a single L-type Ca channel and SR Ca release channels in the junctional local environment. On the cellular level, the model is based on a simplified 3-dimensional sarcomere and includes a restricted subsarcolemmal and nonrestricted cytosolic space as well as the SR and a myofibrillar space with Ca buffers (calsequestrin, calmodulin, troponin C). Since the Ca transient originates in the junctional restricted space between sarcolemma and SR, and the curvature of this cleft does not significantly affect the diffusion, the geometric boundary conditions for this space are two infinite planes. Both analytical and numerical solutions of the diffusion equation were derived. The results show that in the cleft the situation is fundamentally different from an unrestricted hemisphere. In the cleft, an asymptotic steady-state Ca distribution does not exist during opening of a single L-type Ca channel. Therefore, the Ca concentration continues to increase during the open time of a channel. This time-dependence of [Ca] in the cleft may provide a mechanism for a variable delay in the Ca signal transmission. More importantly, the open-time of a particular Ca channel may be crucial for the local [Ca] and for the generation of elementary events in EC-coupling (e.g. Ca sparks). (Supported by SNF)

Tu-Pos62

CALCIUM RELEASE FROM THE SR CAUSED BY SPONTANEOUS OPENING OF CA^{2+} CHANNEL IN RAT VENTRICULAR MYOCYTES. ((S. Adachi-Akahane, L. Cleemann, and M. Morad)) Dept. Pharmac. & Inst. for Cardiov. Sciences, Georgetown Univ. Med. Ctr., Washington, DC 20007. (Spon. by N. Briggs)

Ca^{2+}-influx through L-type Ca^{2+} channel has been shown to be the primary pathway for triggering Ca^{2+} release from the SR in ventricular myocytes. If so, spontaneous opening of the Ca^{2+} channel could cause local release of Ca^{2+} from the SR. In order to explore this idea, we examined Ca^{2+}-release from the SR at membrane potentials sub-threshold for activation of Ca^{2+} channel (-90 to -50 mV). Simultaneous recording of membrane current and Fura-2 signal were conducted using single rat ventricular myocytes dialyzed with 2mM Fura-2. We found that not only basal $[Ca^{2+}]_i$ increased slowly by depolarization from -90mV to -60mV, but also I_{Ca}- or caffeine-gated Ca^{2+} release were larger when activated from -90 compared to -60mV, consistent with partial depletion of Ca^{2+} content of SR at -60mV. The rise in basal $[Ca^{2+}]_i$ upon depolarization from -90 to -60mV was suppressed by the addition of 0.1mM Cd^{2+} or equimolar replacement of extracellular Ca^{2+} by Ba^{2+}, suggesting increased open probability of Ca^{2+} channel at -60mV may mediate the response. (-)BayK8644 (1μM) further increased the basal $[Ca^{2+}]$ at -60mV, but had little or no effect at -90mV. Prolonged exposures to caffeine and thapsigargin abolished the slow rise in $[Ca^{2+}]_i$ at -60mV. These results indicate that opening of the Ca^{2+} channel, even at sub-threshold voltages, lead to stochastic local Ca^{2+} releases, thus, significantly altering the Ca^{2+} content of the SR. Supported by NIH HL16152.

Tu-Pos63

CALCIUM SPARKS OCCUR AT THE JUNCTION OF THE SARCOPLASMIC RETICULUM (SR) AND THE TRANSVERSE TUBULES (T-TUBULES) IN HEART **((M.R. Lederer, A.M. Gómez, H. Cheng and W.J. Lederer)) Dept. Physiol, Univ Maryland Sch. Med. and Med. Biotechnology Center, Baltimore MD, USA**

Ca^{2+} sparks in heart muscle cells are local increases in $[Ca^{2+}]_i$ that are due to elementary SR Ca^{2+} - release events (Cheng, et al. *Science* **262**, 740,1993; Cannell et al *Science* **268**,1045, 1995). The Ca^{2+} -sparks arise as ryanodine receptors (RyR) open spontaneously or are triggered to open by the Ca^{2+} -influx of sarcolemmal L-type Ca^{2+} channels. Extracellular markers were used to locate the t-tubules within heart muscle cells, differential interference contrast (DIC) microscopy was used to locate Z-lines of heart muscle cells while simultaneous location of Ca^{2+} -sparks was possible using the Ca^{2+} -sensitive indicator, fluo-3. A laser-scanning confocal microscope was used to limit the plane of view to a thickness of about 0.8 μm. We used cells isolated from healthy Sprague-Dawley rat hearts by standard methods. The imaging reveals that the majority of both spontaneous and triggered Ca^{2+} -sparks observed in ventricular myocytes occur very close to the t-tubules and at the Z-lines. Furthermore, during Ca^{2+} -overload, the spontaneous Ca^{2+} -sparks that occur with increased frequency also occur at the t-tubules as do the Ca^{2+} -sparks that initiate propagating waves of increased $[Ca^{2+}]_i$ (i.e. "Ca^{2+} waves"). Finally, the elementary Ca^{2+} -release events that sustain the propagating Ca^{2+} waves also occur at the t-tubules as suggested by Cheng, Lederer & Cannell, *Am. J. Physiol.* 1995, In Press. This work supports the earlier findings of diverse groups that the majority of RyRs are located very close to t-tubules and Z-lines in mammalian cardiac ventricular myocytes and provides support for the functional coupling between the sarcolemmal Ca^{2+} channels and the RyRs during normal excitation-contraction coupling.

This work was supported by the NIH and the Spanish Ministry of Education and Science. MRL was a Claude Bernard research fellow.

Tu-Pos64

CYCLIC ADP-RIBOSE AND Ca^{2+}-SPARK ACTIVITY AND CALCIUM-INDUCED CALCIUM RELEASE (CICR) IN HEART CELLS. **((T. Shioya, L.F. Santana, A.E. Ruoho, J. Cleary, W.J. Lederer)) Dept. Physiology, Univ. Maryland Sch. Med. and Med. Biotechnology Center, Baltimore MD, USA and Dept. Pharmacology, Univ. Wisconsin Sch. Med., Madison, WI, USA**

Cyclic ADP-ribose (cADPr), an intermediate metabolite of NAD^+, has been shown to alter Ca^{2+} signaling in heart and other tissues. Because it is readily available inside the cell and because its concentration can be modulated by multiple means, cADPr has been considered to be a candidate "endogenious modulator" of Ca^{2+}-release from intracellular Ca^{2+} stores in many cell types. We examined the effect of cADPr on $[Ca^{2+}]_i$ dynamics in rat ventricular myocytes using the whole cell patch-clamp method. The $[Ca^{2+}]_i$ level was simultaneously monitored using fluo-3 and a laser-scanning confocal microscope. SR Ca^{2+}-release was examined using Ca^{2+}-sparks as an indicator of elementary release events (see Cheng, et al. Science 262:740, 1993; Cannell et al ibid. 268:1045, 1995). We examined the action of cADPr by introducing it into the cell by the patch-clamp pipette. Changes in cADPr could be made using the internal perfusion technique (see Soejima & Noma Pflugers Arch 400:424, 1984). Application of cADPr to the intracellular compartment produced complex actions on Ca^{2+}-spark occurrence. We will discuss our findings in terms of modern excitation-contraction coupling theory. **Supported by the NIH and the Maryland affiliate of the American Heart Association.**

Tu-Pos65

ELEMENTARY EVENTS OF I_{NA}- AND I_{CA}-TRIGGERED EC-COUPLING

((E. Niggli and P. Lipp)) Dept. Physiology, University of Bern, Switzerland (spon. by A. Azzi)

In cardiac myocytes the trigger for SR Ca release is a Ca influx across the sarcolemma. Ca current via L-type Ca channels serves as the main trigger, but a possible contribution of the Na/Ca exchange is discussed. While there is evidence that reverse mode Na/Ca exchange is able to generate tonic contractions on the time-scale of seconds, we investigated the possible contribution of this pathway in the millisecond time-domain since it may be important during early steps in cardiac ec-coupling. The intracellular Ca concentration was recorded with a confocal microscope in patch-clamped guinea-pig ventricular myocytes. While the I_{Ca} triggered SR Ca release events were subcellularly homogeneous, I_{Na} induced release was occasionally accompanied by subcellularly localized Ca transients ("Ca sparks"). These non-uniformities during I_{Na} were characterized by a surge of low-frequency components in a power spectral analysis. Application of verapamil (5 µM) resulted in a partial inhibition of I_{Ca}. The I_{Ca} induced Ca transients now also showed Ca sparks, while the I_{Na} triggered Ca release became completely homogeneous. Thus, in the absence of verapamil partial loss of voltage control resulted in occasional openings of L-type Ca channels during I_{Na}. These openings trigger Ca sparks that could be identified on top of the release induced by I_{Na} via reverse mode Na/Ca exchange. Based on these spatial properties we were able to distinguish between the two Ca influx pathways that could trigger Ca release. Thus spurious activation of Ca channels does not contribute to I_{Na} induced Ca release. This finding further supports the importance of reverse-mode Na/Ca exchange during early steps in cardiac ec-coupling. (Supported by SNF).

CARDIAC EXCITATION

Tu-Pos66

SWELLING-INDUCED CHLORIDE AND POTASSIUM CURRENTS IN CAT VENTRICULAR MYOCYTES. ((Ramesh Gopal and Robert E. Ten Eick)) Dept. of MPBC, Northwestern University, Chicago, IL 60611.

Cardiac myocyte swelling occurs during a variety of pathological processes. However, neither its mechanism nor implications are well understood. We have found that osmotic swelling causes an outward current (I_{Swell}) in feline ventricular myocytes which appears to consist of two components. Under K^+-free conditions, i.e. K^+ omitted in the external solution and internal K^+ replaced with Cs^+, the osmotically-induced current reverses within 5 mV positive to the Nernst potential for Cl^-. In Cl^--free solutions, I_{Swell} appears to be carried by K^+. The Cl^--dependent component can be inhibited by DIDS and the K^+-dependent component by internally applied TEA (10 mM). An outward current with similar characteristics can be induced with positive intracellular baropressure (2-5 cmH_2O) applied to the patch pipette. This particular K^+ and Cl^--dependent swelling-induced current has not been previously described. It is expected to alter both the resting potential and the action potential of myocardial cells and could influence the rhythmicity of the diseased, pathological heart.

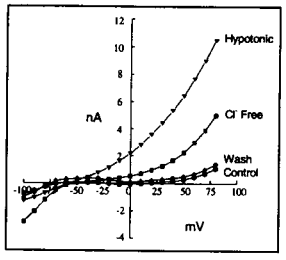

Tu-Pos67

PHOSPHOLEMMAN CHANNEL ACTIVITY RECONSTITUTED FROM CARDIAC SARCOLEMMAL VESICLES ((Zhenhui Chen, J. Randall Moorman, Larry R. Jones)) Indiana University, Indianapolis, IN; University of Virginia, Charlottesville, VA.

Phospholemman (PLM), a 72 amino acid protein with single transmembrane domain, forms ion channels in lipid bilayers. PLM was previously characterized as a recombinant protein expressed and purified from Sf21 insect cells. Here we purified PLM from canine cardiac sacolemmal vesicles, and analyzed its channel activity in planar bilayers. Natural and recombinant PLM exhibited indistinguishable channel activity. Both proteins showed multiple conductance states, cationic/anionic conductance switching, and voltage-dependent closing at extreme membrane potentials. The figure shows the I-V relationship of natural PLM in 200mM:50mM KCl solutions analyzed over 10 second voltage ramp from -100mV to +100mV. The existence of both negative and positive reversal potentials during a single voltage ramp is indicative of cation- and anion-selective conductance switching. Thus, cardiac sarcolemmal PLM, like recombinant PLM, behaves as an ion channel exhibiting complex modes of ionic conductance.

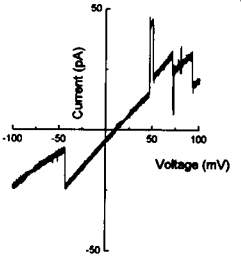

Tu-Pos68

4-AMINOPYRIDINE AND CHOLINE CHLORIDE ACTIVATE THE ACETILCHOLINE INWARD RECTIFYING POTASSIUM CURRENT IN A VOLTAGE- AND TIME-DEPENDENT WAY *. **((R.A. Navarro-Polanco and J.A. Sanchez-Chapula)) CUIB, Universidad de Colima, Apdo. Postal 199, Colima, Col., 28000, Mexico.**

The efects of 4-aminopyridine (4-AP) 1 mM, choline chloride (ChCl) 10 mM and carbachol 0.3 µM were studied in adult cat atrial myocytes using the whole cell and single channel analysis of the patch clamp technique. 4-AP and ChCl produced and increase in a background potassium current and induced a delayed rectifying-like outward potassium current. Carbachol as previously found, activated in a time-independent way the actilcholine inward rectifying potassium current or $I_{K(ACh)}$. In cell attached experiments, using a potassium concentration of 145 mM in the pipette, we found that 4-AP, ChCl and carbachol applied in the pipette solution activated potassium channels that show inward rectification, conductances of 41, 41.9 and 42.3 pS respectively. The open time was 176 µs with 4-AP, 186 µs with ChCl and 162 µs with carbachol. In experiments using a two pulses protocol, from an HP of -80 mV, depolarizing pulses to potentials between -30 and +50 mV of 2.5 s of duration were applied and back to -80 mV for 2.5 s. During the depolarizing pulses the openings were scarcely visible, because of the strong inward rectification of the channel. In the presence of 4-AP and ChCl in the pipette, when membrane potential was repolarized to -80 mV, the open probability increased mainly at the beginning of the pulse, decreasing with time. The open probability of the channel during the repolarizing pulse to -80 mV increased as the voltage of the depolarizing pulse was increased. This results suggest that 4-AP, ChCl and carbachol activate $I_{K(ACh)}$. However, 4-AP and ChCl activate the channel in a voltage- and time-dependent manner. Supported by CONACYT, Mexico*.

Tu-Pos69

POTASSIUM AND CALCIUM CURRENTS IN REMODELED RAT VENTRICULAR MYOCYTES FOLLOWING EXPERIMENTAL MYOCARDIAL INFARCTION. **((D. Qin, Z-H. Zhang, P. Jain, V. Battula, M. Boutjdir and N. El-Sherif))** ***SUNY Health Science and VA Medical Centers, Brooklyn, NY 11209.*** **(Spon. by N. El-Sherif)**

Left ventricular remodeling following myocardial infarction is associated with hypertrophy of non-infarcted myocardium and electrophysiological alterations. Whole-cell patch-clamp techniques were used to characterize the transient outward K^+ current (I_{to}) and L-type Ca^{2+} current (I_{Ca-L}) in remodeled left ventricular cells of rats 3 to 5 weeks post-infarction (PI). Results were compared with sham-operated rats (S). Membrane capacitance of S cells was 126±38 pF (n=50) vs 210±52 pF (n=60) of PI cells, $P<0.001$. Action potential duration (APD) at 1 Hz was prolonged in PI cells. APD_{50} and APD_{90} were 22.2±5.6 and 56.2±8.9 ms in S cells (n=9) compared with 37.8±5.1 and 134.0±28.0 ms in PI cells (n=8), $P<0.001$. Two components of I_{to}, fast component (I_{to-f}) and slow component (I_{to-s}), were detected in both S and PI cells. Amplitudes of I_{to-f} and I_{to-s} had no obvious changes, but the current densities were significantly lower in PI cells. Density of I_{to-f} = 21.4±4.0 in S (n=14) vs 13.0±5.1 pA/pF in PI cells (n=28) at +60 mV, $P<0.001$, and density of I_{to-s} = 4.9±1.9 in S vs 3.4±0.8 pA/pF in PI cells, $P<0.01$. There were no apparent alterations in steady-state activation and inactivation of I_{to-f} and I_{to-s}. Although the amplitude of I_{Ca-L} was 57% larger in PI cells (2.2±0.7 nA) than that in S cells (1.4±0.4 nA, $P<0.01$), the density of I_{Ca-L} was same in both cells (9.6±2.6 in PI, n=11, vs 9.5±2.9 pA/pF in S cells, n=15, $P=0.959$). No change in steady-state inactivation of I_{Ca-L} was found. We conclude that the density of both I_{to-f} and I_{to-s} is decreased while the density of I_{Ca-L} is unchanged in remodeled PI left ventricular cells. The changes in I_{to-f} and I_{to-s} may explain the prolongation of APD in these cells and may contribute to arrhythmogenecity of post-infarction remodeled myocardium. (*Data were expressed as mean±SD.)

Tu-Pos70

MinK-induced outward currents in *Xenopus* oocytes recorded with the macropatch technique.

H Musa, SM Taffet*, M Delmar, J Jalife & JMB Anumonwo. Dept of Pharmacology, and Dept. of Microbiology & Immunology* SUNY HSC. Syracuse, NY.

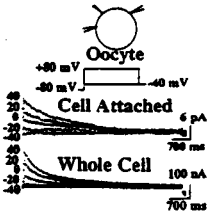

The slowly activating K+ current (I_{sK}) associated with minK expression has whole cell biophysical and regulatory properties similar to the delayed rectifier current I_{Ks}. We have determined the properties of macropatch I_{SK} in oocytes. Cells were injected with 100 ng murine minK mRNA and currents were recorded in the two electrode voltage clamp mode. A third electrode recorded from a localized patch of membrane (macropatch) in the cell attached mode. Depolarizing pulses were applied using the two electrode voltage clamp circuit. The Figure shows recording protocol and representative traces of I_{SK} tail currents recorded simultaneously in cell attached and whole cell configurations. Voltage-dependent activation properties recorded by the macropatch accurately reflected the behavior of the whole cell currents (n=4). Kinetics of current activation were also similar in whole cell and patch currents. Time constants of activation were 246 ± 81 msec (tau1) and 5133 ± 1579 msec (tau2) for whole cell, and 208 ± 69 msec and 2607 ± 681 msec (mean±SD) respectively for patch currents, (n=4). Phorbol 12,13 didecanoate (PDD) inhibited whole cell and patch currents by 50% and 35%, respectively. These data show the feasibility of the macropatch technique for recording a small number of minK channels expressed in oocytes.

Tu-Pos71

EVIDENCE FOR AN INTRINSIC pH-SENSITIVE MECHANISM OF INWARD RECTIFICATION OF THE INWARD RECTIFIER K CHANNEL IRK1. ((R-C. Shieh, S.A. John, J-K. Lee and J.N. Weiss)) UCLA School of Medicine, Los Angeles, CA 90095.

Inward rectification of IRK1 channels has been attributed to voltage-dependent block by intracellular Mg and polyamines. Additionally, we present evidence for an intrinsic gating mechanism. In excised giant inside-out patches from oocytes expressing wild-type IRK1 channels, voltage-dependent inactivation of outward current persisted after prolonged (>5 min) wash in Mg-free, polyamine-free bath solution (100 KCl, 5 EDTA, 5 HEPES, pH 7.2). The time course of outward current was well-fit by two components: an inactivating component with two voltage-independent time constants (τ_1~750 ms, τ_2 ~100 ms), and a non-inactivating component (pedestal current) which was voltage-dependent ($V_{1/2}$ +30 mV, $z\delta$~4 in symmetrical 100 mM K), consistent with a serial 2 open state, one closed state gating model. Raising pH_i from 7.2 to 9.0 accelerated the inactivation rate (τ_1~400 ms, τ_2 ~60 ms) without affecting the voltage-dependence of the pedestal current. In contrast, block of outward IRK1 currents by Mg or polyamines was retarded at pH 9.0, making it unlikely that retention of these agents accounted for the residual inactivation process. The voltage dependence of the intrinsic gating process followed V_m-V_K rather than V_m, and was shifted in the negative direction in the IRK1 mutant D172N. This intrinsic gating process was absent in wild-type ROMK1. These results suggest that an intrinsic, pH_i-sensitive gating mechanism contributes to the inward rectification of IRK1.

Tu-Pos72

EVIDENCE FOR RAPID AND SLOW COMPONENTS OF DELAYED RECTIFIER OUTWARD K^+ CURRENTS IN HUMAN VENTRICULAR CELLS. ((G.-R. Li, J. Feng, L. Yue, M. Carrier and S. Nattel)) Montreal Heart Institute, University of Montreal, Montreal, Quebec, Canada H1T 1C8.

The delayed rectifier outward K^+ current (I_K) has been shown to have pharmacologically and kinetically distinct components, I_{Kr} (rapid I_K) and I_{Ks} (slow I_K). The present study was designed to determine whether the normal human ventricle contains corresponding components. The whole-cell voltage-clamp technique was used to study I_K in single myocytes enzymatically isolated from the right ventricle of three explanted human hearts with an isolation method designed to optimize the yield of cells expressing I_K. In the 35 cells studied, 33 cells showed a significant I_K tail (> 50 pA). Application of 5 μM E-4031 revealed that I_K in human ventricular cells was composed of E-4031 resistant and E-4031 sensitive components, with both components present in 32/33 cells and only E-4031 resistant current in 1/33. E-4031 sensitive currents activated rapidly with a half activation voltage ($V_{½}$) of -14±4 mV and a slope factor (K) of 7.7±2.7 mV, and showed inward rectification, while the E-4031 resistant component activated more slowly with a $V_{½}$ of 9.4±2.5 mV and K of 11.8±2.9 mV. The envelope of tails analysis showed a time-dependent change in ratio of $I_{K,tail}/I_{K,step}$ under control conditions. E-4031 eliminated time dependent changes in the ratio, indicating that the E-4031 resistant current was dominated by one component. The E-4031 resistant current was strongly suppressed by indapamide, which has been reported to block selectively I_{Ks}. E-4031 significantly increased action potential duration to 90% repolarization from 336±16 to 424±19 ms ($p<.01$) in five cells, indicating the functional importance of I_K. These results provide evidence that the human ventricle expresses both I_{Kr} and I_{Ks}, and that I_K is important in human ventricular repolarization.

Tu-Pos73

EXTRACELLULAR POTASSIUM MODULATES THE GATING, BUT NOT THE RECTIFICATION, OF THE RAPIDLY-ACTIVATING CARDIAC DELAYED RECTIFIER I_{Kr}. ((T. Yang, D.J. Snyders and D.M. Roden)) Vanderbilt University School of Medicine, Nashville, TN 37232.

Increasing extracellular potassium ($[K^+]_o$) unexpectedly increases the amplitude of the rapidly-activating cardiac delayed rectifier I_{Kr} in guinea pig myocytes and in oocytes expressing *HERG*. This effect might be attributable to changes in state transitions, permeation, or rectification. In these studies we have determined the effect of altering $[K^+]_o$ on I_{Kr} in AT-1 cells, derived from mouse atrium. As in other systems, E_{rev} was $[K^+]_o$-dependent and increasing $[K^+]_o$ increased I_{Kr}: after a 1 sec pulse to +20 mV, activating I_{Kr} was 2.5±0.4 pA/pF at 1 mM $[K^+]_o$ (±SE, n=16), 3.8±0.4 pA/pF at 4 mM $[K^+]_o$ (n=13), and 5.9±0.9 pA/pF at 20 mM $[K^+]_o$ (n=8). Increasing $[K^+]_o$ exerted a minimal effect on the kinetics of I_{Kr} activation (τ at +20 mV: 237±32 msec [4 mM] vs 201±31 [20 mM], n=6). In contrast, there was slowing of deactivation and of recovery from fast inactivation. Deactivation τ_{fast} was 62±5 vs 118±30 msec (-90 mV), deactivation τ_{slow} was 162±10 vs 318±16 msec, and $\tau_{recovery}$ (-120 mV) was 1.5±0.3 msec vs 3.4±0.4 msec. Increasing $[K^+]_o$ up to 60 mM did not alter I_{Kr} rectification, and evidence of fast inactivation ("hooks") actually became more prominent. The mechanism underlying I_{Kr} rectification is unlike that for the inward rectifier for two reasons: (1) we have previously shown that eliminating $[Mg^{2+}]_i$ does not alter I_{Kr} rectification; and (2) at $[K^+]_o$ 4-60 mM, the slope conductance below E_{rev} did not depend on $\sqrt{[K^+]_o}$, but was roughly constant (250-270 pS/pF). Thus (1) as in other systems, I_{Kr} in AT-1 cells is paradoxically increased by elevating $[K^+]_o$; (2) inward rectification and fast inactivation are both preserved at high $[K^+]_o$; (3) the data suggest that the $[K^+]_o$-dependent increase in activating current is determined by $[K^+]_o$-dependence of I_{Kr} state transitions.

Tu-Pos74

A REGULATORY EFFECT BY EXTRACELLULAR CATIONS ON IRK1 WHEN EXPRESSED IN *XENOPUS* OOCYTES ((J.M. Owen, R. Leach, C.C. Quinn, J.B.C. Findlay and M.R. Boyett.)) Departments of Physiology and Biochemistry & Molecular Biology, University of Leeds, UK

We have investigated the block of the inward rectifier IRK1 by the naturally occurring extracellular cations Mg^{2+}, Ca^{2+} and Na^+ and compared the block to that of Ba^{2+}. *Xenopus* oocytes were injected with IRK1 mRNA and 36 h later membrane currents were recorded using the two electrode voltage clamp technique. Recordings were made in solutions containing either 10 or 90 mM K^+; Na^+ was substituted by N-methyl D-glucamine. The cation affinity of IRK1 was quantified by measuring the K_d value (concentration required to decrease the current by 50%) at 0 mV. In 10 mM K^+ solution, the K_d values (in mM) were 8 ± 2 (Mg^{2+}), 21 ± 4 (Ca^{2+}), 0.026 ± 0.002 (Ba^{2+}) and 4532 ± 1167 (Na^+), with electrical binding distances (δ) of 0.11 ± 0.02, 0.08 ± 0.03, 0.37 ± 0.01 and 0.55 ± 0.05 respectively (mean ± SEM, n=5-7). In 90 mM K^+ solution, K_d increased to (in mM) 48 ± 6 (Mg^{2+}), 65 ± 10 (Ca^{2+}) and 0.14 ± 0.04 (Ba^{2+}) with no significant change in δ. These results show that the cations block IRK1 in a concentration and voltage dependent manner, and that Mg^{2+} and Ca^{2+} may both bind to a superficial site whilst Na^+ and Ba^{2+} bind to a deeper site. It is possible that Mg^{2+}, Ca^{2+} and Na^+ exert a significant blocking effect on IRK1 at normal physiological $[K^+]$ (~5 mM). *Supported by the British Heart Foundation.*

Tu-Pos75

COMPARISON OF REPOLARIZATION OF CELLS FROM DIFFERENT LAYERS OF MYOCARDIUM IN VITRO AND IN VIVO. ((E.A.Sosunov, E.P.Anyukhovsky, and M.R.Rosen)) Columbia University, New York, NY 10032.(Spon. by R.Robinson)

Previous microelectrode studies have described a unique population of cells (M cells) in the deep midmyocardium having long action potential durations (APD) and high maximum rates of phase 0 depolarization. We used standard microelectrode techniques to record APs in canine ventricular epicardial (EPI), endocardial (ENDO) and midmyocardial cells (M cells). We found that after an abrupt lengthening of cycle length (CL), the APD in M cells reached a new steady-state much faster than in EPI or ENDO: time to 90% of the new steady state ($t_{90\%}$) = 13.3±0.7 min (X±SEM) in ENDO, 12.8±1.1 min in EPI, and 2.6±0.4 min in M cells ($p<.05$ cf EPI or ENDO) when CL changed from .4 to 1 s. On transition from CL=.4 to 4 s, APD in M cells changed biphasically reaching a maximum at 3.8±0.3 min and then decaying to its steady state level. In contrast, EPI and ENDO APD increased monotonically. In situ, we used plunge and surface electrodes to register activation-recovery intervals (ARI) of bipolar electrograms obtained from different myocardial layers of the left ventricle in conditions of AV block and His-bundle pacing. At CL from .3 to 2 s, ARI were equal in all myocardial layers from EPI to ENDO. ARI coincided with APD of M cells recorded *in vitro* in the physiological range of CL from .3 to .7 s. When CL changed from .3 to 1 s, the ARI followed the time course typical of M cells *in vitro* ($t_{90\%}$ = 2.6±0.5, 2.5±0.4, and 2.3±0.4 min for EPI, 5 mm sub EPI, and ENDO, respectively). Thus, there is no difference in duration of repolarization among myocardial layers in the intact canine heart: all cell layers are similar to M cells *in vitro*, rather than EPI or ENDO *in vitro*.

Tu-Pos76

THE NOVEL CARDIOPROTECTIVE AGENT BMS-180448 ACTIVATES A POTASSIUM CONDUCTANCE IN CARDIAC AND VASCULAR SMOOTH MUSCLE. ((N.J. Lodge and M.A. Smith)) Bristol-Myers Squibb Pharmaceutical Research Institute, Princeton, NJ 08543.

Exposure of voltage-clamped guinea pig ventricular myocytes to the novel cardioprotective agent BMS-180448 (300 μM) produced an inhibition of I_K followed by the delayed (5.5 ± 0.5 min) activation of a large time-independent potassium current. At 100 μM, BMS-180448 produced only inhibition of I_K. The BMS-180448 activated current was refractory to block by 30 μM glyburide but was largely inhibited by 100 μM alinidine (84 ± 6 % inhibition at +40 mV). Cromakalim (100 μM)-activated currents were fully inhibited by 3 μM glyburide and 79 ± 4 % blocked by 100 μM alinidine. The current responses to BMS-180448 were unaffected by the inclusion of 10 mM UDP in the pipette. BMS-180448 (100 μM) also increased ^{86}Rb efflux from rabbit ventricular muscle slices. The increased efflux was enhanced in solutions containing low calcium. Additionally, BMS-180448 produced a concentration-dependent increase in ^{86}Rb efflux from aortic strips; efflux responses were increased in low calcium medium and fully antagonized by 3 μM glyburide. Thus, BMS-180448 activates a potassium conductance in both cardiac and smooth muscle. The cardioprotective action of BMS-180448 is observed at 1-30 μM. If the BMS-180448 evoked potassium conductance underlies this effect, we must assume that only a small fraction of BMS-180448 sensitive potassium channels need to be open in order to confer protection and/or that the conditions encountered during ischemia enhance the potency of the drug. Inhibition of I_K may also play a role in the observed cardioprotection.

Tu-Pos77

Regulation of HERG-Induced Current (I_{Kr}) by Protons

J Horta, SM Taffet*, M Delmar, J Jalife & JMB Anumonwo. Dept. of Pharmacology, and the Dept. of Microbiology & Immunology* SUNY HSC, Syracuse, NY.

We have studied the proton regulation of I_{Kr} induced by the human ether-a-go-go-related gene (HERG) in Xenopus oocytes. Cells were injected with a 50 nl mixture of cRNA (2μg/μL) and the proton-sensitive dye, SNARF (seminaphthorhodafluor) and were placed in a bicarbonate-buffered solution. Combined intracellular and extracellular acidification (pH_i/pH_o) was achieved by gassing the solution with 40% CO_2. Acidification of extracellular space alone (pH_o), was carried out using HEPES-containing saline solution, buffered to 7.6 or 6.6. To measure intracellular pH, oocytes were illuminated with 534 nm light and emitted light was monitored at 590 nm (acidic peak) and 640 nm (basic peak) using a video camera-based optical system. Intracellular pH was determined from the 590/640 ratio. I_{Kr} was recorded using the two electrode voltage-clamp. Acidification (pH_i/pH_o) inhibited I_{Kr} amplitude. Pulse current at 0 mV was reduced by 75 %, from 2.64 ± 1.10 μA to 0.66 ± 0.32 μA (mean, ± SEM, n=5). Also, the time constants of activation (at 0 mV) and deactivation (at -40 mV) were reduced by 25%. pH_o affected only the deactivation kinetics; time constants were 314 ± 53 ms (tau1) and 1498 ± 365 ms (tau2) in control, and respectively were 157 ± 34 ms and 621 ± 187 ms (n=4) during acidification of the extracellular space alone. pH_o had a minor effect on I_{Kr} amplitude. The pKa for the pH_o effect on deactivation was 7.07 ± 0.4 (n=3). Zn^{2+}, which interacts with the histidyl imidazole ring, had a similar effect as pH_o. We conclude that the proton effect is intracellular for activation but extracellular for deactivation. The extracellular site presumably, is on the histidine residue(s) of the HERG channel. The data also suggest that activation and deactivation may be controlled at independent sites on the channel protein.

Tu-Pos78

SPECIES DISTRIBUTION OF THE CARDIAC POTASSIUM CHANNEL ERG ((R.S. Wymore, R.T. Wymore, D. McKinnon, J. Dixon and I.S. Cohen)) Physiology and Biophysics , and Neurobiology and Behavior, SUNY at Stony Brook, NY 11794.

Strong interest developed in the potassium channel HERG when a series of mutations in this gene were demonstrated to be linked to one inherited form of the cardiac disease, the long QT syndrome (LQT2; Curran *et al.*, **Cell 81:** 299-307). Recently two laboratories have expressed HERG in *Xenopus* oocytes, and generated currents both similar and dissimilar in properties to the ventricular delayed rectifier current I_{Kr} (Sanguinetti, *et al.*, 1995. **Cell 81:** 299-307; Trudeau, *et al.*, 1995. **Science 269:** 92-95). While the current inwardly rectified like I_{Kr}, both its kinetics of activation, and pharmacologic sensitivities differed from those of I_{Kr}. One difficulty might be that most studies of I_{Kr} have been in guinea pig, while the expressed erg is from human. Given the uncertainty of relating the expression data with that obtained from cardiac myocytes, we believe that correlative data of a different type will be valuable. By cloning cDNA fragments of erg from various species, and then performing RNase protection assays on a variety of cardiac preparations, we hoped to determine whether the RNA levels seemed consistent with the amount of I_{Kr} observed in electrophysiologic studies. Erg mRNA is expressed at significant levels in hearts of dog, rabbit, human and guinea pig. Since it is readily detected in guinea pig heart, where I_{Kr} has been well characterized, erg remains a candidate alpha subunit for I_{Kr}. It now remains to do functional studies of the guinea pig erg homologue to determine if biophysical differences between HERG and I_{Kr} are species related. Supported by HL20558, and NS29755 from NHLBI.

Tu-Pos79

EARLY REPOLARIZING CURRENTS IN MAMMALIAN HEART. ((Andrew C. Zygmunt and Danielle Robitelle)) Masonic Medical Research Laboratory, Utica, NY 13501

We investigated the ionic basis of I_{to1} and determined the role of I_{to1} and $I_{Cl(Ca)}$ in early repolarization. Whole cell currents were recorded in cells isolated from epicardial and midmyocardial layers of the dog ventricle. I_{to1} was measured in the presence of 300 mM $CdCl_2$ in Na-free solutions. When pipettes contained 2 mM Cl^-, substitution of external Cl^- with methanesulfonate reduced peak outward current, suggesting a Cl^- component to I_{to1}. Substitution of external Cl^- when pipettes contained 132 mM Cl^- did not result in the expected overlapping inward Cl and outward K currents. Moreover, substitution of K^+ with Cs^+, sucrose, or N-methyl-D-glucamine abolished I_{to1} when external and internal Cl^- concentrations were normal. *We concluded that methanesulfonate inhibits I_{to1}.* Amphotericin perforated-patch technique was used to record action potentials (APs) and currents in the same cell. Blockers of I_{to1} and $I_{Cl(Ca)}$ were used in low concentrations to avoid nonspecific effects. We determined that 1 mM 4AP did not affect Ca current or $I_{Cl(Ca)}$, and that neither 0.5 mM SITS nor 200 μM DIDS had any effect on Ca current or I_{to1}. Although $I_{Cl(Ca)}$ and I_{to1} at 10 mV were comparable in amplitude at a basic cycle length (BCL) of 0.9 sec, block-ade of these two currents had different effects on repolarization. APs exhibited a spike and dome morphology, but the depth of the notch that precedes the plateau varied considerably among cells. 1 mM 4AP blocked I_{to1}, reduced the depth of the notch, lowered the dome, and significantly shortened AP duration (APD). Voltage clamp experiments indicate that elevation of the notch permits early activation of the Ca current, resulting in less inward current to support the plateau late in the AP, and APD shortens. Conversely, SITS and DIDS blocked $I_{Cl(Ca)}$, elevated the dome and shortened APD. The effects of these blockers on APD was significantly smaller than the effect of 4AP on APD. In cells with a shallow notch, SITS or DIDS reduced the notch, elevated the dome, and shortened APD. *We conclude that I_{to1} and $I_{Cl(Ca)}$ contribute importantly to early repolarization, but that the density of I_{to1} determines the depth of the notch and the timing of I_{Ca} and $I_{Cl(Ca)}$.*

Tu-Pos80

INACTIVATION IN A MAMMALIAN K^+ CHANNEL (hKv1.4) ((J.P. Johnson, L. Nie, A.L. George, P.B. Bennett)) Departments of Pharmacology Vanderbilt School of Medicine, Nashville, TN 37232. (Spon. by A. Saito)

The molecular mechanism of inactivation of Shaker related potassium channels is believed to involve a cytoplasmic amino terminal domain that blocks the ion conducting pore (ball-and-chain hypothesis). Mutations of a cloned human A-type K^+ channel (hKv1.4, HK1) were made to evaluate the role of the amino terminus in inactivation. *In vitro* transcribed cRNA was injected into *Xenopus* oocytes to induce ion channel expression and allow functional assay by two-electrode voltage clamp. Wild type HK1 inactivates completely in less than 200 msec. Deletion of 40 amino acids near the amino terminus (residues 8-47) resulted in a macroscopic current which showed no inactivation in 200 msec. Shortening of the putative chain by deletion of residues 48-79, 80-120, 121-159, or 31-159 resulted in currents which inactivate slower, not faster (as predicted) than wild type. An insertion of 9 amino acids between residues 19 and 20 had no effect on current inactivation. These results indicate that HK1 rapidly inactivates by a mechanism which involves the amino terminus as in *Shaker B*. The lysine in the pore (*Shaker B* equivalent T449K) does not induce fast inactivation, as in Shaker B. Shortening of the putative chain had an opposite effect as that seen in Shaker B, and lengthening it had no effect, contrary to the prediction of the ball-and-chain hypothesis. The data also implies that the simple ball-and-chain model may be insufficient to describe fast inactivation in mammalian channels.

Tu-Pos81

MARKED SPATIAL DISPERSION OF REPOLARIZATION ACROSS THE VENTRICULAR WALL IN A MODEL OF LONG QT SYNDROME (LQTS) AND TORSADE DE POINTES (TdP). ((EB Caref, M Restivo, S Zhang, H Yin, M Piracha, N El-Sherif)) VA Medical & SUNY Health Science Centers, Brooklyn, NY

We have previously described a canine model of LQTS and TdP using the neurotoxin anthopleurin-A (AP-A). The drug delays Na inactivation and results in bradycardia-dependent prolongation of action potential duration (APD) and the QT interval, and TdP. Recent microelectrode studies in canine transmural preparations have shown that subepicardial (EPI), midmyocardial (M) and subendocardial (END) cells respond differently to changes in cycle length (CL), with M cells having the steepest APD-CL relationship. We investigated the presence of spatial dispersion of repolarization in the AP-A model by studying the steady state relationship of activation-recovery intervals (ARI, dV/dt_{min} of QRS to dV/dt_{max} of T wave) to CL across the left ventricular (LV) free wall. ARIs were measured from 10 plunge needle electrodes, each containing 8 unipolar electrodes (50μm diameter, 1mm spacing, interneedle distance = 5mm). Recordings were obtained during constant AP-A infusion at CLs of 400 - 1400 ms. RESULTS: At a CL of 400 ms, ARIs ranged from 220 to 240 ms with no significant difference across the LV wall. At a CL of 600 ms, ARIs at M sites started to lengthen more compared to EPI and END sites. At CLs of 1000 - 1400 ms, ARIs at M sites were significantly longer than ARIs of EPI and END sites. At CL of 1400 ms, ARIs across the wall ranged from 602 ± 15 (EPI) to 692 ± 56 (M) with a mean dispersion of 90 ms. ARI dispersion at transitional zones ranged from 17 ms/mm to 102 ms/mm). CONCLUSION: The study illustrates for the first time in vivo the presence of spatial dispersion of repolarization across the LV wall due to differences in the recovery-CL relationship at different zones. The marked spatial dispersion of repolarization may provide a substrate for the TdP in LQTS.

Tu-Pos82

OPTICAL MAPPING OF EARLY-AFTERDEPOLARIZATION FORMATION IN THE EPICARDIUM OF THE LANGENDORFF-PERFUSED GUINEA PIG HEART. ((M Restivo, EB Caref, BR Choi, N El-Sherif, G Salama)) SUNY Health Science Center at Brooklyn, Brooklyn, NY, VA Medical Center, Brooklyn, NY, and *University of Pittsburgh, Pittsburgh, PA. (Spon. by G. Romero)

The role of bradycardia-dependent earlyafterdepolarization (EAD) formation to the induction of polymorphic ventricular tachycardia (PVT) was examined in the ventricular epicardial surface of 8 Langendorff-perfused guinea pig hearts using the potentiometric florescent dye RH421 (150-300 nmoles), imaged with a 128 channel photodiode array. EADs and PVT were induced with 100 μg/L Anthopleurin-A, an agent known to prolong action potential duration (APD) and induce EADs by delaying inactivation of inward Na+ current. At cycle lengths (CL) of 800-1500 msec, marked dispersion of APD (ΔAPD = 50-400 ms) was observed. At CLs of 2-8 sec, additional APD dispersion and EADs were observed at multiple epicardial sites. APD dispersion and EADs were reversibly suppressed by rapid pacing (CL < 400 msec). Non-propagated EADs decayed in amplitude from the primary site of origin (λ=1.7±.2 mm). Propagation of EAD occurred when the primary site neighbored sites of shorter APD. Propagation of EAD into contiguous zones of spatially prolonged APD, resulted in long lines of functional conduction block. However, a complete reentrant circuit was not mapped within the epicardial optical field (13x13 mm). In one heart, a CL of 8 sec produced APD prolongation > 3 sec, followed by multiple EAD firing and spontaneous PVT/VF. Conclusion: In guinea pig model of AP-A induced arrhythmia, extrasystolic activity is due to EAD, which, combined with a concomitant substrate of disperse repolarization provides a substrate for reentrant activation. EAD-dependent triggered activity and dispersion of repolarization can occur within the epicardium of guinea pig exposed to AP-A. The mechanism(s) underlying arrhythmia generation in this particular model does not appear to require the involvement of M-cells.

Tu-Pos83

EARLY AND LATE AFTERDEPOLARIZATIONS IN RABBIT VENTRICULAR MYOCYTES INDUCED BY NORADRENALINE AND DEPOLARIZING CURRENT. ((A.O. Verkerk, M.W. Veldkamp, A.C.G. van Ginneken, L.N.Bouman)) Dept. of Physiology, AMC, 1105 AZ Amsterdam (Spon. by T.Blangé)

The effect of two components of cardiac ischemia, release of catecholamines and depolarization, on action potential and membrane currents were studied in isolated myocytes from rabbit ventricle. Cells were superfused with normal Tyrode's solution (33-35 °C), noradrenaline (NA) was added in a concentration of 10^{-10} to 10^{-6} M. Membrane potential and -currents were recorded with conventional whole-cell patch clamp. Injection of depolarizing current alone increased action potential duration (APD) significantly and beyond a critical current level membrane potential stabilized in the plateau range. No early after depolarizations (EAD's), delayed after depolarizations (DAD's) or oscillations in membrane potential were seen during APD prolongation or sustained depolarization. Injection of depolarizing current in presence of NA resulted in: 1) a reduction in APD; 2) an increase in critical current; 3) an increased incidence of EAD's and plateau oscillations. In some occasions irregular, spontaneous activity and DAD's were found. In voltage clamp the following changes after addition of 1 μM NA were noted: 1) a reduction in inward rectifying K^+-current I_{K1}; 2) an about twofold increase in calcium current ($I_{Ca,L}$); 2) an increase in a slowly activating, outward current; 3) an increased incidence of transient inward currents. We speculate that DAD's result from an increased $[Ca^{++}]_i$, while plateau oscillations and EAD's may originate from the increased $I_{Ca,L}$ and slow outward current.

Tu-Pos84

INSIGHTS INTO THE METHOD OF ACTION OF THERAPEUTIC DOSES OF LIDOCAINE ON MAMMALIAN CARDIAC TISSUE. ((A. Varghese, D. Noble and R. Winslow)) Laboratory of Physiology, University of Oxford, Parks Road, Oxford OX1 3PT, UK.

Biophysically detailed models of electrical activity in single cardiac atrial cells have been used to study spatial propagation of action potentials in cell networks modeling cardiac tissue. The basic cell model, a system of 17 ordinary differential equations was augmented with the modulated receptor model, comprising 2 additional differential equations, of drug blockade of ion channels. In this report we present the results of a study of the action of the class I antiarrhythmic drug, Lidocaine. The response to simple pulsing protocols was a complex response of Wenckebach-like phenomena depending on drug dose and pacing frequency. In addition different dynamics were observed in single-cell and multicellular simulations: large drug doses were required to inhibit the generation of action potentials in single cells whereas therapeutically relevant doses are sufficient to have the same effect in chains of cells.

Supported by the Burroughs-Wellcome Fund, the Wellcome Trust and the British Heart Foundation.

Tu-Pos85

NOVEL EXTRACELLULAR MICROELECTRODES WITH HIGH SPATIAL RESOLUTION SHOW VARIATIONS IN INTRAMURAL LONGITUDINAL CONDUCTION IN ISCHEMIC PAPILLARY MUSCLES ((W.T. Smith IV, D.B. Brosnan*, H.T. Nagle*, H. Yang, T.A. Johnson, and W.E. Cascio)) *North Carolina State University, Raleigh, NC and the University of North Carolina at Chapel Hill, Chapel Hill, NC.

Isolated, ischemic rabbit papillary muscles suspended in an O_2-free atmosphere were utilized to model an ischemic boundary. Silicon/iridium microelectrodes, (Center for Neural Communication Technology, University of Michigan) with pad size 75 μm^2 and intersite spacing of 100 μm, ascertained intramural conduction during normal arterial perfusion and no-flow ischemia. Signals comparable with those collected via traditional silk-wick Ag/AgCl recording electrodes, with very high signal-to-noise ratios, were obtained by reducing mean electrode site impedance 63%, from 1714 to 640 kΩ, by an activation process in which a 1 Hz square wave (-0.8V and 0.75V potential) is applied across each site in series for 600 cycles while the electrode is submerged in a moderately alkaline solution of 0.3M Na_2HPO_4. Input voltage clamping during delivery of the stimulation pulse prevented saturation of the operational amplifiers. Activation times were measured from five vertically aligned consecutive electrode sites perpendicular to the longitudinal axis of the muscle in two experiments during ischemia. Mean activation delay of all sites increased to 3.5 ms after 8-12 min of ischemia. Conduction within 100 μm of the surface was slowest, with 4.3 ms mean delay, while deeper sites were sequentially and progressively less delayed. Sites 500-600 μm beneath the surface demonstrated only 2.1 ms delay. These results indicate that conditions at the surface of the papillary muscle cause slower conduction during ischemia than at deeper intramural layers. The disparity in activation time at sites within 500 μm in the rabbit papillary preparation may have important ramifications for the initiation and maintenance of ischemic arrhythmias at the ischemic boundaries.

Tu-Pos86

WHY DO FLECAINIDE AND ENCAINIDE ENHANCE SUDDEN CARDIAC DEATH? ((Teresa Ree Chay* and Y. S. Lee**)) *University of Pittsburgh, Pittsburgh, Pennsylvania 15260 USA and **Hangyang University, Ansan, Korea.

In this work, we explore theoretically why some antiarrhythmic drugs are proarrhythmic, while others are antiarrhythmic. In order to do that, we first study the behavior of reentry that occurs in a ring by bifurcation analysis. When the conduction velocity is plotted against the ring size, one can locate a phase transition (PT) from which sustained reentry (solid line) emerges from non-sustained reentry (dashes). This transition occurs sharply; however, it is smooth and continuous. In the region of PT, cycle length oscillates with an interesting pattern. From this bifurcation diagram, we can explain why some sodium blockers are deadly to heart patients with myocardial infarction: A heart patient who suffered myocardial infraction has a scar whose circumference may not exceed 300Δx (~9cm). As long as the scar size is smaller than ~9cm, the impulse that circulates around the scar cannot be sustained (see the g_{Na} =10 curve in A and the g_{Ca} = 0.2 curve in B). However, when sodium or calcium channel blockers are administered, the heart that previously lied in the dashed zone (non-sustained) moves to the horizontal zone (sustained). This explains why the patients with an ischemic heart can develop sudden cardiac death. The potassium channel blockers, on the other hand, suppress reentry by shifting PT to the right (see frame C). Thus, this type of drugs is useful to the patients who are prone to ventricular fibrillation.

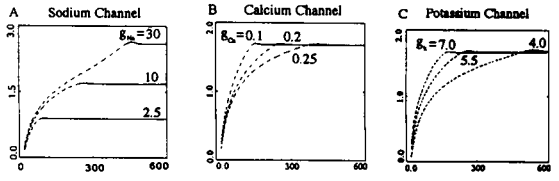

Tu-Pos87

INDUCTION OF VERY SLOW AND DISCONTINUOUS CONDUCTION BY PALMITOLEIC ACID IN LINEAR STRANDS OF RAT VENTRICULAR MYOCYTES. ((S. Rohr, A.G. Kléber, and J.P. Kucera)) Dept. of Physiology, U. of Bern, Buehlplatz 5, CH-3012 Bern, Switzerland.

Computer simulations have shown that a decrease in gap junctional conductance results in discontinuous conduction at the cellular level, which is characterized by a much lower macroscopic velocity than that obtained by a reduction of the fast sodium inward current (INa) alone. With the present experiments, we tried to test these predictions by combining patterned growth of neonatal rat ventricular myocytes in culture with high resolution optical multisite recording of transmembrane voltage (MSORTV). Linear strands of myocytes (1 cm long, 80 to 200 μm wide) were obtained using photolithographic techniques as described previously. The preparations were stained with the voltage sensitive dye di-8-ANEPPS and conduction was assessed using a linear array of photodiodes, which monitored up to 0.9 mm of the strands with a spatial resolution of 50 μm. Propagating action potentials were elicited by extracellular stimulation (2 Hz). Experiments were performed at 35°C and tetrodotoxin (TTX, 22 μM) or palmitoleic acid (PA, 20 μM) was added to the superfusate. Block of INa with TTX resulted in a reversible decrease of dV/dtmax from 93.2 ± 4.5 V/s (mean ± S.D.) to 18.7 ± 1.8 V/s (n=7), which was accompanied by a homogeneous slowing of conduction from 32 ± 2 to 13 ± 1 cm/s. No conduction blocks could be observed during TTX superfusion suggesting that the calcium inward current (ICa) alone ensured safe propagation in these preparations. During application of 20 μM PA aimed at decreasing gap junctional conductance, dV/dtmax was transiently decreased from 109.1 ± 3.0 V/s to 39.1 ± 10.1 V/s, while conduction was slowed from 28.7 ± 4 cm/s to 1.7 ± 1.0 cm/s (n=7). In contrast to the TTX experiments, this slowing was characterized by discontinuous conduction at the microscopic level resulting in local conduction velocities between two neighboring recording sites as low as 2 mm/s (average of all experiments 5.3 ± 2.3 mm/s). Eventually, after extended time periods of exposition to PA (> 20 min.), impulse propagation invariably failed. Thus, our results show that (i) complete suppression of INa in cultured rat neonatal myocytes induces slow but still continuous conduction which is likely to be carried by ICa, while (ii) partial uncoupling leads to very slow conduction, which is characterized by discontinuities at the microscopic level and eventually by conduction blocks.

Tu-Pos88

BIPHASIC EFFECTS OF L-PALMITOYL-CARNITINE ON CARDIAC L-TYPE Ca^{2+} CHANNELS.

((Qi-Yi Liu and Robert L. Rosenberg)) Departments of Pharmacology and Physiology, Univ. of North Carolina at Chapel Hill, Chapel Hill, NC 27599.

Myocardial ischemia causes disturbances of lipid metabolism, leading to accumulation of long chain acylcarnitines (LCAC) such as L-palmitoyl-carnitine (L-PC) that may be responsible for electrophysiological alterations. Voltage-gated calcium channels help control the conduction velocity in nodal cells and other regions of slow conduction, help determine action potential durations, and play a key role in setting the strength of atrial and ventricular contractions. We have therefore investigated the effect of L-PC on cardiac L-type Ca^{2+} channels incorporated into planar lipid bilayers and studied in the presence of DHP agonist (+) 202-791. We found that upon the addition of 1 μM L-PC in ***trans*** (intracellular) or ***cis*** (extracellular) chambers, average open probability (Po) increased ~8.5 fold during the first minute. The Po remained elevated for ~5 min before returning to baseline. At 10 μM L-PC ***cis***, the period of increased Po lasted only 2 min, followed by an inhibition of Po below the starting baseline. Therefore, higher concentrations (L-PC > 10 μM, ***cis***) and longer exposures (> ~3 min) inhibited rather than stimulated the channel activity. In addition, long exposure of the channels to 10 μM L-PC ***cis*** caused a reduction in the unitary conductance from ~26 pS to ~21 pS (in 100 mM Ba^{2+}). These transient changes in L-type channel activity could play a role in some of the electrophysiological changes seen during ischemia. (supported by NIH HL49449)

Tu-Pos89

POLYUNSATURATED FATTY ACID (PUFA) INHIBITION OF IONIC CURRENTS IN RAT VENTRICULAR MYOCYTES.

((K. Bogdanov, T. Vinogradova, E. Lakatta and H. Spurgeon)) Gerontology Research Center, Baltimore, MD 21224 and Cardiology Research Center, Moscow 121552, Russia

Experiments in animal models and clinical trials in humans suggest that dietary addition of PUFA's provides protection against lethal arrhythmias. The basis for this likely resides in PUFA effects on specific cardiac ion channels. Using the whole cell patch clamp technique, we studied the effects of linoleic (C18:2n-6), eicosapentaenoic, EPA (C20:4n-3), docosahexaenoic (C22:5n-3) and arachidonic, AA (C20:4n-6) acids on K^+ and Ca^{2+} currents in rat ventricular myocytes. At low concentrations (5-10 uM) all PUFA's except AA inhibited , by about 40%, the transient outward current (I_{to}) (Fig A) without affecting other K^+ or Ca^{2+} currents , and markedly prolonged the action potential (Fig B). AA inhibited I_{to} but also augmented a non-inactivating K current; the later effect did not occur with eicosatetraynoic acid, non-metabolizable analog of AA. Higher concentrations of PUFA's further inhibited I_{to} and also inhibited I_{Ca} and the delayed rectifier K current. Depressant effects of high concentrations of PUFA's on I_{Na} were also noted. Thus, at high concentrations PUFAs have a non specific effect to inhibit several ion channels; at low concentrations the PUFA's preferentially inhibit I_{to} and prolong the AP.

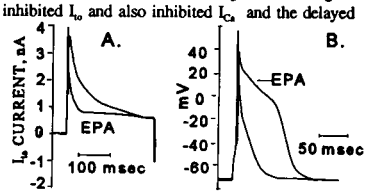

Tu-Pos90

Ca^{2+} PERMEATION THROUGH Na^+ CHANNELS IN GUINEA-PIG VENTRICULAR MYOCYTES.

((N. Leblanc, D. Chartier, M. Martin, and W.C. Cole*)). Montréal Heart Institute, University of Montréal, Montréal, Québec, and *University of Calgary, Calgary, Alberta, CANADA.

This study was undertaken to test the hypothesis that Ca^{2+} can permeate tetrodotoxin(TTX)-sensitive Na^+ channels in cesium-loaded whole-cell voltage clamped guinea-pig ventricular myocytes. Unless otherwise stated, all experiments were carried out in the absence of Na^+ in the perfusate. With 10 mM Ca^{2+} in the bathing medium, 50 ms step depolarizations (-50 to + 25 mV) from HP = -100 mV elicited two types of voltage-dependent transient inward current: 1) a small (< 400 pA) and rapid component (I_{fast}) which activated near -45 mV and peaked around -30 mV; and 2) a larger but slower component (I_{slow}) that activated near -25 mV and peaked near + 20 mV. Both current components disappeared following equimolar replacement of extracellular Ca^{2+} by Mg^{2+} suggesting Ca^{2+} was the main charge carrier flowing through both I_{fast} and I_{slow}. While I_{slow} could be unequivocally identified as a dihydropyridine-sensitive L-type Ca^{2+} current, the nature of I_{fast} remained elusive. TTX inhibited I_{fast} in a dose-dependent manner with an IC_{50} = 2.4 μM. Veratridine (1-50 μM) reduced the amplitude of I_{fast} elicited by step depolarizations to -30 mV (primarily consisting of I_{fast}) and induced slowly decaying inward tail currents following repolarization to negative holding potentials. Cell exposure to 10 and 50 μM extracellular Na^+ inhibited I_{fast} by 21.2 ± 3.9% (n = 23) and 14.0 ± 3.0% (n = 14), respectively, while 1 μM (n = 14) was without effect. Application of 200 μM Na^+ produced a small enhancement of I_{fast} (+ 6.2 ± 4.1%, n = 14) which was just at the limit of significance (p = 0.079). Our data support the notion that Ca^{2+} can permeate cardiac Na^+ channels in the absence of external Na^+. Supported by the Québec Heart and Stroke Foundation and MRC of Canada.

Tu-Pos91

THE ROLE OF SODIUM CURRENT (I_{Na}) IN ALTERED CELL FUNCTION DURING OXIDATIVE STRESS.

((P.L. Barrington)) Department of Biomedical Sciences, UIC College of Medicine at Rockford, Rockford, IL 61107.

Previously it was reported that H_2O_2 and t-butyl hydroperoxide (t-butyl OOH) do not alter the slowly inactivating I_{Na} of feline ventricular myocytes. This observation contradicts the predictions of Bhatnagar, et al. (1990) that t-butyl OOH should reduce the Na window current. Fast I_{Na} current-voltage (IV) relationships and slowly inactivating I_{Na} were monitored in isolated feline ventricular myocytes using whole-cell voltage clamp techniques. Ionic composition of solutions isolated I_{Na} either by using Cs substitution for K and F inside the pipette, or by using "physiological" pipette solutions with K and Ca current blocking compounds added to the external solution. Fast I_{Na} IV relationships were determined at reduced Na^+ gradients (TMA substitution). The slow I_{Na} was assessed with physiological Na^+ gradients and voltage ramps from -100 to 0 mV. Temperatures of experiments were set from 15 to 33 °C. At room temperature using Cs and F solutions no differences were seen in IV relationships or in slow I_{Na} between cells exposed to 1.4 mM t-butyl OOH for 30 min or left untreated. The peak inward IV was reduced after 10 min when t-butyl OOH exposure was increased to 14 mM at 30°C. Reduction in the slow I_{Na} also was noted following exposure to 1.4 mM t-butyl OOH at 30 °C for 15 minutes using "physiological" solutions. Induction of changes in I_{Na} during exposure to t-butyl OOH required warm temperatures and either high concentration of oxidant or prolonged exposure. This suggests that Na channel damage is unlikely to be an early contributor to oxidative stress.

Tu-Pos92

BLOCK OF CARDIAC CA CHANNEL BY FREE RADICALS REQUIRES TRANSMEMBRANE CA ENTRY AND INTRACELLULAR PROTEIN KINASE ACTIVITY

((Taiji Furukawa, Ako Yamazaki, Kazuyuki Suzuki, Yasuhiko Nakamura, Kyoko Nakayama, Yasuyuki Maruyama, Toshio Sagawa and Masao Nishimura)) First Department of Medicine, Teikyo University School of Medicine, Tokyo, Japan

In order to investigate which factors are responsible for modulation of L-type cardiac Ca current (I_{Ca}) by free radicals, we conducted whole cell voltage clamp experiments using isolated guinea pig ventricular myocytes. I_{Ca} was evoked by step depolarization of 200 ms from -40 to 0 mV. In the presence of 100 μM *t*-butyl hydroperoxide (TBH), a potent free radical generator, bubbled with 100% oxygen, I_{Ca} was reduced by 28±5% and 14±2% at the cycle lengths of 10 and 60 s, respectively (n=6, P<0.05). In contrast, when the extracellular Ca was replaced by equimolar Ba, TBH did not exert a blocking action of the Ba current (I_{Ba}) because I_{Ba} measured 108±5% of control values even at the cycle length of 10 s (n=7). Since I_{Ca} block by TBH was revealed to require transmembrane Ca influx, involvement of intracellular protein kinase to modulate Ca channel function was investigated. When the myocytes were pretreated with 100 μM H-7, a broad spectrum protein kinase inhibitor, I_{Ca} block by TBH was attenuated to only 15±6% of the control values at the cycle length of 10 s (n=6, P<0.05). These results suggest that (1) Ca channel block by free radicals is dependent on transmembrane Ca entry and intracellular protein kinase activity, and (2) membrane lipid peroxidation by free radicals may not be a single mechanism underlying impaired Ca channel function during reperfusion injury.

Tu-Pos93

SIGNIFICANT POSTNATAL CHANGES IN HUMAN CARDIAC SODIUM CHANNELS.

((Craig W. Clarkson and Chuntong Chang)) Department of Pharmacology, Tulane University School of Medicine, New Orleans, LA

Previous studies in rat myocytes have shown that cardiac Na channels can undergo significant postnatal changes in their gating behavior. In this study we investigated whether similar postnatal changes occur in human atrial myocytes by comparing the gating behavior of Na channels in single myocytes isolated from heart tissue obtained from newborn (0-1 month) and adult (>10 years old) patients undergoing open heart surgery. The cardiac Na current was measured using the whole cell voltage clamp technique (Na_o=10 mM, Na_i=10 mM, 16°C). The voltage dependencies for Na current activation and inactivation in all cells exhibited a spontaneous time-dependent hyperpolarizing shift, but there was no definable age-dependence to the shifts observed. In contrast, there were significant age-related differences in the V_{mid} values for channel inactivation and activation, and in Na current density (pA/pF). For example, after a 6-8 minute perfusion interval, the mean V_{mid} for channel inactivation in cells from newborn tissue was -109.0±3.0 mV (n=9) compared to -94.5±1.1 mV (n=11) for adult tissue (P<0.01). The mean V_{mid} for channel activation was also significantly more hyperpolarized in cells from newborn tissue (V_{mid} = -49.2±1.9 mV) compared to adult tissue (V_{mid} = -39.5±1.2 mV)(P<0.05). In addition, the Na current density in newborn tissue (59.5±11.0 pA/pF) was significantly lower compared to adult tissue (88.0±6.1 pA/pF)(P<0.05). These results confirm that there are significant postnatal changes in the human atrial Na current.

Tu-Pos94

SINGLE CELL PCR TO DETECT CARDIAC MYOCYTE SPECIFIC GENE EXPRESSION ((K. Krown, A. Dubin, C. Nguyen, G. Harris and R. Sabbadini)) Dept. of Biology San Diego State Univ., San Diego CA 92182.

Northern analysis, RNAse protection assay and RT-PCR are commonly used for gene expression studies. A major drawback of these methods is the inability to demonstrate the cell origin of the mRNA, if the RNA has been extracted from a tissue, such as the heart, consisting of heterogeneous cell populations. In the heart, for example, one finds not only cardiac muscle cells (myocytes) but also other cell types (i.e. fibroblasts, neurons, macrophages, VSM, endothelial cells). In situ hybridization is a method for localizing transcripts in cells, but this only gives a signal if there is appreciable abundance of transcript. In an attempt to determine if the cardiac myocyte itself expresses certain myocyte-specific genes that are in low abundance, we have applied a single-cell RT-PCR (scPCR) technique to individual cells. Cardiac myocytes are patch-clamped in the whole cell configuration. The cell cytoplasmic contents are aspirated into the patch pipette and then subjected to RT-PCR. Accordingly, we have used the scPCR to evaluate the expression of several cardiac genes, including the TNFα type I receptor (TNFRI) and the myocyte-specific gene product, ANF. Current studies involve use of the scPCR method to quantify the differential expression of selected genes. These data are the first to indicate that scPCR is an efficient tool for detecting cardiac myocyte-specific gene expression Supported by AHA, NIH and MDA.

Tu-Pos95

CARDIAC COMETS: METHOD FOR DETECTING TNFα-INDUCED APOPTOSIS IN CARDIAC MYOCYTES ((K. Krown, T. Page, C. Nguyen, V. Gutierrez, A. Dubin, and R. Sabbadini)). Department of Biology and Molecular Biology Institute, San Diego State University, San Diego, CA 92182

Tumor necrosis factor alpha (TNFα) is an inflammatory cytokine that is responsible for many of the cardiotoxic and negative inotropic effects which occur during septic shock, tissue transplant and HIV infection. In this study, we demonstrate for the first time that TNFα induces apoptosis in cultured rat myocardial cells. The percentage of apoptotic cells in the population was quantified by single cell gel electrophoresis of nuclei exhibiting DNA fragmentation patterns characteristic of apoptosis (i.e. cardiac comets). Since the sphingolipid second messenger system has been implicated in TNFα action in several cell types, including cardiac cells, we examined the role of these signaling molecules in mediating TNFα's ability to produce apoptosis. The intracellular lipid second messenger, sphingosine (SPH), was very effective in producing cardiac comets, while C2 ceramide was not as effective as either SPH or TNFα in stimulating apoptosis. HPLC analysis of rat ventricular cells demonstrate that TNFα stimulates a rapid production of endogenous sphingosine by cardiac cells. Results from single cell RT-PCR, ^{125}I-TNFα ligand binding, and Western blots identify the receptor mediating TNFα's action as the type I TNFα receptor (TNFRI, p60). These data suggest that the sphingomyelin signal transduction cascade operating via the TNFRI could be responsible for TNFa actions on cardiac cell, including apoptosis. We postulate that the cardiodepressant effects of TNFα seen in several clinical conditions are not only due to acute negative inotropic effects but also may be complicated by TNFα-induced cell death which reduces the number of working myocardial cells. Supported by MDA, AHA and NIH.

Tu-Pos96

PROBING THE ORDER WITHIN NEONATAL HEART RATE VARIABILITY. ((John C. Nelson, Rizwan-uddin, J. Randall Moorman)) Schools of Medicine and Engineering, University of Virginia, Charlottesville VA.

Heart rate variability is high in healthy newborn infants and low during severe illness. One difference is *scaling*-the differences from one RR interval to the next are several-fold higher in health. Another possible difference is that the *order*-the non-randomness of the arrangement of the intervals-is altered during illness. To test order, we measured the predictability of an HRV time series, incrementally added noise (Gaussian random numbers) or order (logistic map in a chaotic regime), and then measured predictability again. If the effect of added noise (or order) on the predictability of low and normal HRV were the same, we would conclude that they have similar degrees of order.

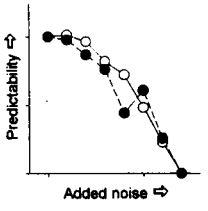

We first normalized each data set to remove the effects of scaling. To predict the n+1st RR interval, we searched the preceding m RR intervals for the y intervals (ending at an interval z) whose first differences most closely matched those of the intervals n-y to n. The predicted n+1st interval was then taken to be the z+1st interval. Predictability is based on the difference between the actual and predicted n+1st intervals. For each data set, we systematically varied m, y and n, and predicted 100 points. The Figure shows a similar decrease in predictability as noise is added to both low (open) and normal (filled) HRV; similar results were obtained by adding order. These findings support the idea that low and normal HRV are scaled versions of one another, and that there are no large changes in ordering.

Tu-Pos97

MINOXIDIL INDUCED CARDIAC HYPERTROPHY IN GUINEA PIGS. ((J. van der Velden, G.J.M. Stienen, P. Borgdorff and A.F.M. Moorman*)) Department of Physiology, Free University and the *Department of Anatomy and Embryology, University of Amsterdam, Amsterdam, The Netherlands. (Spon. by H.V. Westerhoff)

Adult guinea pigs were treated with minoxidil (120 mg/L) in their drinking water to induce cardiac hypertrophy. The composition of myosin heavy chains in age-matched control (n=11) and minoxidil treated (n=17) guinea pigs was investigated using two monoclonal antibodies directed specifically against α-myosin heavy chain and ß-myosin heavy chain in ELISA. Furthermore the rate of ATP consumption and force development were measured during isometric contraction in chemically skinned trabeculae taken from the same hearts. ATP consumption was derived from NADH absorbance in an enzyme-coupled assay. Minoxidil treatment resulted in an increase in left ventricular dry weight by 17%. Right ventricular weight did not increase. No change in ventricular myosin heavy chain composition was found. Maximum isometric ATP consumption and force were the same for control and minoxidil treated guinea pigs. Calcium sensitivity of force and ATPase activity were not affected by minoxidil treatment. These results indicate that moderate cardiac hypertrophy does not affect the economy of contraction in guinea pigs.

Tu-Pos98

ELECTRO-ELASTIC COUPLING IN MODELING MEMBRANE ELECTROPORATION. ((V. Dorman, M.B. Partenskii and P.C. Jordan)) Dept. of Chemistry, Brandeis University, Waltham, MA 02254-9110.

Coupling between quasielastic and electric degrees of freedom can cause such peculiarities at electrified interfaces as a negative branch of differential capacitance (under charge control), instabilities and phase transitions (under either charge or potential control) (Partenskii, Dorman and Jordan, Int. Rev. Phys. Chem., 1996). The electromechanical model of such phenomena in membranes, first suggested by Crowley (Biophys. J., 1973) is modified to account for the possibility of spontaneous transition to a non-uniform state and for the inherent inhomogeneity of the membrane. It is shown that critical values of the controlled variables corresponding to the appearance of the non-uniform phase depend strongly on a coupling constant accounting for the surface tension. In a non-uniform membrane a transition can occur without significant change of mean membrane thickness (unlike the prediction of the original Crowley model). Dependence of the critical characteristics on the type of electrical control is analyzed. It is concluded that the phenomena considered can play important roles in the initial stages of membrane electroporation and rupture.

Tu-Pos99

MECHANICAL RESTITUTION IN FAILING SHHF/MCC-CP RAT HEARTS. ((Prakash Narayan, Sylvia A. McCune, Charlene M. Hohl and Ruth A. Altschuld)) Department of Medical Biochemistry, The Ohio State University, Columbus, OH 43210.

Mechanical restitution in failing SHHF-Mcc/cp rat hearts was compared with normotensive controls. Hearts were perfused in the Langendorff mode (temperature = 32°C), with a balloon inserted into the left ventricle to enable pressure measurements. The hearts were paced at a basic cycle length of 333 milliseconds. After a priming period of a 100 beats, test stimuli were introduced at varying intervals from 150 ms to 600 ms. Developed pressures in response to the test stimuli were normalized with respect to the previous steady state beat. While the controls produced significant force at the shortest test interval, viz. 150 ms, the failing hearts did not do so until 210 ms. The curve from the failing hearts was right-shifted with respect to their normotensive counterparts (τ = 241 ms for control, n = 7 vs. τ = 287 ms for failing, n = 9). Furthermore, 200 nM thapsigargin failed to increase τ in the control hearts. These results suggest that mechanical restitution can be explained by the fractional release of calcium from the sarcoplasmic reticulum. Increasing the test interval allows for an increase in the amount of calcium released. The sarcoplasmic reticulum calcium release channels from failing hearts can then be construed to be more refractory to calcium release.

Supported by HL48835.

Tu-Pos100

SURAMIN IS A POTENT ACTIVATOR OF THE SHEEP CARDIAC RYANODINE RECEPTOR. ((R. Sitsapesan and A. J. Williams)) NHLI, Imperial College, University of London, SW3 6LY, UK.

The adenine nucleotide binding site on the cardiac ryanodine receptor is fairly non-specific as agents as diverse as ATP, adenosine and cyclic ADP-ribose appear to increase open probability (Po) by binding to this site. We investigated if suramin, a P_2-purinoceptor antagonist, could also modulate the Po of sheep cardiac ryanodine receptors. Vesicles of heavy sarcoplasmic reticulum (SR) were incorporated into planar phospholipid bilayers and current fluctuations through single ryanodine receptor channels were recorded under conditions where Ca^{2+} was the permeant ion. The cytosolic and luminal [Ca^{2+}] were maintained at 10 μM and approximately 50 mM respectively. The channel could be fully opened by micromolar concentrations of suramin added to the cytosolic channel face. The effect of suramin was completely reversible. Unlike ATP activation of the channel which is characterized by very brief opening and closing events, suramin caused marked prolongation of the open lifetimes. For example, 10 μM suramin increased Po from 0.017 ± 0.010 to 0.264 ± 0.025 (SEM; n=4) and mean open lifetimes from 0.77 ± 0.11 to 21.26 ± 11.64 ms (SEM; n=4). It therefore appears unlikely that suramin increases Po by interacting with the adenine nucleotide binding site on the cardiac ryanodine receptor.

This work was supported by the British Heart Foundation.

Tu-Pos101

EFFECTS OF ADP AND INORGANIC PHOSPHATE ON THE SHEEP CARDIAC RYANODINE RECEPTOR. ((H. Kermode, R. Sitsapesan & A.J. Williams)) NHLI, Imperial College, University of London, SW3 6LY, UK.

It has been demonstrated that ADP and inorganic phosphate (Pi) can release Ca^{2+} from the cardiac sarcoplasmic reticulum (SR) (Smith & Steele, J. Physiol. 458, 457-473, 1992). We aimed to investigate the effects of ADP and Pi on the gating of the cardiac ryanodine receptor and to compare these effects with those of ATP. Native sheep cardiac ryanodine receptors were reconstituted into planar phospholipid bilayers and experiments were performed under voltage-clamp conditions using Ca^{2+} as the permeant ion. Cytosolic free [Ca^{2+}] was maintained at 10 μM. Our results demonstrate that ATP fully activates the channel, with an EC_{50} value of 0.24 mM. In contrast, ADP under the same conditions is unable to cause full channel activation. The channel has a maximum open probability (Po) of 0.578 ± 0.214 (S.E.M., n=4) in the presence of 20 mM ADP and the EC_{50} value is 1.2 mM. These results indicate that ADP may act as a partial agonist at the adenine nucleotide binding site. Pi is also able to activate the channel at concentrations of 10 mM and above. For example, 100 mM Pi increases the Po from 0.009 ± 0.003 (n=5) to 0.244 ± 0.206 (n=3). In conclusion, we demonstrate that both ADP and Pi can activate the sheep cardiac ryanodine receptor and this may contribute to the observed effects of these compounds on Ca^{2+} release from the cardiac SR.

This work was supported by the British Heart Foundation.

Tu-Pos102

INTRACELLULAR ACIDOSIS INDUCED BY LACTATE AND ACETATE AFFECTS SR Ca^{2+} UPTAKE IN ISOLATED GUINEA-PIG VENTRICULAR MYOCYTES. ((C.M.N. Terracciano and K.T. MacLeod)) Imperial College of Science, Technology and Medicine, NHLI, Cardiac Medicine, Dovehouse Street, London SW3 6LY, U.K.

The effects of intracellular acidosis obtained by extracellular application of 20 mM lactate (L) or 20 mM acetate (A) (external pH=7.4 ± 0.05) on Ca^{2+} regulation mechanisms in guinea-pig ventricular myocytes were investigated. Intracellular pH measured with BCECF was 7.03 ± 0.009 (n=6) in L and 7.028 ± 0.022 (n=4) in A (mean$\pm$SEM). Cytoplasmic Ca^{2+} was monitored using indo-1 fluorescence (IF). Rapid cooling was applied to produce a release of Ca^{2+} from the SR. Ca^{2+} uptake was studied during subsequent rewarming. In L the recovery of IF signal during rewarming was slower than control (time-to-50% recovery (T50) in L was 21.5 ± 6.3 % longer than control (n=17)). No difference in T50 of IF was observed in 9 cells superfused with A. To test the role of the SR on Ca^{2+} extrusion from the cytoplasm, paired rapid cooling contractures (RCCs) were performed. The RCC elicited by a second cooling period (RCC_2) is dependent on Ca^{2+} taken up by the SR during the rewarming phase after a previous RCC (RCC_1). In both L and A RCC_2/RCC_1 was smaller compared with control (by 0.21 ± 0.04 (n=13) and 0.19 ± 0.03 (n=11) respectively). We conclude that, although L and A have different effects on cytoplasmic Ca^{2+} regulation, both these conditions affect SR Ca^{2+} uptake.

Tu-Pos103

EFFECTS OF FCCP ON REST POTENTIATION IN RAT VENTRICULAR MYOCYTES ((R.U. Naqvi, M. Mesenholler and K.T. MacLeod)). Imperial College of Science, Technology & Medicine. NHLI, Cardiac Medicine, Dovehouse Street, London SW3 6LY, UK.

The contribution of the mitochondria in influencing SR Ca load during rest was investigated using the mitochondrial inhibitor FCCP in field-stimulated enzymatically dissociated cells (0.5 Hz, 22°C, 2mM Ca) loaded with indo-1. SR Ca release was induced by rapid cooling of the cells or by rapid application of 10 mM caffeine (caffeine spritz). Two periods of rapid cooling and rewarming separated by a 1 min rest period were used to assess changes in the SR Ca content during rest (results are expressed as mean $\pm$ SEM, n=12). In normal Tyrode the size of the second rapid cooling contracture (RCC2) was 15.4 ± 2.2 % greater than the first (RCC1). Repeating in 0Na/0Ca solution reduced this rest potentiation of SR content to 5.01 ± 1.8 %. Addition of FCCP (1μM) and oligomycin (1μM) to the 0Na/0Ca solution gave two distinct results. In 75% of the cells, RCC2 was 15.63 ± 3.19 % smaller than RCC1. In the remaining cells it was abolished completely, but a caffeine spritz applied immediately after this second cooling was able to produce a large release of Ca and a cell contraction. Hence, Ca loading of the SR via both reverse Na/Ca exchange and the mitochondria contributes to the rest potentiation characteristic of rat myocytes. Furthermore, FCCP can have different effects on SR Ca release induced by cooling or caffeine.

Tu-Pos104

CLONING AND CHARACTERIZATION OF 5' UPSTREAM REGULATORY REGION OF THE CALCIUM RELEASE CHANNEL GENE OF CARDIAC SARCOPLASMIC RETICULUM. ((K. Nishida, K. Otsu, T. Toyofuku, M. Yabuki and M. Tada)) Department of Medicine and Pathophysiology, Osaka University Medical School, Suita, Osaka 565, Japan.

Calcium release channel of cardiac sarcoplasmic reticulum (CRC) plays an important role in exitation-contraction coupling. The expression of CRC is regulated at the level of transcription during development and is altered in pathological status. To examine the transcriptional regulation mechanism of CRC gene, we isolated and characterized a 5'-flanking region of this gene. The transcription start site was identified at 335 bp upstream from the initiation codon by primer extension method. Sequence analysis revealed that the core promoter region lacks TATA and CAAT boxes, but contains a GC box-like element in the position -64 to -51, which complexed with Sp1 when examined by gel shift assays. Deletional and mutational analysis of CRC-reporter fusion gene constructs in transient transfection assays defined the two positive regulatory regions from -89 and -84 and from -74 to -66. The GC box has shown no promoter activity by itself, but introduction of mutations into this region resulted in decrease in promoter activity, indicating the regions, from -89 to -84 and from -74 to -66, by interacting the GC box are crucial for the expression of CRC gene. Transient transfection experiment in skeletal muscle cell line, C2C12 suggested that the region between -209 and -90 has a negative regulatory element to repress the expression of CRC gene in skeletal muscle cells.

Tu-Pos105

NOVEL MODULATORS OF SARCOPLASMIC RETICULUM CALCIUM RELEASE CHANNELS I. CALAMUS SECONDARY METABOLITES TECTORIDIN AND 3'-HYDROXY TECTORIDIN. ((K.R. Bidasee[1], V. Patel[2] A.Maxwell[3] and H.R. Besch, Jr.[1])) [1]Dept. of Pharmacol. and Toxicol., and [2]Pathology, Indiana Univ. Sch. of Med., Indianapolis, IN 46202-5120 and [3]Dept. of Chem., Univ. of the West Indies, Trinidad.

Crucially involved in regulation of free intracellular calcium ion concentrations in a variety of tissues, calcium-release channels (CRCs) are molecular entities of current interest as potential therapeutic targets. The neutral alkaloid ryanodine specifically modulates conductance of CRCs, activating (opening) them at low (<uM) concentrations and deactivating (closing) them at higher concentrations. We have recently produced activator selective agonists of the CRCs, including C_{10}-O_{eq} β-alanyl ryanodine (BARy) and C_{10}-O_{eq} guanidno propionyl ryanodine (GPRy) that are less toxic than the parent ryanodine when administered i.v. to rats. These results suggest the possibility that closing, rather than opening of CRCs, may be central to the toxicity of ryanodine. In our ongoing evaluation of tropical biota that may exhibit BARy- and GPRy-like activity, we have isolated two active principals, tectoridin (TTR) and 3'-hydroxy tectoridin (3OHT) from the Ayuvedic plant *Acorus calamus* Linn. In [^{3}H] ryanodine displacement binding affinity assays, TTR and 3OHT demonstrated IC_{50} values of 22μM (K_d= ca. 5μM) and 25μM (K_d= ca. 5.7μM), respectively compared to the BARy IC_{50} values of 2.8nM (K_d= ca. 1nM) and GPRy of 2.1nM (K_d= ca. 0.5nM). In calcium efflux assays with junctional sarcoplasmic reticulum membrane vesicles (JSRV), unlike BARy and GPRy that both afforded only activator actions, even at concentrations as high as 3mM (ca. 700-fold their K_d values), TTR and 3OHT exhibited biphasic effects. TTR and 3OHT activated CRCs at lower concentrations (maximally at 500μM, to a full efficacy 85% that of GPRy) and deactivated at higher concentrations (to a maximal of 45% of full closure at saturating concentrations). The inability of *Acorus* secondary metabolites to effect full closure of CRCs may underlie their reduced toxicity in Ayuvedic medicinal preparations.

Supported in part by the Showalter Trust.

Tu-Pos106

9-Me-7-Br-EUDISTOMIN-D (MBED), A POTENT AND SELECTIVE Ca^{2+} RELEASER FROM CARDIAC SARCOPLASMIC RETICULUM (SR).
((P. Lahouratate, and J. Guibert)) SmithKline Beecham Laboratoires Pharm., BP-58, 35762 Saint Grégoire, France.

MBED, is a potent Ca^{2+} releaser from skeletal muscle SR (Kobayashi *et al.*, Experientia 45:782-3, 1989), but its selectivity is unknown. Caffeine (CAF) is the standard tool for activating SR Ca^{2+} release but its use can be complicated by phosphodiesterase (PDE) inhibition and interaction with the contractile proteins. We compared the ability of CAF and MBED to release Ca^{2+} from cardiac SR vesicles prepared according to Webster *et al.*, (JMCC. 26:1273-90, 1994) and incubated (30°C) in (mM) KCl, 90; K-MOPS, 18; KH_2PO_4, 5; MgATP, 1; Na_2-phosphocreatine, 5; CPK, 20 μg/ml (pH 7.05). The Ca^{2+} release, assessed from the transient increase in fluorescence of extravesicular fluo-3 (3 μM), was expressed relatively to that produced by Br-A23187. MBED released a similar amount of Ca^{2+} but was 1000-fold more potent than CAF (fig.). Ryanodine or ruthenium red inhibited to a similar extent this Ca^{2+} release. In contrast to CAF, MBED did not quench fluo-3 fluorescence and did not affect myofibrilar ATPase activity at pCa 6.0. At concentrations producing max Ca^{2+} release, MBED (10 μM) inhibited SR-PDE by only 34% compared to 89%, for CAF (10 mM). Due to its high potency and selectivity, MBED represents an ideal tool to trigger Ca^{2+} release from cardiac SR.

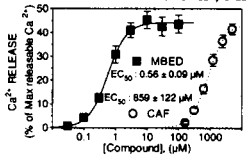

Tu-Pos107

ALTERNATIVE SPLICING IN HUMAN CARDIAC MUSCLE RYANODINE RECEPTOR mRNA.
((B.M.A. Bertrand, R.E.A. Tunwell and F.A. Lai)) MRC National Institute for Medical Research, Mill Hill, London NW7 1AA, UK.

The ryanodine-sensitive calcium release channel (RyR) is responsible for calcium release from intracellular stores and plays a fundamental role in excitation-contraction coupling in cardiac muscle. By PCR and sequence analysis, we identified an alternatively spliced region in the mRNA of the human cardiac muscle ryanodine receptor (human cRyR). This region was characterized by the presence or the absence of a stretch of 30bp generating two variants 30bp(+) and 30bp(-), respectively. Exclusion of these 30bp results in the absence of 10 amino acid residues corresponding to Phe^{1480}-Gly^{1489} of the human cRyR. The cloned cDNA sequences flanking this insert were identical in 30bp(+) and 30bp(-). Using primers adjacent to this 30bp insertion in PCR with human genomic DNA, we found that this insertion corresponded to an exon of 30bp flanked by introns of 0.5 and 1.4 kbp. This shows that the heterogeneity of mRNA is generated by alternative use of this 30 bp exon. Studies with different adult rabbit tissues (heart, cerebellum, cerebral cortex, hippocampus, etc.) showed that all these tissues lacked this 30bp insertion. In the human cardiac RyR, this 10 amino acid sequence is located in the modulatory region of the protein. The putative variant isoforms may result in heterogeneities in channel activity and regulation. Elucidation of the effects of alternative splicing on human cRyR function will provide further insights into the roles of cRyR in the excitation-contraction coupling of cardiac muscle.

Tu-Pos108

RECTIFICATION OF SKELETAL MUSCLE RYANODINE RECEPTOR MEDIATED BY FK506 BINDING PROTEIN.
((Jianjie Ma, Manjunatha B. Bhat and Jiying Zhao)) Department of Physiology and Biophysics, Case Western Reserve University, Cleveland, Ohio 44106. (Spon. by T. Hoshiko)

Cytosolic receptors for immuno-suppressant drugs, FK506 binding protein (FKBP12), maintain tight association with ryanodine receptors (RyR) in skeletal muscle. With SR membrane vesicles isolated from rabbit skeletal muscle, we observed ~20% of the Ca release channels (52/262 experiments) which conducted current unidirectionally from SR lumen to myoplasm (in the opposite direction, the channel deactivated with fast kinetics). The interaction with endogenous FKBP12 seemed to account for the asymmetric opening of the Ca release channel, as rectification of the channel was eliminated by perchlorate (10 mM), which could be restored through further addition of exogenous FKBP12 (0.6 μM). The normal (non-rectifying) Ca release channel exhibited similar rectification in the presence of exogenous FKBP12, only after prior treatment with perchlorate. Both on- and off-rates of FKBP12 binding to the RyR showed clear dependence on membrane potential, suggesting that the binding sites of FKBP12 reside in or near the conduction pore of the Ca release channel. FK506 (10 μM) caused frequent appearence of residual conductance in the rectifying Ca release channel, without changing the rectification property of the channel. Thus, interaction between FKBP12 and RyR had two consequences on the Ca release channel: voltage dependent block of the ion conduction pathway and altered interaction within the RyR complex.

Tu-Pos109

HETEROLOGOUS EXPRESSION OF SKELETAL MUSCLE RYANODINE RECEPTOR IN CHO CELLS.
((Manjunatha B. Bhat*, Mitchell L. Drumm@, Hiroshi Takeshima# and Jianjie Ma*)), Depts. of Physiology and Biophysics* & Pediatrics@, Case Western Reserve Univ., Cleveland, OH, #Dept. of Pharmacol., Saitama Med. School, Saitama, Japan.

Skeletal muscle ryanodine receptor cDNA (SkRyR) [Nature, 339:439] was expressed in chinese hamster ovary (CHO) cells using liposome-based transfection method. The expression of protein was assayed by immuno-western blot using antibody against rabbit SkRyR. Subcellular fractionation using sucrose density gradient identified the expressed RyR specifically in the ER membranes. In addition to a high molecular weight band (~560 kD) that corresponds to native SkRyR,CHO cells transfected with SkRyR cDNA also contain a lower band (~450 kD), both of which were recognized by antibody against SkRyR (see Fig.). Although such patterns have been reported to be due to possible proteolytic degradation (Takeshima et al, Nature 339:439; Chen et al., Biochem 32:3743), an alternative explanation includes translation of the protein from an alternate initiation site within the cDNA. When microsome membranes from transfected CHO cells were incorporated into planar lipid bilayer, single channel currents characteristic of skeletal muscle calcium release channel could be recorded.

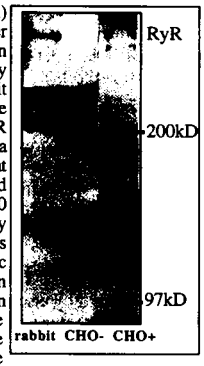

Tu-Pos110

DIABETIC ALTERATIONS IN PHOSPHOLAMBAN(PLB) PROTEIN EXPRESSION; REGULATORY EFFECTS ON SARCOPLASMIC RETICULUM(SR) Ca^{2+} TRANSPORT
((Hac Won KIM and Y. S. LEE)) Dept. of Pharmacology, Univ. of Ulsan College of Medicine, Seoul 138-040, Korea

Diabetic cardiomyopathy has been suggested to be caused by the intracellular Ca^{2+} overload in the myocardium, which is partly due to the defect of calcium transport of the cardiac SR. In the present study, both of the maximal Ca^{2+} uptake and the affinity for Ca^{2+} were decreased in the diabetic rat SR in comparison with the control. We examined whether the decrease of the cardiac SR function in streptozotocin-induced diabetic rat is associated with the phosphorylation level of the PLB. The levels of PLB phosphorylation were increased in diabetic cardiac SR. Phosphatase treatment of PLB before phosphorylation did not change the level of phosphorylation. Thus the increased phosphorylation level in diabetic rat could not be due to the autonomic alterations in chronic metabolic states. To determine whether the increased PLB phosphorylation level is associated with the increased PLB expression, western blot analysis was performed. The level of Ca^{2+}-ATPase was decreased in diabetic hearts, however, PLB level was increased. Consequently, the relative PLB/ Ca^{2+}-ATPase ratio was 1.6 in diabetic hearts, and these changes correlated with changes in the EC_{50} of the SR Ca^{2+} uptake for Ca^{2+}. It was also well correlated with the levels of mRNAs for PLB and Ca^{2+}-ATPase. However, insulin treatment reverse these parameters to normal levels. Since PLB is the inhibitor of SR Ca^{2+}-ATPase, the increase of PLB and the decrease of Ca^{2+}-ATPase levels in the diabetic state could explain well the functional defect of SR. (Supported by Grants from AILS, and KOSEF)

Tu-Pos111

Activation of the Skeletal Muscle Ryanodine Receptor by Peroxide is inhibited by Thiol Reducing and Alkylating Agents.
((T.G. Favero[1], A.C. Zable[2], and J.J. Abramson[2])) [1]Biology Department, University of Portland, and [2]Physics Department, Portland State University.

Hydrogen peroxide (H_2O_2) at millimolar concentrations has been shown to induce Ca^{2+} release from sarcoplasmic reticulum (SR) vesicles and stimulate [^{3}H]ryanodine binding to its receptor. We observe that, peroxide stimulation of Ca^{2+} channel activity was reversed by the addition of the thiol reducing agent, dithiothreitol (DTT), and the thiol alkylating reagent, n-ethylmaleimide (NEM). Following activation by 1 mM peroxide, DTT inhibited ryanodine binding in a concentration dependent manner with complete reversal of peroxide activation by 1 mM DTT. However, DTT (1 mM) was unable to reduce the stimulation of ryanodine binding induced by 10 mM peroxide, even though peroxide was detoxified by the addition of catalase. As demonstrated by SDS-PAGE, the presence of DTT also dissociated the ryanodine receptor from a large disulfide-linked protein complex formed by the addition of peroxide. Similar to DTT, NEM also inhibited peroxide stimulation of ryanodine binding in a concentration dependent manner with complete inhibition of the ryanodine receptor at 100 uM. NEM (1 mM) also completely inhibited ryanodine binding when stimulated by ATP and doxorubicin. These results suggest that reducing and alkylating reagents target sulfhydryl (SH) groups that participate in closing down the SR Ca^{2+} release channel. Supported by AHA Oregon Affiliate.

Tu-Pos112

LONG-TERM STIMULATION IMPROVES CONTRACTILE PROPERTIES OF CULTURED ADULT RAT CARDIOMYOCYTES. ((E. Holt, P.K. Lunde, O.M. Sejersted and G. Christensen)) Inst Exp Med Research, Univ of Oslo, Ullevaal Hospital, N-0407 Oslo, Norway. (Spon. by J. Storm)

To examine whether electrical or mechanical activity affect cardiac contractile performance, isolated adult rat cardiomyocytes were stimulated for 20 hrs. Cells were isolated after retrograde perfusion of hearts with a trypsin/ collagenase solution and cultured on laminine in flasks in a serum free medium with added taurine (5 mM), insulin (0.1 mM) and triiodothyronine (10^{-10} M). Continous field stimulation (5 V·cm^{-1}) at 1 Hz (bipolar pulses of 5 ms duration) was achieved by two rod shaped graphite electrodes. In a random, blind design, unstimulated (U) and stimulated (S) cells were tested in an inverted microscope which allowed continuous length recording. Fractional shortening was 14.12 ± 0.72% and not different at 0.25 Hz, but fell to 8.05 ± 0.94% at 2 Hz in U, but only to 12.02 ± 0.66% in S ($p<0.005$). At this frequency both velocity of shortening and relaxation rate were slower in U than in S ($p<0.05$). Measurements of Ca^{2+} transients were done at 1 Hz after loading with fura-2 AM. Resting Ca^{2+} ratio signals equalled 0.28 ± 0.01 and 0.26 ± 0.01 in U and S ($p<0.05$) and peak Ca^{2+} transient ratios were 0.64 ± 0.02 and 0.81 ± 0.04 ($p<0.005$). Rate of fall of Ca^{2+} was slower and caffeine-induced Ca^{2+} transients were smaller in U than in S. Moreover, the content of ryanodine receptors was 1.35 ± 0.06 pmol/mg and 1.23 ± 0.06 pmol/mg in U and S cells, respectively (ns). We conclude that continuous long-term stimulation of adult rat ventricular cardiomyocytes in primary culture improves contractile performance and is associated with altered calcium handling.

Tu-Pos113

CONTROL OF CALCIUM IN SINGLE VASCULAR SMOOTH MUSCLE CELLS BY ARGININE-VASOPRESSIN

((J. R. Holda and L. A. Blatter)) Department of Physiology, Loyola University Chicago, Maywood, IL 60153

Arginine vasopressin (AVP) is a peptide hormone known to increase intracellular calcium ($[Ca^{2+}]_i$) in vascular smooth muscle. The control of $[Ca^{2+}]_i$ in single rat aortic smooth muscle cells (A7r5 cell line) by AVP was investigated using the fluorescent Ca^{2+} indicator indo-1. AVP (10 nM) induced a rapid and transient increase in $[Ca^{2+}]_i$ followed by a prolonged plateau phase of elevated $[Ca^{2+}]_i$. $[Ca^{2+}]_i$ immediately returned to baseline after removal of AVP. AVP failed to increase $[Ca^{2+}]_i$ in cells that were internally perfused with heparin. Stimulation with caffeine also induced a transient increase of $[Ca^{2+}]_i$. These results suggest that the initial (non-plateau) phase of the $[Ca^{2+}]_i$ transient is due to release of Ca^{2+} from IP_3-sensitive intracellular stores, with the possible contribution from ryanodine-sensitive stores. The plateau phase of the $[Ca^{2+}]_i$ transient was abolished in Ca^{2+}-free solutions. Furthermore, NCDC (phospholipase inhibitor and putative blocker of receptor mediated Ca^{2+} entry in smooth muscle) caused an immediate return of $[Ca^{2+}]_i$ to baseline when applied during the plateau phase. These results indicate that Ca^{2+} influx is required to maintain the plateau phase during AVP stimulation and that phospholipase activation may be a prerequisite. Removal of extracellular Ca^{2+} caused a small and reversible decrease of $[Ca^{2+}]_i$. AVP induced $[Ca^{2+}]_i$ transients under Ca^{2+}-free conditions, although repetitive stimulation resulted in a progressive decrease and eventual abolishment of $[Ca^{2+}]_i$ transients due to depletion of the stores. After the stores were depleted in the absence of extracellular Ca^{2+}, exposing the cells to extracellular Ca^{2+} caused a rapid, large and prolonged increase in $[Ca^{2+}]_i$ that slowly returned to baseline. This observation is consistent with the hypothesis that empty stores signal activation of Ca^{2+} influx pathways. The rate at which $[Ca^{2+}]_i$ returned to baseline during this phase was dramatically increased by AVP. This suggests that AVP, along with triggering Ca^{2+} release and influx, may also have a novel role in stimulation of Ca^{2+} sequestration or efflux.

Tu-Pos114

Thiol Reducing Agents Antagonize Skeletal Muscle Ryanodine Receptor.

((A.C. Zable[1], T.G. Favero[2], and J.J. Abramson[1])) [1]Physics Department, Portland State University and [2]Biology Department, University of Portland.

Reduced glutathione (GSH) inhibits Ca^{2+} stimulated [^{3}H]ryanodine binding to the sarcoplasmic reticulum and, in single channel experiments, it also inhibited the gating activity of the reconstituted Ca^{2+} release channel. The effect of GSH in both the [^{3}H]ryanodine binding and single channel measurements was dose dependent. Scatchard analysis demonstrates that the interaction between GSH and the ryanodine receptor both decreased the binding affinity of ryanodine for its receptor (increased K_d) and the maximal binding occupancy (B_{max}). In addition, GSH does not to modify the Ca^{2+} dependence of [^{3}H]ryanodine binding. In single channel experiments, GSH (5mM), added to the cis side of the BLM, lowers the open probability (P_o) of a Ca^{2+} (50 μM) stimulated Ca^2 channel without modifying the single channel conductance. Subsequent perfusion of the cis chamber with an identical buffer, containing 50 μM Ca^{2+} without GSH, re-establishes Ca^{2+} stimulated gating channel gating. GSH does not appear to inhibit channel gating when added to the trans side of the BLM. Similar to GSH, the thiol reducing agents dithiothreitol (DTT) and β-mercaptoethanol (BME) also inhibit high affinity [^{3}H]ryanodine binding to sarcoplasmic reticulum membranes. In contrast to GSH, oxidized glutathione (GSSG) stimulates high affinity [^{3}H]ryanodine binding. These results provide evidence that glutathione interacts with reactive thiols associated with the Ca^{2+} release channel/ryanodine receptor complex. These results support the previous observation (Liu et. al. 1995) that hyperreactive thiols are involved in the gating of Ca^{2+} release channel. Furthermore, the present report suggests that the location of these key thiols appears to be on the cytoplasmic face of the SR membrane. Supported by AHA Oregon Affiliate.

Tu-Pos115

MILLISECOND KINETICS OF CALCIUM RELEASE INDUCED BY PHOTOLYSIS OF CAGED IP_3 IN PEELED SKELETAL MUSCLE FIBERS. ((M.G. Higgins, D.D. Thomas, L.V. Thompson, D.A. Huetteman, *S.K. Donaldson)) University of Minnesota, Minneapolis, MN 55455; *Johns Hopkins University, Baltimore, MD 21205.

Inositol 1,4,5-Trisphosphate (IP_3) elicits Ca^{2+} release in both smooth and skeletal muscle. Walker et al. (Nature 327: 249-252, 1987) elicited IP_3-induced tension transients in both but found that tension development in skinned skeletal fibers was too slow to be attributed to excitation-contraction (EC) coupling. However, Ca^{2+} release is much faster than end-to-end tension generation in the skinned fiber preparation. In the present study, Ca^{2+} release was measured directly and fiber tension was recorded continuously. IP_3 was released by laser pulse photolysis of caged IP_3, and IP_3-induced Ca^{2+} release was measured as Fluo-3 fluorescence in mechanically peeled (sarcolemma removed) single, rabbit skeletal muscle fibers. The IP_3-induced Ca^{2+} transient had a $t_{1/2}$ of 15.8±3.2 msec, consistent with action potential-induced Ca^{2+} release (Vergara et al., 1992, Adv. Exp. Med. Biol. 311, 227-236). End-to-end fiber tension had a $t_{1/2}$ of 11.8±1.8 sec, consistent with Walker's results. This study extends previous work by including a direct measurement of IP_3-induced Ca^{2+} release in single skeletal muscle fibers. Our results support the hypothesis that IP_3 acts as an important second messenger in skeletal muscle EC coupling. NIH AM 37163, AR 32961.

Tu-Pos116

PHOSPHOLAMBAN-DEPENDENT EFFECTS OF C12E8 ON CALCIUM TRANSPORT AND MOLECULAR DYNAMICS IN THE HEART ((Yongli Shi, Brad S. Karon, and David D. Thomas)) Department of Biochemistry, University of Minnesota Medical School, Minneapolis, MN 55455

We have studied the effects of the nonionic detergent $C_{12}E_8$ on Ca-ATPase enzymatic activity and oligomeric state (detected by time-resolved phosphorescence anisotropy, TPA), in skeletal and cardiac sarcoplasmic reticulum (SR). In skeletal SR, $C_{12}E_8$ inhibits the Ca-ATPase, both at high (μmolar and above) and low (submicromolar) Ca. In cardiac SR, $C_{12}E_8$ inhibits at high Ca but activates at low Ca. Thus $C_{12}E_8$ activates enzymatic activity only in cardiac SR and only under conditions (submicromolar Ca) where phospholamban (PLB) regulates (inhibits) the enzyme (Lu and Kirchberger, *Biochemistry* 33:5056). TPA on skeletal SR at low and high Ca, and on cardiac SR at high Ca, shows that the Ca-ATPase is present as monomers and small oligomers, but $C_{12}E_8$ induces aggregation of the enzyme. In cardiac SR at low Ca, the Ca-ATPase is already highly aggregated, and $C_{12}E_8$ partially dissociates these aggregates. Thus the TPA results provide a simple physical explanation for the functional effects: **$C_{12}E_8$ inhibits the ATPase when it aggregates the enzyme** (skeletel SR at high and low Ca; cardiac SR at high Ca), **but the detergent activates when it dissociates ATPase oligomers** (cardiac SR at low Ca). $C_{12}E_8$ reverses both the physical and functional effects of PLB on the Ca-ATPase. The results provide insight into the role of PLB in regulating the Ca-ATPase in cardiac SR.

Tu-Pos117

MOLECULAR DYNAMICS DURING ACTIVE CALCIUM PUMPING (Min Zhao and David D. Thomas) Dept. of Biochemistry, University of Minnesota Medical School, Minneapolis, MN 55455.

We have used time-resolved phosphorescence anisotropy (TPA) to probe the rotational dynamics of Ca-ATPase in skeletal sarcoplasmic reticulum (SR). Most previous studies on this system have been done with dyes attached to Lys-515 on the Ca-ATPase, which inactivate the enzyme by inhibiting the binding of ATP. Therefore, in the present study, we labeled the Ca-ATPase predominantly at Cys-674 with erythrosin 5'-iodoacetamide (ErIA), with 100% retention of the Ca-dependent ATPase activity. TPA was performed at 4°C with 2 μM Ca-ATPase. Ca was found to increase the initial anisotropy decay without affecting the residual anisotropy, suggesting that Ca decreases sub-μsec internal rotation in the Ca-ATPase. In contrast, ATP increases the sub-μsec internal rotation. In the presence of both Ca and ATP, the effects were intermediate and additive. AMPPCP has the same effects as ATP, showing that the changes are due to nucleotide binding, not to ATP hydrolysis. The changes in internal dynamics, due to binding of Ca or ATP, are accompanied by more subtle changes in global rotational dynamics.

Tu-Pos118

STRUCTURE AND MOLECULAR DYNAMICS OF PHOSPHOLAMBAN AND ITS MUTANTS BY EPR

((Christine B. Karim, John D. Stamm, Larry R. Jones*, and David D. Thomas)) Department of Biochemistry, University of Minnesota Medical School, Minneapolis, MN 55455, and *Krannert Institute for Cardiology, Indiana University School of Medicine, Indianapolis, IN 46202.

The structure and molecular dynamics of recombinant phospholamban (PLB) and its mutants, L37A and C41L, were probed using electron paramagnetic resonance (EPR) of a thiol-reactive spin label (MTSSL), targeting Cys 36, 41, and 46 in the hydrophobic C-terminal domain. In PLB and C41L, only two Cys residues were reactive, while in L37A all three Cys were reactive. After labeling, SDS-PAGE showed that PLB and L37A remained predominantly pentameric and monomeric, respectively, but labeling converted C41L from a tetramer to a monomer. The 25° EPR spectra of the two spin-labeled mutants (both monomers in SDS) showed single spectral components with high rotational mobility, while the spectrum of the pentameric PLB had a substantial contribution from a more restricted component. Low-temperature EPR spectra showed clear evidence of spin-spin interactions in L37A, but not in PLB or C41L, showing that spin-spin interactions are predominantly intramolecular and involved the label on C41. We conclude that Cys 36 and 46 are reactive in PLB, and the pentameric structure leads to restriction at one or both of these sites, providing a sensitive measurement of PLB oligomeric state that should be useful in future studies.

Tu-Pos119

THE OLIGOMERIC STRUCTURE OF PHOSPHOLAMBAN IN MEMBRANES, PROBED BY FLUORESCENCE ENERGY TRANSFER.

((Ming Li, Răzvan L. Cornea, Eric J. Olson, Larry R. Jones† and David D. Thomas)) Dept. of Biochemistry, University of Minnesota Medical School, Minneapolis, MN 55455. †Krannert Institute of Cardiology, Indiana Univ., Indianapolis, IN 46202.

Phospholamban (PLB) is an amphipathic peptide that regulates Ca-ATPase activity in cardiac sarcoplasmic reticulum. PLB exists as a homo-pentamer under the conditions of SDS-polyacrylamide gel electrophoresis (Jones et al., 1986), and it has been proposed that pentamerization of PLB is required for its regulatory function. Therefore, it is important to determine the oligomeric structure of PLB in biological membranes. We have used both steady-state and time-resolved fluorescence to measure the energy transfer between subunits of recombinant PLB, in order to determine its oligomeric state. Separate populations of PLB were labeled with fluorescent donor and acceptor at Lys-3. These two samples were then mixed in different ratios under conditions shown to produce complete subunit exchange. Significant energy transfer between PLB subunits was observed in both SDS and in phospholipid bilayers, confirming that PLB is oligomeric, but the oligomeric structure is different in the two cases. The measurements were also performed on PLB mutants in order to obtain a rigorous correlation between the oligomeric structure and function of PLB.

Tu-Pos120

CYSTEINE REACTIVITY AND OLIGOMERIC STATES OF PHOSPHOLAMBAN AND ITS MUTANTS

((Christine B. Karim, Joseph M. Autry*, David D. Thomas and Larry R. Jones*)) Department of Biochemistry, University of Minnesota Medical School, Minneapolis, MN 55455, and *Krannert Institute for Cardiology, Indiana University School of Medicine, Indianapolis, IN 46202.

In order to test a model for the pentameric structure of phospholamban (PLB), we characterized recombinant PLB and two of its mutants by the reactivity of Cys toward DTNB [5', 5'- dithiobis (2-nitrobenzoic acid)], and by oligomeric state on SDS-PAGE. For PLB in SDS at pH 7.5, two out of the three residues Cys 36, 41 and 46, located in the hydrophobic transmembrane region, reacted with DTNB, with very slight destabilization of the pentameric structure. When PLB was denatured in guanidine at pH 8.1, all three Cys reacted. Stoichiometric labeling of the three cysteines disrupted, but cleavage of the disulfide bonds with DTT re-established the pentameric structure. In the tetrameric mutant C41L, the remaining two cysteine residues reacted with DTNB, which reversibly destabilized the tetrameric structure. All three cysteines reacted with DTNB in the monomeric mutant L37A. We conclude that Cys 41 is the unreactive Cys in PLB-WT, and that this residue is located at a crucial site for maintenance of the pentameric structure.

Tu-Pos121

DECAMETHONIUM INCREASES CAFFEINE INDUCED CA^{2+}-RELEASE OF SKINNED SKELETAL MUSCLE FIBRES.

((R.H.A. Fink, O. Harney, C. Weber & C. Veigel)) II. Institute of Physiology, University of Heidelberg, INF 326, D-69120 Heidelberg, Germany

We have used Decamethonium (DEM) to block the SR-K^+-conductance of skinned skeletal fast and slow twitch muscle fibres during caffeine induced Ca^{2+}-release measured as force transient. The fibres were isolated from e.d.l. or soleus muscles of Balb-C mice and chemically skinned using saponin. The Ca^{2+}-loading and release procedure was similar to that used by Fink & Stephenson (1987, Pflügers Arch. 409: 474). Test releases were carried out with DEM in a concentration range of 0.1 to 4 mM when the drug was only present during the caffeine induced transient of isometric force as indicator of the Ca^{2+}-release. In the presence of DEM the transients increased up to threefold in peak and twofold in area under the transient as relative measures of Ca^{2+}-release when compared to control releases without DEM. When varying the caffeine concentration from 5 to 30 mM the rate of force development increased with DEM. These results may at least partly be explained by indirect effects on the ionic milieu in the SR (see Fink & Veigel, 1996, Acta physiol. scand., in press).

MUSCLE PHYSIOLOGY: CHANNELS AND RECEPTORS

Tu-Pos122

THAPSIGARGIN INDUCES A RAPID, RYANODINE-INHIBITABLE CALCIUM RELEASE FROM SKELETAL MUSCLE SARCOPLASMIC RETICULUM.

((C. G. Palahniuk, and J.S.C. Gilchrist)). Department of Oral Biology, University of Manitoba, Winnipeg, Canada, R3E 0W2

The sesquiterpine lactone, thapsigargin (Tg), is a specific inhibitor of SERCA-type Ca^{2+}-ATPase pumps in skeletal, cardiac and smooth muscle. The reported effect of Tg is a net elevation of cytosolic Ca^{2+}. The purpose of this study was to investigate the action of Tg on SR Ca^{2+} uptake and Ca^{2+} release. SR Ca^{2+} transport was monitored through the fluorescence of Calcium Green-2 (λ_{ex}=488nm/λ_{em}=540nm) in response to extraluminal Ca^{2+} transients. Using conventional Pi assay procedures we confirmed Tg potently inhibited SR Ca^{2+}-ATPase activity. In Ca^{2+} transport assays under conditions where the size of the intraluminal Ca^{2+} sink exceeded the extraluminal Ca^{2+} load, Tg (1-10μM) delayed the time course of ATP-dependent Ca^{2+} accumulation by SR vesicles (0.5-1 mg·ml^{-1}). When Tg (1-10μM) was added to SR vesicles that were submaximally loaded with Ca^{2+}, the intraluminal Ca^{2+} threshold required for ryanodine- and Ca^{2+}-induced Ca^{2+} release (CICR) markedly decreased in a concentration dependent manner. Under identical conditions, Tg (≥10μM) also directly induced a rapid release of Ca^{2+}. In this case, Ca^{2+} re-accumulation was prolonged and vesicles remained sensitive to further CICR. At higher concentrations Tg (≥20μM) caused a rapid release of Ca^{2+} which was not re-accumulated by the SR vesicles. However, under conditions of ryanodine inhibition of CICR, Tg-induced Ca^{2+} release was markedly diminished. Thus, Tg inhibition of the SR Ca^{2+}-ATPase appears to stimulate SR Ca^{2+} release through the ryanodine receptor. In general, Tg appeared not to affect SR Ca^{2+} transport until the Ca^{2+} release channel was fully open and maximal CICR had occurred. This curious action of Tg upon SR Ca^{2+} transport was reflected in its effect upon [^{3}H]-ryanodine binding to SR vesicles. In the absence of ATP, Tg did not promote the binding of [^{3}H]-ryanodine. On the contrary, 100 μM Tg inhibited (50%) the binding of [^{3}H]-ryanodine. In the presence of mM concentrations of ATP, however, 10 μM Tg consistently elevated [^{3}H]-ryanodine binding by over 50%. These observations provide preliminary evidence that the actions of the Ca^{2+}-ATPase and ryanodine receptor in SR vesicles in regulating SR Ca^{2+} transport are coupled

(Supported by the Medical Research Council of Canada)

Tu-Pos123

NICOTINAMIDE ADENINE DINUCLEOTIDE EFFECTS UPON SKELETAL MUSCLE SARCOPLASMIC RETICULUM CALCIUM RELEASE AND RYANODINE BINDING.

((J.S.C. Gilchrist, C. Palahniuk, and R. Bose)) Departments of Oral Biology and Pharmacology, University of Manitoba, Winnipeg, Manitoba, Canada. R3E 0W2

In this study, we investigated nicotinamide adenine dinucleotide effects upon SR Ca^{2+} uptake and Ca^{2+} release. Ca^{2+} transport was assayed by monitoring Calcium Green-2 fluorescence (λ_{ex}=488nm/λ_{em}=540nm) in response to extraluminal Ca^{2+} transients. Cisternal SR vesicles (0.5-1 mg.ml^{-1}) were selectively loaded with Ca^{2+} in the absence of co-precipitating anions by ATP-dependent Ca^{2+} uptake. NADH (750 μM) and NADPH (4-8 mM) were found to (a) directly induce Ca^{2+} release and, (b) markedly sensitize SR vesicles to ryanodine-induced and Ca^{2+}-induced Ca^{2+} release (CICR). Sensitization effects were manifest as a reduction in the intraluminal Ca^{2+} threshold requirement for Ca^{2+} release. With NADH, in particular, SR vesicles remained remarkably sensitive to the repetitive triggering of Ca^{2+} release by this nucleotide. Indeed, the profile of repetitive NADH-induced Ca^{2+} release and Ca^{2+} re-uptake was virtually indistinguishable from the kinetic profile observed with CICR. In contrast, NAD (1 mM) and NADP (4 mM) desensitized SR vesicles to ryanodine- and Ca^{2+}-induced release of Ca^{2+}. NAD markedly attenuated ryanodine stimulation of release channel opening and diminished the magnitude of CICR. NADP had similar effects by substantially increasing the intraluminal Ca^{2+} requirement for CICR. The inhibitory effects of NAD were not prevented by the presence of DTT. Other adenine nucleotide effects were also examined. Only AMP-PNP, ADP and cyclic AMP possessed Ca^{2+} releasing activity. ATP and AMP did not directly induce Ca^{2+} release. Potency of nucleotide activation of Ca^{2+} release paralleled nucleotide stimulation of [^{3}H]-ryanodine binding (AMP-PNP≈NADH>ADP>NADPH>ATP≈AMP>cyclic AMP≈NAD>NADP). In this study the most interesting phenomenon was the contrary effects of the reduced versus oxidized nicotinamide adenine dinucleotides. Thus, SR vesicles may be uniquely sensitive to the redox status of nicotinamide adenine dinucleotides. This may represent a mechanism by which SR Ca^{2+} transport may be regulated by intracellular redox status.

(Supported by the Medical Research Council of Canada)

Tu-Pos124

CHOLINERGIC REGULATION OF $[Ca^{2+}]_i$ AND ION CHANNELS IN HUMAN ESOPHAGEAL SMOOTH MUSCLE CELLS. ((G.R. Wade, H.G. Preiksaitis, Y. Jiao, & S.M. Sims)) The Department of Physiology, The University of Western Ontario, London, Ontario, CANADA. (Sponsored by M. Karmazyn)

Intracellular Ca^{2+} concentration ($[Ca^{2+}]_i$) plays a key role regulating contraction of smooth muscle. It has been reported that extracellular Ca^{2+} is required for cholinergic excitation of esophageal smooth muscle, with little evidence for the involvement of intracellular Ca^{2+} stores. We investigated cholinergic regulation of $[Ca^{2+}]_i$ and ion channels in freshly dispersed human esophageal muscle cells. In single channel studies of the large conductance Ca^{2+}-dependent K^+ channel (K_{Ca}), ACh caused contraction accompanied by a transient increase in channel open probability. This occurred when channels were isolated from ACh by the electrode and when cells were clamped near 0 mV using 135 mM K^+ in the bath. These results are consistent with the involvement of a cytosolic second messenger. When we investigated the participation of Ca^{2+} stores using fura-2 fluorescence, ACh caused elevation of $[Ca^{2+}]_i$ from a basal level of 153 ± 44 nM to 457 ± 155 nM. Ca^{2+} transients from 129 ± 26 nM to 276 ± 42 nM were also elicited in Ca^{2+} free solutions and caffeine elicited similar transients, implicating Ca^{2+} stores. We have previously demonstrated that ACh-mediated release of Ca^{2+} from stores causes acute inhibition of Ca^{2+} current (I_{Ca}) in gastric and tracheal smooth muscles. Using perforated-patch recording, we identified L-type Ca^{2+} current in human esophageal muscle. ACh caused an acute reduction of I_{Ca} with peak amplitude reduced by $58\pm5\%$. We conclude that muscarinic excitation of human esophageal smooth muscle involves release of Ca^{2+} from intracellular stores. We are investigating the signalling events underlying the regulation of K_{Ca} and I_{Ca}. SUPPORTED BY M.R.C. OF CANADA.

Tu-Pos125

DETERMINATION OF RELEASABLE CALCIUM IN ISOLATED RABBIT TRIADS/TERMINAL CISTERNAE((J.W. Kramer, and A.M Corbett)) Dept. of Biochemistry & Molecular Biology; Wright State University, Dayton, OH 45435

Isolated skeletal muscle triad/terminal cisternae vesicles were actively loaded with 160, 320, and 480 nmol/mg calcium. The loaded vesicles were then subjected to chemical depolarization in the presence and absence of 15 mM caffeine. Through the use of the calcium sensitive dye, Fura-2, calcium release was monitored and measurements were taken which represented calcium released due to depolarization, and then again after 1 hour to determine the percentage of loaded calcium that was released from the vesicles. After 1 hour, in the absence of caffeine, the vesicles released 67-92% of loaded calcium. In the presence of caffeine, the vesicles released 85-113% of the loaded calcium (mean of 96% released). This data shows that all of the loaded calcium is releasable, proving that little added calcium is bound to vesicular membranes. The amount of calcium that was released upon depolarization was approximately doubled in the vesicles that were loaded with 320 and 480 nmol/mg calcium in the presence of 15 mM caffeine, but, unlike other studies, total calcium release was not complete in 10 sec. Further studies will be performed to determine whether this increase is an effect on junctional or non-junctional ryanodine receptors.

Tu-Pos126

PHOSPHOLAMBAN EXPRESSION IN TRANSGENIC MICE PROLONGS FAST-TWITCH SKELETAL MUSCLE RELAXATION ((J.P. Slack, I. L. Grupp, D.G. Ferguson and E. G. Kranias)) University of Cincinnati, Cincinnati, OH 45267. (Spon. by T. Kirley)

Phospholamban (PLB) is a regulator of the affinity of the sarcoplasmic reticulum (SR) Ca^{2+}-ATPase (SERCA2) for calcium and a key modulator of myocardial contractility. *In vitro* reconstitution and cell culture expression studies have shown that PLB can also regulate SERCA1, the fast-twitch skeletal muscle isoform of the SR Ca^{2+}-ATPase, resulting in decreased rates of SR Ca^{2+}-uptake. To determine whether this regulation can be of physiological relevance, we generated a transgenic (TG) mouse that ectopically expressed PLB in fast-twitch skeletal muscle, a tissue normally devoid of PLB. The myosin light chain 1f promoter and its enhancer were used to drive skeletal muscle specific expression of PLB. Western analysis of fast-twitch skeletal muscle homogenates revealed expression of phospholamban, and indirect immunofluorescence labeling demonstrated that the expressed protein was co-localized with SERCA1 in the SR membranes. Examination of isometric twitch contractions of the extensor digitorum longus (EDL) indicated that the introduction of PLB into fast-twitch skeletal muscle was associated with a prolongation in the time to half-relaxation compared to wild-type(WT) muscles (13 msec in TG *vs* 7 msec in WT) . These findings suggest that PLB can regulate SERCA1 *in vivo* and this leads to decreases in the rates of relaxation of fast-twitch skeletal muscle, consistent with its inhibitory effects on SR Ca^{2+}-uptake.

Tu-Pos127

CHARACTERIZATION OF Na^+ EFFLUX AND Na^+ INFLUX USING THE FLUORESCENT INDICATOR, SBFI: DUAL EFFECTS OF DOPAMINE ON Na^+ HOMEOSTASIS IN VASCULAR SMOOTH MUSCLE CELLS. ((M.L. Borin)) Dept. of Physiol., Univ. of Maryland Sch. Med., Baltimore, MD 21201.

The goal of these experiments was to determine the effect of dopamine on Na^+ influx, Na^+ efflux and Na^+ pump activity by measuring changes in intracellular Na^+ concentration ($[Na^+]_i$) in SBFI-loaded smooth muscle cells. The protocol consisted of 3 steps: (1) preincubation of the cells in Na^+-free medium, to deplete intracellular Na^+; (2) exposure to Na^+-containing, K^+-free medium (Na^+ pump is inhibited; a rise in $[Na^+]_i$ reflects Na^+ influx); (3) exposure to K^+-containing Na^+-free medium (Na^+ influx is inhibited and Na^+ pump is activated; a decline in $[Na^+]_i$ reflects Na^+ efflux). The rise in $[Na^+]_i$ consisted of a rapid and a slow phase; the rapid phase reflected, presumably, the activation of the Na^+/H^+ exchange. The decrease in $[Na^+]_i$, which was a combination of the Na^+ pump-mediated and passive Na^+ efflux, had an average time constant (τ) of 1.8 min. Inhibition of the Na^+ pump with ouabain substantially slowed the decline in $[Na^+]_i$ (τ = 8 min). Na^+ pump kinetics were determined by plotting the rate of the ouabain-sensitive Na^+ efflux as a function of $[Na^+]_i$. This method allowed determination of the pump rates below resting $[Na^+]_i$ and provided a correction for passive Na^+ fluxes. The rate of Na^+ pumping was saturable and dependent on $[Na^+]_i$, with a K_m of 10 mM and V_{max} of 24 mM.

Dopamine (10-200 μM) inhibited the influx of Na^+ in a dose-dependent manner; IC_{50} for initial rate of the rise in $[Na^+]_i$ was 100 μM. Furthermore, dopamine also reduced the rate of Na^+ efflux (e.g., τ increased to 3.5 min in the presence of 100 μM dopamine). The latter effect was due to the inhibition of the Na^+ pump because passive Na^+ efflux was not affected). The inhibition of the Na^+ pump was due to a reduction in its turnover rate ($\approx$ 2-fold reduction in V_{max} in the presence of 200 μM dopamine). In contrast to the reduction in V_{max}, the affinity of the Na^+ pump for Na^+ was not affected by dopamine.

In summary, (1) fluorescent measurements of $[Na^+]_i$ with SBFI provide a convenient way of characterizing of Na^+ fluxes in single cells; (2) dopamine inhibits both Na^+ influx and Na^+ pump-mediated Na^+ efflux in vascular smooth muscle cells.
Supported by NIH HL50700 and AHA Maryland Affiliate Grant-in-Aid

Tu-Pos128

EXPRESSION OF THE T704M HYPERKALEMIC PERIODIC PARALYSIS MUTATION IN MOUSE ((L.A. Slobotski*, C.M. Gomez*, J.W. Day*, P.A. Iaizzo*)) *Department of Anesthesiology and Program in Biomedical Engineering; *Department of Neurology, University of Minnesota, Minneapolis, MN 55455.

Hyperkalemic periodic paralysis (HyperPP) is an autosomal dominant muscle disease transmitted with a high rate of penetrance. Several distinct clinical phenotypes of this disease have been described and are known to be due to different point mutations in the adult, TTX-sensitive skeletal muscle sodium channels. We have designed a transgene construct for expression of the human sodium channel alpha subunit in mice based on the promoter for the mouse muscle creatine kinase gene. We have generated a transgenic mouse line that over-expresses the human T704M sodium channel mutation several-fold above endogenous mouse alpha subunit. In situ phenotypic analysis is ongoing by exposing the gastrocnemius to a high (7-9 mM) potassium solution to simulate the human HyperPP provocation test. Force, EMG and ionic conductance measurements are being obtained in the presence and absence of specific pharmacologic agents (e.g. anesthetics) so that we can gain insight into hyperkalemic periodic paralysis and into the structure-function relationship of the human adult skeletal muscle sodium channel.

Tu-Pos129

DISTINCT LOCAL ANESTHETIC AFFINITIES IN HUMAN Na^+ CHANNEL ISOFORMS. ((D.W. Wang, L. Nie, A.L. George and P.B. Bennett)) Department of Pharmacology. Vanderbilt University, Nashville, TN 37232.

Molecular genetics and cloning have revealed the existence of at least five unique voltage gated Na^+ channels encoded by distinct genes and expressed in different tissues. Lidocaine is a widely used local anesthetic and antiarrhythmic drug that is believed to exert its clinically important action by blocking Na^+ channels. We find that the cardiac and skeletal muscle isoforms also have distinct local anesthetic affinities. The recombinant skeletal muscle (hSkM1) and cardiac sodium channels (hH1) were transfected into tsA201 cells and studied under identical conditions using whole-cell voltage clamp. Tonic block at high concentrations of lidocaine (0.1 mM) was greater in hH1 than in hSKM1. This was also true for use-dependent block where 25 μM lidocaine produced an inhibition equivalent to 0.1 mM in the skeletal muscle isoform. Thus, the cardiac isoform was at least four times as sensitive as the skeletal muscle isoform. Pulse protocols optimized to explore inactivated state block revealed a similar time- and concentration- dependence except that the hSkM1 (IC_{50} = 172 μM, N=6) five to eight times less sensitive ($p<0.05$) to block by lidocaine than the hH1 (IC_{50} = 21 μM, N=13). We conclude that the cardiac sodium channel is intrinsically more sensitive to inhibition by lidocaine.

Tu-Pos130

GENISTEIN AND L-TYPE Ca^{2+} CHANNEL ANTAGONISTS INHIBIT Ba^{2+} ENTRY IN A10 VASCULAR SMOOTH MUSCLE CELLS (VSMC). ((J. Di Salvo, S. E. R. Nelson and T. S. Chien)) Med. & Mol. Physiol., Univ. of Minnesota-Duluth, Duluth, MN 55812.

Recently, we suggested that receptor-activated increases in $[Ca^{2+}]_i$ in VSMC may be dependent on tyrosine kinase activity (TKA). Because Ba^{2+} is used to study Ca^{2+} channel function, we studied Ba^{2+} entry in A10 VSMC. Ba^{2+} entry can be monitored by electrophysiological techniques, or by ratiometric fluorescence analysis of fura-2 loaded cells. We sought to study (a) Ba^{2+} entry in intact fura-2 loaded A10 VSMC, (b) the sensitivity of Ba^{2+} entry to antagonists for L-type Ca^{2+} channels, and (c) if Ba^{2+} entry was suppressed by genistein, an inhibitor of TKA. Exposure of cells to 5 mM Ba^{2+} produced a monotonic increase in the 340/380 fluorescence ratio which attained a maximal value within 4-6 min and was maintained for up to 30 min. Preincubation with genistein (148 μM) resulted in 80-100% inhibition of the Ba^{2+} response. Similarly, 50-100% inhibition occurred after preincubation with L-channel antagonists (10 μM) including nicardipine, nifedipine, verapamil, and diltiazem. In contrast, treatment with 200 μM cromakalim, a K^+_{ATP} channel opener, did not alter the response. Thus, Ba^{2+} entry occurs in resting A10 VSMC through a pathway behaving as an L-type Ca^{2+} channel. The results suggest that the pathway may be modulated by TKA.

Tu-Pos131

VASOPRESSIN (AVP) ACTIVATION OF A7r5 VASCULAR SMOOTH MUSCLE CELLS (VSMC): PROTEIN TYROSINE PHOSPHORYLATION (PTP) AND $[Ca^{2+}]_i$. ((N. Kaplan, E.K. Stauffer, and J. Di Salvo)) Med. & Mol. Physiol., Univ. of Minnesota-Duluth, Duluth, MN. 55812. (Spon. by D. Levitt)

AVP increases PTP and $[Ca^{2+}]_i$ in VSMC. To determine if these events were coupled, we studied effects of tyrosine kinase inhibitors (TKI) on AVP induced increases in PTP and $[Ca^{2+}]_i$ in A7r5 VSMC loaded with fura-2. AVP (20 nM) induced a transient increase in $[Ca^{2+}]_i$ followed by a smaller sustained increase. In most cells, 60% of the transient was due to influx of extracellular Ca^{2+} and 40% to release of intracellular Ca^{2+}. In all cells, the sustained increase was due to Ca^{2+} influx only. Genistein (148 μM) blocked the transient and sustained components of the response. In contrast, 105 μM lavendustin A, a different TKI, suppressed the transient by only 30%. Another TKI, tyrphostin 47 (80 μM), did not alter either component. Special conditions were required to study PTP. AVP induced a transient increase in PTP in cells preincubated with 10 mM vanadate, a tyrosine phosphatase inhibitor. Time courses for AVP induced transient increases in PTP and $[Ca^{2+}]_i$ were similar. Vanadate alone increased PTP and induced a small increase in $[Ca^{2+}]_i$. Genistein blocked PTP induced by AVP+vanadate, and increases in $[Ca^{2+}]_i$ induced by vanadate alone. Unexpectedly, lavendustin or tyrphostin enhanced vanadate induced PTP and precluded assessment of AVP induced PTP. Lavendustin enhanced the vanadate induced increase in $[Ca^{2+}]_i$. Under conditions where changes in PTP could be measured, the results suggested that AVP activated increases in PTP may be coupled to AVP activated mechanisms that regulate influx of extracellular Ca^{2+} and release of intracellular Ca^{2+}.

Tu-Pos132

ACETYLCHOLINE AND PROTEIN KINASE C ACTIVATION INHIBIT DELAYED RECTIFIER K^+ CURRENT IN GUINEA PIG TAENIA COLI MYOCYTES ((N.M. Magoski and W.C. Cole)) The Smooth Muscle Research Group, Faculty of Medicine, University of Calgary, Calgary, AB, Canada, T2N 4N1.

The effects of acetylcholine (ACh; 10 μM) and protein kinase C (PKC) activation with analogs of diacylglycerol (DAG) on delayed rectifier K^+ current (K_{dr}) in myocytes from guinea pig taenia coli was studied using whole-cell patch clamp technique. The pipette and bath contained (in mM): 110 K-gluconate, 30 KCl, 5 Na_2ATP, 0.5 $MgCl_2$, 10 BAPTA, 5 Hepes, 1 GTP, (pH 7.2) and 120 NaCl, 3 $NaHCO_3$, 4.2 KCl, 1.2 KH_2PO_4, 0.5 $MgCl_2$, 10 glucose, 10 Hepes, 1.8 $CaCl_2$, (pH 7.4), respectively, at 20°C. Net end-pulse current and K_{dr} tail current amplitudes were determined with 250 ms steps to -50 and +20 mV and a subsequent step to -40 mV, respectively. ACh depressed end-pulse and tail current amplitude of K_{dr}. The active DAG analog, 1,2-diC_8 reduced K_{dr} in a dose-dependent fashion: for example, 1 & 10 μM caused ~61 & ~100% decline in the amplitude of K_{dr} tails at -40 mV, respectively. The inactive DAG analog, 1,3-diC_8, had little effect on K_{dr} at 1 μM. Dialysis for 15 to 20 min with the specific PKC inhibitor, chelerythrine (50 μM), had no effect on K_{dr} but it reduced the inhibition of the current by 1,2-diC_8. These data suggest the presence of a signal transduction pathway for inhibtion of K_{dr} in taenia coli smooth muscle cells which involves muscarinic receptors and PKC activation. Supported by MRC (WCC).

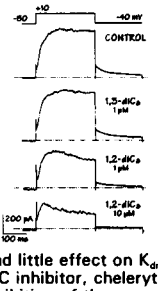

Tu-Pos133

TIME-DEPENDENT RELAXATION OF RAT AORTA BY BACTERIAL LIPOPOLYSACCHARIDE IS BLOCKED BY TEA. ((L.H. CLAPP & S.J. HALL)) Cardiovascular Research, UMDS Smooth Muscle Group, St. Thomas's Hospital, London SE1 7EH, U.K.

In isolated blood vessels, application of lipopolysaccharide (LPS) causes relaxation and hyporeactivity to vasoconstrictors. These effects are thought to be mediated primarily by the vascular synthesis of nitric oxide (NO) through the induction of NO synthase (iNOS). We have investigated whether activation of K^+ channels is responsible for the effects of LPS. Helical strips of rat aorta (-endothelium) were perfused with physiological saline at 37 °C. Tissues were precontracted with 1μM phenylephrine (PE) and incubated with and without 0.1μg/ml of LPS. Time controls showed that PE contractions relaxed by only 17 ± 3.5% (n=6) after 4 hours, while LPS caused a significantly ($p<0.01$) greater relaxation compared to controls (55.5 ± 4.6, n=13). Furthermore muscle strips pre-incubated with 10 mM TEA, produced relaxation to LPS that was not significantly different to controls. Reversal of LPS effects occurred if TEA was given after LPS, implying that this agent is not blocking induction of iNOS. L-arginine (1mM) applied several hrs after LPS caused additional relaxation of rat aorta (to 20.6±2.8%, n=10), which was partially reversed by 10 mM TEA (68.7±4 %, n=7). Both TEA and L-arginine had no significant effect on PE contractions under control conditions. These results suggest that LPS causes time-dependent relaxation by activation of TEA-sensitive K^+ channels. *Supported by the Wellcome Trust*

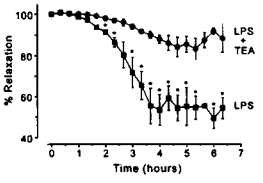

Tu-Pos134

Activation of Potassium Channels by ATP in Murine Colonic Smooth Muscle Cells ((S.D.Koh, K.S.Kim*, and K.M.Sanders)) Department of Physiology, School of Medicine, University of Nevada Reno, NV 89557 *Department of Physiology, College of Medicine, Hanyang University, Seoul 133-791, Korea

ATP induces hyperpolarization in murine and human colonic smooth muscle cells as measured with conventional microelectrode techniques. The hyperpolarization induced by ATP is not blocked by charybdotoxin, 4-aminopyridine(4-AP), or tetraethylammonium (TEA), but can be blocked by apamin(10^{-7} M). This suggests that ATP may activate small conductance Ca^{2+} activated K-channels that have been described in skeletal muscle(Blatz and Magleby, 1986) and hepatocytes(Capoid and Ogden, 1989). To date, these channels have not been observed in mammalian smooth muscle. We have studied activation of K-channels by ATP in isolated murine circular muscle cells with the whole cell and single channel configurations of the patch clamp technique. Two types of K-current, a rapidly inactivating component and non-inactivating component sensitive to 4-AP(10mM) and TEA(1mM) were observed in dialyzed cells. ATP(1mM) did not increase outward current under these conditions. We also studied the effects of ATP in cells with amphotericin B-perforated patches. In these cells ATP increased outward current(12.3 ± 0.7%, n=3). Pretreatment with apamin blocked the ATP-induced outward current(n=3). Recordings from cell attached patches showed that ATP increased open probability(NP_o 0.12 ± 0.5) of a 12pS K-channel at -60 mV. NP_o of these channels under control conditions was very low(i.e., <0.001). EGTA(5mM) decreased NP_o of the channels activated by ATP in excised patches. These data suggest that the apamin sensitive conductance responsible for part the inhibitory neural regulation of gastrointestinal muscles may be mediated by 12pS, apamin-sensitive class of Ca^{2+} activated K-channels. (supported by NIH DK 41315)

Tu-Pos135

EFFECTS of NS-1619 on CONTRACTILE PROPERTIES and TRANSMEMBRANE CURRENTS in ISOLATED URINARY BLADDER DETRUSOR TISSUE and MYOCYTES. **((Jeffrey H. Sheldon, N. Wesley Norton and Thomas M. Argentieri)) Wyeth-Ayerst Research, Cardiovascular and Metabolic Diseases, Princeton, NJ. 08543-8000**

The effects of the putative maxi-K channel opener NS-1619 on contractility and transmembrane currents were studied in isolated rat urinary bladder strips and in enzymatically dissociated guinea pig bladder detrusor smooth muscle cells, respectively. Detrusor strips were precontracted with 20 mM KCl. Exposure to NS-1619 produced a concentration-dependent decrease in the spontaneous contraction amplitude and frequency with an IC_{50} of 15.7±3.2 μM (mean±SEM, n=4). After drug, tissues could be contracted with carbachol (10 μM) or iberiotoxin (IbTx, 100 nM), but not by glyburide (6 μM). Transmembrane currents were assessed using standard whole cell voltage clamp techniques. Exposure to NS-1619 (10, 30 and 100 μM, 5 min.; n= 2-6) produced a concentration-dependent increase in outward current at potentials greater than 10 mV (step protocol: V_h=-50mV, V_t=-60 to 40 mV, t= 850 ms) that was reversed by IbTx or by wash-out. NS-1619 (30 μM, n=6) produced both an increase in steady-state outward current (105±38% @ 30 mV, $p<0.05$), as well as a decrease in the calcium window current (ramp: -60 to 40 mV @3.34 mV/sec.). IbTx reversed the effects of NS-1619 on outward steady-state current, but had no effect on the inhibition of steady-state calcium current. NS-1619 (30 μM, n=4) decreased peak calcium current amplitude (V_h=-40mV, V_t=-40 to 50 mV, t= 200 ms) by 71±7 % ($p<0.05$) and was partially reversed upon wash-out. Peak calcium current activation was at 0 mV for both control and NS-1619 treated cells. In conclusion, NS-1619: (i) inhibits contractility of isolated detrusor tissue, (ii) increases an IbTx-sensitive outward current in a dose dependent manner, consistent with activation of a maxi-K^+ current, and (iii) inhibits both peak and steady-state L-type calcium current.

Tu-Pos136

PROLONGED EXPOSURE OF VASCULAR SMOOTH MUSCLE CELLS TO CYTOCHALASIN D DOES NOT AFFECT THE ACTIVITY OF THE LARGE CONDUCTANCE CALCIUM ACTIVATED K CHANNELS. ((J.R. Serrano, R. Matteo, C.A. Obejero-Paz and A. Scarpa)) Dept. Physiol & Biophys, School of Medicine . Case Western Reserve University. Cleveland , Ohio 44106.

Several reports suggest that cytoskeleton is involved in the modulation of ion channels in different cells. Changes in cytoskeleton characteristics of vascular smooth muscle (VSM) cells have been observed during development or several pathological conditions. This in principle could affect the properties of ion channels necessary to maintain a normal excitability of these cells. Here we investigated the effects of 0.14 μg/ml cytochalasin D (CD) applied during 24 h on large conductance Ca activated K channels from fresh isolated rat aorta VSM cells. Single channel currents were recorded at the resting membrane potential of the cells (-40 to -60 mV) using the cell attached configuration of the patch clamp technique. Cells were depolarized using a high extracellular K^+ (low Ca^{+2}) solution. Cells treated with CD showed a rounded morphology as compared with the spindle like shape of control cells. In both preparations the percentage of patches showing channel activity was comparable (control: 8 out of 39 cells (21%); CD: 12 out of 37 (32%)). The single channel conductance was not affected by CD ((Mean ± SD) Control: 196±31 pS (n=8) and CD: 163±10 (n=10) respectively). Channel activity was investigated at steady membrane potentials. NPo was calculated from records lasting more than 30 s. Similar parameter values were found in both populations ((Median and Range) Control: 0.14%, 0.03-7.39% (n=8), CD: 0.06%, 0.02-0.19%.(n=10)). These results suggest that the open probability and conductance of large Ca^{+2} activated K^+ channels in VSM cells is unaffected by the disruption of the actin filament network. Supported by NIH HL41618.

Tu-Pos137

REDUCED MEMBRANE RESISTANCE AND INCREASED INWARD CHLORIDE CONDUCTANCE IN CULTURED TRISOMY 16 MOUSE TONGUE MUSCLE CELLS SUGGEST A MECHANISM FOR THE HYPOTONIA IN HUMAN DOWN SYNDROME S. Peng, S. I. Rapoport, and Z. Galdzicki
Lab of Neuroscience, NIA. NIH. Bethesda, MD 20892

Trisomy 16 (Ts16) mouse is a genetic animal model of Down syndrome (DS; human Ts21). DS patients develop hypotonia in striated muscle. Tongue muscle is an example. A whole-cell patch-clamp method was used to study membrane properties of isolated Ts16 and diploid control tongue muscle cells in primary culture prepared from mouse embryos.

Patch clamp recordings were done in physiological solutions with 1 mM $CdCl_2$. Cells were treated with 0.1 μM colcemid before tests. Membrane resistance (R_m) and capacitance (C_m) were measured at a holding potential of -60 mV. Mean Ts16 cell R_m was 369 MΩ (SEM, ±31; n=26), whereas control R_m was 505 MΩ (SEM, ±38; n=33). Thus the mean Ts16 cell R_m was 27% less than that of control. We did not detect a significant difference in C_m between the two groups of cells. Furthermore, we applied depolarization voltage steps to elicit total membrane current at holding potential of -60 mV. The mean of normalized maximum outward conductance ($G_{max,out}/C_m$) was 491 pS/pF (SEM, ±58; n=25) and 840 pS/pF (SEM, ±78; n=33) for Ts16 and control cells, respectively. Thus the $G_{max,out}/C_m$ of the Ts16 cells was 42% lower than that of control, but there was no significant difference in inward current or conductance. Direct measurements on Cl^- current in absence of K^+ showed that the mean of $G_{max,out}/C_m$ was 344 pS/pF (SEM, ±29 n= 26) and 104 pS/pF (SEM, ±15 n=25) for Ts16 and control cells, respectively. Therefore, the cause of hypotonia could be the increased Cl^- conductance, which interacts with action potential initiation.

Tu-Pos138

CALCIUM-ACTIVATED CHLORIDE CURRENT IN PULMONARY ARTERY SMOOTH MUSCLE CELLS. ((X.-J. Yuan and L.J. Rubin)) Division of Pulmonary Medicine, University of Maryland School of Medicine, Baltimore, MD 21201.

Many agonists induce membrane depolarization by promoting Ca^{2+} influx through Ca^{2+} channels and releasing intracellular Ca^{2+}. Activation of Ca^{2+}-activated Cl^- (Cl_{Ca}) channels may be one of the mechanisms by which increased $[Ca^{2+}]_i$ causes membrane depolarization. In this study, we characterized the biophysical and pharmacological properties of Cl_{Ca} currents ($I_{Cl(Ca)}$) in primary cultured (for 3-6 days) smooth muscle cells of rat pulmonary artery (PA). Whole-cell Cl^- currents were recorded by patch clamp techniques, and $[Ca^{2+}]_i$ was measured with fura-2 using quantitative fluorescence microscopy system. The external solution included (mM): 141 NaCl, 1.8 $CaCl_2$, 1.2 $MgCl_2$, 4.7 KCl, 10 HEPES, 10 glucose (pH 7.4); the internal (pipette) solution included (mM): 135 CsCl, 5 ATP, 4 $MgCl_2$, 10 TEA-Cl, and 10 HEPES (pH 7.2). Depolarizations elicited an inward Ca^{2+} current (I_{Ca}), followed by a sustained outward current which reverses near Cl^- equilibrium potential (E_{Cl}=0.2 mV). Repolarizing voltage steps produced a large inward tail current (I_{tail}) which also reverses at a potential close to E_{Cl}. The amplitude of I_{tail} positively correlates to the amplitude of I_{Ca}. Replacement of extracellular Ca^{2+} with equimolar Ba^{2+} abolished I_{tail}, while significantly augmented I_{Ca}. I_{tail} was also blocked by the Cl^- channel blocker, niflumic acid (10-50 μM), and nitroprusside, a nitric oxide-generating compound. In the absence of extracellular Ca^{2+}, cyclopiazonic acid, an inhibitor of Ca^{2+}-ATPase in sarcoplasmic reticulum (SR), increased $[Ca^{2+}]_i$ by releasing Ca^{2+} from SR, and thus elicited an inward Cl^- current at a holding potential of -70 mV. These results indicate that rat PA smooth muscle cells possess Cl_{Ca} channels which are activated by depolarization-induced Ca^{2+} influx and agonist-induced Ca^{2+} release. This Cl^- current may contribute to the agonist-induced membrane depolarization in PA smooth muscle cells.

Tu-Pos139

A POTENTIAL ROLE FOR Ca^{2+}-ACTIVATED Cl^- CHANNELS IN THE DEVELOPMENT OF MYOGENIC TONE IN PRESSURIZED RABBIT MESENTERIC ARTERIOLES?. ((C.V. Rémillard & N. Leblanc)) Dept. of Physiology, U. of Montréal, and Research Centre, Montréal Heart Institute, Montréal, Québec, Canada H1T 1C8.

Recent findings have indicated that Ca^{2+}-activated Cl^- channels ($I_{Cl(Ca)}$) may act as modulators of membrane potential in smooth muscle. This study was designed to elucidate the potential role of $I_{Cl(Ca)}$ in the generation of myogenic tone. Rabbit resistance mesenteric arteriole (ID < 100μm) segments were cannulated and subjected to increasing transmural pressure steps (0-50 mmHg) prior and following agonist application. In the absence of an agonist, nifedipine (1μM) had no effect on pressure-induced diameter changes, suggesting little contribution by sarcolemmal Ca^{2+} channels to resting tone following increased pressure. However, nifedipine reversed most of the constriction induced by phenylephrine (PE; 1μM), an α_1-agonist, suggesting that activation of voltage-dependent Ca^{2+} channels plays a major role in the α_1-adrenergic-induced contractile response. A blocker of $I_{Cl(Ca)}$, niflumic acid (NfA; 100μM), was used to verify the contribution of $I_{Cl(Ca)}$ to myogenic tone. TEA (1mM) was also added to the bathing solution to block Ca^{2+}-activated K^+ channels (K_{Ca}) channels since NfA has been shown to activate this channel. TEA alone produced little effect on the pressure-diameter relationship, but accentuated the constriction induced by PE. When arteries were preconstricted with 500nM PE and 1mM TEA, subsequent exposure to NfA produced relaxation in 2 vessels, and constriction in 2 other vessels; pressure-diameter relationships exhibited complex biphasic characteristics. In the absence of endothelium, NfA produced a significant relaxation of the PE-TEA preconstricted arteries. This relaxation is consistent with a hyperpolarization of the membrane potential following inhibition of $I_{Cl(Ca)}$. These results indicate a possible role for $I_{Cl(Ca)}$ in the development and maintenance of myogenic tone in rabbit mesenteric arterioles. Supported by grants from the HSFC (C.V.R.) and MRC (N.L.).

Tu-Pos140

NITRIC OXIDE INHIBITS SARCOPLASMIC RETICULUM Ca^{2+} RELEASE IN PORCINE TRACHEAL SMOOTH MUSCLE CELLS ((Y.S. Prakash, M.S. Kannan and G.C. Sieck)) Depts. of Anesthesiology and Physiology & Biophysics, Mayo Foundation, Rochester, MN 55902 and Department of Veterinary PathoBiology, University of Minnesota, St. Paul, MN 55108. (Spon. C.F. Louis).

Nitric oxide (NO) released from nonadrenergic, noncholinergic inhibitory nerves of porcine tracheal smooth muscle (TSM) relaxes tone through cGMP-dependent mechanisms. In this study, we investigated the effect of s-nitroso-n-acetylpenicillamine (SNAP), a NO donor, on sarcoplasmic reticulum (SR) Ca^{2+} release induced by acetylcholine (ACh) or caffeine. In freshly-isolated, single porcine TSM cells using a video fluorescence imaging technique, intracellular Ca^{2+} ($[Ca^{2+}]_i$) was measured as the ratio of fura-2 emissions when excited at 340 and 380 nm. With an extracellular Ca^{2+} concentration of 0 and 2.5 mM, SNAP (0.1-1.0 μM) attenuated the $[Ca^{2+}]_i$ in response to ACh (0.1-1.0 μM). Exposure to caffeine (50 mM) after an ACh response resulted in an elevation of $[Ca^{2+}]_i$ that was smaller than the initial ACh response. Pre-exposure to SNAP did not alter this caffeine response. However, SNAP inhibited caffeine responses in cells that were not pre-exposed to ACh. Exposure to SNAP alone resulted in a significant reduction of basal $[Ca^{2+}]_i$ .When the cells were stimulated with ACh in zero Ca^{2+} and SNAP, addition of 2.5 mM resulted in an immediate elevation of $[Ca^{2+}]_i$. These results suggest that SNAP inhibits SR Ca^{2+} release via both the IP_3 and ryanodine receptors, with no effects on Ca^{2+} uptake into SR and Ca^{2+} entry from the extracellular space. Supported by NIH grant HL#51736-02C, Mayo Fdn., and Univ. of Minnesota. MSK was a recipient of an Abbott Fellowship.

Tu-Pos141

MODULATION OF THE RYANODINE – RECEPTOR CHANNEL IN VASCULAR SMOOTH MUSCLE. ((J. Y. Su)) Dept. of Anesthesiology, Box 356540, University of Washington, Seattle, WA 98195-6540

This study was performed to examine the effect of modulators of the ryanodine–receptor Ca^{2+} channel on caffeine–induced tension transients in saponin-skinned strips of aorta (AO) and femoral artery (FA) from the rabbit. The skinned arterial strips were cycled in solutions to load Ca^{2+} into and to release Ca^{2+} from the SR using caffeine (a load–release cycle). In each skinned strip, three cycles were performed: a control, a conditioning (the releasing solution contained ± $[ryanodine]_i$ and $[caffeine]_i$, $[Ca^{2+}]_i$, or $[Mg^{2+}]_i$ ± ryanodine), and finally a test. Ryanodine (0.3 nM – 1 μM), in the presence of 25 mM caffeine, caused a dose–dependent depression of caffeine–induced tension transients (ryanodine depression) to a similar degree in AO and FA (IC_{50} = 9.5 ± 2 nM *vs.* 7.9 ± 3 nM for pCa 6.8 – 7.0, or 0.23 ± 0.014 μM *vs.* 0.23 ± 0.018 μM for pCa > 9). Ryanodine depression was a function of $[caffeine]_i$, or $[Ca^{2+}]_i$ (pCa < 6.0) which was potentiated by caffeine, and an inverse function of $[Mg^{2+}]_i$ (($[caffeine]_{50}$ = 3.22 ± 0.26 mM *vs.* 2.13 ± 0.19 mM, pCa_{50} = 5.81 ± 0.18 *vs.* 5.76 ± 0.43, and 7.52 ± 0.133 *vs.* 8.26 ± 0.54 (+25 mM caffeine), and pMg_{50} = 4.88 ± 0.65 *vs.* 3.18 ± 0.24, for AO and FA, respectively)). Thus, AO (*vs.* FA) is less sensitive to the effect of $[caffeine]_i$ but more sensitive to pMg_i and the ryanodine–receptor SR Ca^{2+}–release channels in vascular smooth muscle are modulated as are those in striated muscle. Supported by NIH GM 48243.

Tu-Pos142

L(+)-LACTATE AFFECTS CALCIUM UPTAKE AND RELEASE BY THE SARCOPLASMIC RETICULUM (SR) OF FAST-TWITCH MUSCLE. ((M.A. Andrews, and T.M. Nosek‡)) NY Coll. Osteopath. Med., Old Westbury, NY 11568 and ‡Med. Coll. Georgia, Augusta, GA 30912-3000

During even mild exercise, the intracellular concentration of L(+)-lactate (LL) increases from a resting level of 1 - 2 mM to 10 - 20 mM. We have previously demonstrated that this level of LL significantly inhibits maximum Ca^{2+}-activated force generation in Triton-skinned muscle fibers (*Biophys.J. 68:A169, 1995*). Here we have investigated the effect of LL on Ca^{2+} uptake and Ca^{2+}-induced Ca^{2+} release (CICR) from single saponin-skinned fast-twitch (EDL) muscle fibers of adult rats. Experiments were conducted at room temperature, and at a constant ionic strength of 170 mM, and pH of 7.0. The basic experimental protocol was as previously described (*Am.J.Physiol. 261:H620, 1991*), with the Ca^{2+} content of the SR being determined from the magnitude of the contractile response to 25 mM caffeine. Under control conditions, a 15 second exposure to pCa 6.6 produced loading of the SR to approximately 90% of maximum (reached at 60 seconds). Loading at 15 seconds, but not at 60 seconds, was significantly decreased by 10, 20 and 30 mM LL to 81 ± 6%, 87 ± 4% and 92 ± 4% (n = 12 - 13) of control, respectively. After control loading of the SR for 15 seconds, a 30 second releasing period in a control bathing solution of pCa 5 released 15 ± 2% (n = 26) of the Ca^{2+} in the SR. LL did not cause an efflux of Ca^{2+} from the SR in the absence of stimulating Ca^{2+}. However, in the presence of pCa 5, increasing LL progressively increased Ca^{2+} release (27 ± 3%, 33 ± 3%, and 37 ± 7% in 10, 20, and 30 mM LL, respectively; n = 6 - 8). We conclude that in saponin-skinned fibers, increasing LL into the range found with mild exercise slows the rate of Ca^{2+} uptake by the SR and increases the Ca^{2+} sensitivity of CICR. (Support: NIH AR40598 to TMN; NYCOMRI to MAA).

Tu-Pos143

ADENOSINE RECEPTOR ACTIVATION AND PKC-ε TRANSLOCATION IN RAT VENTRICULAR MYOCYTES. ((J. William Lester and Polly A. Hofmann)) Dept. of Physiology, Univ. of Tennessee, Memphis, TN 38163.

Previously we showed treatment of rat ventricular myocytes with the adenosine A_1/A_3 agonist R-phenylisopropyladenosine (R-PIA) or the protein kinase C (PKC) activator dioctanoylglycerol decreased unloaded shortening velocity (V_{max}) to a similar extent (Lester et al., *Biophys J.* 1995, 68:A60). These data suggest adenosine effects are mediated by PKC activation. The purpose of the present study was to determine if adenosine receptors are linked to activation of the primary PKC isoform in rat ventricle, PKC-ε. Translocation of PKC-ε from the cytosol to the membrane, an initial step necessary for PKC activation (Bell, *Cell.* 1986, 45:631.), was used as a measure of PKC activation. Following enzymatic isolation ventricular myocytes were treated for 1 or 5 minutes with the indicated agent, homogenized, and separated into cytosolic and membrane fractions. Samples were electrophoresed on 12% SDS acrylamide gels and immunoblotted with polyclonal anti-PKC-ε antibody. To establish the correlation between PKC translocation and activation in our system, we initially examined effects of direct (phorbol ester) and indirect (α-adrenergic agonist) activators of PKC. Phorbol 12-myristate 13-acetate treatment (1 μM) significantly increased membrane bound PKC-ε and concomitantly decreased cytosolic PKC-ε. To a lesser extent, PKC-ε translocation was also seen with 100 μM phenylephrine (α-adrenergic agonist) + 10 μM propranolol (β-adrenergic antagonist). Finally, myocytes treated with 100 μM R-PIA showed a trend toward increased membranous PKC-ε. This suggests R-PIA activates PKC-ε which in turn may mediate adenosine agonist-induced decrease in V_{max} in ventricular myocytes. (Supported by HL48839).

Tu-Pos144

EFFECT OF CYCLOPIAZONIC ACID ON TRACHEAL SMOOTH MUSCLE. ((R. Espinosa-Tanguma & A.M. Lopez-Dominguez)). Dept. Physiology & Pharmacology. School of Medicine, Universidad Autonoma de San Luis Potosi, S.L.P., Mexico, 78210.

Our aim was to study the effect of the sarcoplasmic-reticulum Ca-ATPase specific inhibitor Cyclopiazonic Acid (CPA) on tracheal rings of guinea-pig. For this purpose tracheal rings were placed in a two ml organ chamber for isometric tension recording. In the presence of Krebs-Henseleith solution CPA (10 μM) produces a transient contraction (72%, n= 10, of that produced by KCl, 80 mM) which is dependent of the releasing of acetilcholine and the opening of voltage-dependent calcium channels, because the cholinergic antagonist atropine (10μM) and the voltage-dependent calcium channel blocker verapamil (10μM) reduced the contraction evocked by CPA (55%, n=7, and 95%, n= 8, respectively). Moreover, preincubation with CPA (10 μM) reduces the contractures induced by 5 μM carbachol (24%, n=8), 80 mM KCl (63%, n=4), and 10 μM histamine (41%, n=6) compared with that produced by the same substance in the absence of CPA. These results support and extend previous reports showing that, in smooth muscle from ureter and ileum (Maggi et al., Br. J. Pharmacol. 114: 127-137, 1995), CPA produces a concentration-dependent transient contraction which is inhibited by the voltage-dependent calcium channel blocker nifedipine and calcium-free solutions, and a depletion of the intracellular calcium stores. Supported by FAIUASLP: C95-FAI-O1-4.4 to R.E.T.

Tu-Pos145

CALCIUM STORES AND CALCIUM OSCILLATIONS IN HUMAN MYOMETRIUM: AN IP_3-DEPENDENT STORE AND A SECOND STORE THAT IS NOT RYANODINE DEPENDENT. ((R. Young, R. Hession)) Dept of Ob/gyn, Medical University of South Carolina, Charleston, SC 29425.

Using confocal laser scanning microscopy in the epifluorescence mode, we observed calcium oscillations in cultured human myometrium following exposure to either oxytocin or thapsigargin. We found that calcium oscillations are not dependent upon calcium in the bathing solution and are not dependent upon either caffeine or ryanodine. In a pixel-by-pixel video analysis of calcium oscillations, we observed that depletion of calcium stores by thapsigargin exposure reduced the number of regions exhibiting oxytocin induced calcium rises, but depletion of calcium stores by oxytocin did not reduce the number of regions exhibiting thapsigargin induced calcium rises. Thus, myometrium contains at least two intracellular calcium stores, one IP_3-dependent (oxytocin dependent), and a second that is not ryanodine dependent.

Tu-Pos146

ACTIVATION OF NON-SELECTIVE CATION CONDUCTANCE BY PURINERGIC RECEPTOR STIMULATION IN CANINE COLONIC MYOCYTES. ((Hye Kyung Lee, Kathleen Keef and K.M. Sanders)) Dept. Physiology & Cell biology, University of Nevada, Reno, NV 89557, U.S.A.

Purinergic receptor stimulation depolarizes the cell membrane of canine colonic muscles. To study underlying ionic mechanisms, ionic currents were measured using whole cell patch clamp technique in cells isolated from circular and longitudinal muscle layers of canine colon at 32 °C. K^+ currents were minimized by internal dialysis with Cs^+, and the Cl^- gradient was adjusted to E_{Cl} = -70 mV. In circular myocytes, ATP (10 μM-3 mM) induced inward currents (I_{ATP}) at -70 mV with an amplitude of -50 ± 6 pA (n=8, 1 mM ATP). The I-V relationship of I_{ATP} was linear with some inward rectification and a reversal potential of -13 ± 2 mV (n=11). I_{ATP} at -70 mV appeared to be carried predominantly by Na^+. P_2 receptor antagonists Suramine (100 μM) and Cibacron Blue 3GA (100 μM) substantially inhibited I_{ATP}. In longitudinal myocytes, both ATP (1-100 μM) and α,β-methylen ATP (0.1-100 μM) induced inward currents at -70 mV with the amplitudes of -78±12 pA (n=3, 100 μM ATP) and -68±17 pA (n=3, 10 μM α,β-methylen ATP). The electrical properties of these currents appeared to be similar to I_{ATP} in circular myocytes. These preliminary results support the presence of P_{2X} receptors in canine colonic myocytes, which mediates the excitation of the muscle via activation of a non-selective cation conductance. (Supported by DK 41315).

Tu-Pos147

MUTATIONS AT A CRITICAL POSITION IN THE OUTER VESTIBULE OF THE NA^+ CHANNEL ALTER PERMEATION AND GATING. ((H. Todt, S. Dudley and H. Fozzard)) Cardiac Electrophysiology Laboratories, University of Chicago, Chicago, IL 60637. (Spon. by E.Page)

Ionic selectivity of Na^+ and Ca^{2+} channels is critically dependent on a set of amino acids which presumably form a narrow ring in the outer vestibule. Whereas each of the four domains contributes a negatively charged residue to the putative selectivity filter of the Ca^{2+} channel, only two negative charges are present in the analogous part of the rat brain II Na^+ channel (I-D384, II-E942). Domain III contributes a positive charge (K1422), domain IV a neutral residue (A1714). The mutation K1422E has previously been shown to alter Na^+ selectivity but changes in channel gating have not been reported. The analogous mutation in the adult rat skeletal muscle Na^+ channel (K1237E), expressed in *Xenopus* oocytes, produced a shift in reversal potential for the fast transient current from 56±5 mV (wild type; n=6) to 9±1 mV (n=6), consistent with a loss of selectivity for Na^+. In addition substantial alterations in gating were observed: the half point of peak conductance was shifted into the negative direction (V_h=-31±2 mV versus -18±1 mV for the wild type) and the slope factor of conductance was increased (5±0.3 vs. 4±0.1). The midpoint of steady state availability was substantially shifted to the hyperpolarizing direction (-86±2 mV vs. -62±0.6 mV). Also the neutral mutation K1237S showed kinetic alterations: The half point of conductance was shifted into the positive direction (V_h=-13±0.5 mV; n=6) whereas the midpoint of steady state availability was more negative than in the wild type (-67±1.4 mV). These alterations in gating cannot be explained by a simple electrostatic effect.

Tu-Pos148

CALCULATION OF MUSCLE STIFFNESS BASED ON DIAGONAL MOVEMENT MODEL OF MYOSIN HEAD ON THIN FILAMENT
((Toshikazu Majima)) Electrotechnical Laboratory, Tsukuba, Ibaraki 305, JAPAN

In the crossbridge theory, the population of active cross-bridges is considered to vary with imposed load. Therefore muscle stiffness has been regarded as a good measure of active fraction of crossbridges. The author proposed a model of muscle contraction based on load dependent sliding direction change of the myosin head on actin molecules during contraction (Majima 1993, J. Muscle Res. Cell Motil. 14:361 (Abstr.); 1995, Biophys. J. 68:324s), where the population of active crossbridges is independent of imposed load. Properties of muscle stiffness derived from the model are discussed.

The calculated stiffness showed gradual increase with increasing load. It shows maxima around 0.8 Po and decreased with further load increase. In the calculation, only the force generated at crossbridges is considered. The interpretation of the result is that the calculated stiffness is corresponding exactly to that of the crossbridges.

A double hyperbolic load-velocity relationship in single muscle fibers has been reported (Edman 1988, J. Physiol. 404:301). Stiffness calculation, using the double hyperbolic load-velocity model, gives a two-phase increase of stiffness with increasing imposed load.

Tu-Pos149

RHEOLOGICAL MODEL OF RESTING FROG MUSCLE FIBRES AND WEAKLY BINDING BRIDGES.
((P Garzella)) SSSA, Via Carducci 40, Pisa 56100, Italy.

A number of experimental findings have suggested the presence of "weakly binding bridges" (with viscoelastic properties) in skinned muscle fibres (B. Brenner et al. 1982, PNAS 79; Schoenberg, Biophysical Journal, 48, 1985). However recent experiments failed to show the presence of these bridges in intact and skinned muscle fibres (P. Garzella, Ph.D. thesis, 1993). To investigate the reasons of this discrepancy I have compared the passive force response to stretch in the same fibre before and after chemical skinning using a simple mechanical model. Fast length changes were applied to one end of frog muscle fibres and resulting force response changes were measured at the other end (4°C,sarcomere length ≈2.2 μm). After the experimental tests the intact fibre was chemically skinned and the measurements repeated. The force responses of a resting muscle fibre can be accounted for by assuming the presence of a viscoelastic element arranged in parallel with a Voigt unit (i.e. a parallel combination of one spring and dashpot). The analysis was based on nonlinear elements. Results from one experiment are shown in the figure. A) Sarcomere length changes (upper traces) and force responses (lower traces, continuous lines) obtained from an intact fibre before and after the skinning. Response of a rheological model (empty circles) composed by (B) a viscous (a), viscoelastic (b) and elastic components. There is a good agreement between the model and the experimental results. The model simulation shows a pure viscous response (a) and this behavior is clearly not in agreement with the properties expected from "weakly binding bridges".

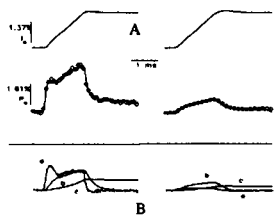

Tu-Pos150

MYOSIN HEAVY CHAIN EXPRESSION IN THE RHYTHMICALLY ACTIVE DILATOR NARIS AND CHRONICALLY STIMULATED RABBIT FAST-TWITCH TIBIALIS ANTERIOR MUSCLES.
((William O. Kline[1], Prasarn Tangkawattana[2], Mamoru Yamaguchi[2] and Peter J. Reiser[1,3])) Exercise Science[1], Veterinary Biosciences[2] and Oral Biology[3], The Ohio State University, Columbus, OH 43210.

Mammalian fast-twitch skeletal muscle can be transformed toward the slow-twitch phenotype by chronic low frequency stimulation (CLFS). A stimulation frequency of 10 Hz is most commonly employed to study the fundamental changes induced by CLFS. One application of CLFS is conditioning skeletal muscle for cardiac assist (cardiomyoplasty). We have examined the expression of myosin heavy chain (MHC) isoforms and the ultrastructural characteristics of rabbit tibialis anterior (TA) muscles (n=3) after 3 weeks of continuous stimulation at 10 Hz. The relative amounts of both types I and IIA MHC increase by ~100% and that of IID MHC decreases by ~70% with this stimulation protocol. There is also marked ultrastructural disruption of myofibers as a result of this stimulation, including the presence of extensive intracellular regions with few myofilaments. The goal of this study was to determine several characteristics, including MHC isoform expression, of a skeletal muscle (dilator naris) which normally contracts repetitively and continuously at a frequency (~3 Hz) that is more similar to the normal heart contraction frequency (3-5 Hz), thus defining a possible end-point for conversion of fast-twitch muscle without marked disruption to perform repetitive work. Surprisingly, the dilator naris expresses relatively little (~5%) type I MHC (~25% in 3 week stimulated TA). The predominant MHC is IIA (~80%) with a small amount (~15%) of IID (no IIB was detected in this muscle). These results may have important implications for cardiomyoplasty conditioning in that a skeletal muscle can perform continuous repetitive work with predominantly fast type MHC at a frequency which is close to that of the cardiac cycle. Supported by NIH Grant AR39652.

Tu-Pos151

CROSSBRIDGE DETACHMENT CONTRIBUTES TO THE TENSION TRANSIENTS OF SKINNED RABBIT PSOAS FIBERS.
((C.Y. Seow, S.G. Shroff, and L.E. Ford)) Dept. of Medicine, U. Chicago, Chicago, IL 60637.

Adding 3 mM 2,3-butanedione monoxime (BDM) to the activating solution of skinned fibers at 2°C decreased isometric force by half, maximum velocity by 31%, and stiffness by 32%, suggesting that BDM detained crossbridges in a low force state (Circulation 88; I-630, 1993). The rapid, transient tension responses (Phases 1-3) to step shortening of sarcomere length could be described by three stiffness components that relaxed rapidly and partially to an intermediate, T_2, force level (J. Physiol. 269; 441, 1977). The three components relaxed with separate monoexponential rate constants that increased with the size of release. The largest of these components comprised about half of the response under reference (non-BDM) conditions and relaxed with the fastest rate constant. BDM caused the amplitudes of the two smaller components to decrease in proportion to the tension drop with almost no change in the amplitude of the largest component and very little change in any of the three time constants for each step size. These results suggest that BDM detained bridges in a state where shortening produced negative force followed by rapid detachment, thereby augmenting the relative tension recovery. The similarity of the fastest component of the responses in the presence and absence of BDM suggests that up to half the reference transient responses may have been due to rapid detachment of initially attached bridges. While the proposed mechanism offers a partial alternative to Huxley & Simmons' (Nature 233, 533, 1971) explanation of the tension transients, it is in keeping with Huxley's later proposal of two stage attachment to explain energetic data (Proc. Roy. Soc. B 183: 83, 1973).

Tu-Pos152

ACTIVE MUSCLE FORCE, THE WEAKLY-TO-STRONGLY BINDING CONFORMATIONAL CHANGE, AND LABELING SH1 AND SH2.
((Mark Schoenberg)) LPB, NIAMS, NIH, Bethesda, MD 20892

Alkylation of the SH1 and SH2 sulfhydryls with phenylmaleimide locks myosin in a weakly-binding configuration. The myosin is incapable of reverting to a strongly-binding configuration even in the absence of nucleotide, and is, not surprisingly, incapable of interacting with actin to produce active force. In order to determine the relative importance of the reactions at SH1 and SH2 for muscle crossbridge function, the method of Reisler, et al., (Biochemistry 13:2014:'74) and Roopnarine and Thomas (BJ. 67:1634:'94) was used to link phenylmaleimide to SH2 alone. It was found that this single modification was sufficient to lock myosin crossbridges in a weakly-binding configuration and eliminate active force production. Using the technique of Roopnarine and Thomas on muscle fibers also allowed study of the behavior of crossbridges having a dinitrophenyl group solely at SH1. These SH1-DNP crossbridges behave differently from the SH2-PM crossbridges. In the presence of MgATP and calcium, they are able to produce active force, although only 10% as much as unmodified crossbridges. Despite this large force reduction, these crossbridges apparently are able to undergo the nucleotide-induced weakly-binding to strongly-binding transition, although the rate constants for this transition are not yet known. To know if the differential effects described are due to differences in the site of the two labels or differences in the labels, it will be necessary to place a penylmaleimide solely at SH1 or a dinitrophenyl solely at SH2.

Tu-Pos153

SPECTROSCOPIC DETECTION OF ACTO-MYOSIN INTERACTIONS BY SITE-DIRECTED FLUORESCENT LABELING OF THE ACTIN BINDING INTERFACE OF MYOSIN.
((W.C. Cooper, L.R. Chrin, and C.L. Berger)) Dept. of Molecular Physiology & Biophysics, Univ. of Vermont, Burlington, VT 05405.

The stiffness of a contracting muscle fiber relative to rigor has been routinely used as a measure of cross-bridge attachment, but recent results have questioned the validity of this approach (Higuchi et al., 1995, *Biophys. J.* **69**:1000 and references within). We are currently developing novel spectroscopic techniques for detecting cross-bridge attachment in actively contracting muscle fibers by labeling selected sites on the actin-binding interface of myosin with fluorescent probes. We have labeled the lower 50 kD subdomain of myosin at Lys-553 with a succinimidyl derivative of fluorescein (FHS) by the method of Bertrand et al. (1995, *Biochem.* **34**:9500), and the upper 50 kD subdomain of myosin near the 50/20 kD junction with an azido methyl-coumarin probe (MC) using an innovative photolabeling protocol. The latter procedure involves transfer of the methyl-coumarin label from a peptide sequence complimentary to the 50/20 kD junction (Chaussepied and Morales, 1988, *P.N.A.S.* **85**:7471) to the upper 50 kD subdomain of myosin. Preliminary results from solution studies indicate that the fluorescence emission from both probes is sensitive to the interaction between actin and myosin.

Tu-Pos154

A-BAND LENGTH, SLACK LENGTH AND TENSION IN SKINNED SOLEUS FIBERS FROM PATIENTS WITH HYPERTROPHIC CARDIOMYOPATHY CAUSED BY A MUTATION IN THE β-MYOSIN HEAVY CHAIN. ((Jody A. Dantzig*, Margot E. Leonard*, Lameh Fananapazir+, Neal Epstein+, Yale E. Goldman*, Rhea J. C. Levine‡, H. Lee Sweeney*)) ‡Med. Col. of PA and Hahneman, 19129, +NHLBI, NIH, 20892, *PA Muscle Inst., Univ. of PA, 19104.

In a severe form of familial hypertrophic cardiomyopathy (HCM), patients have an Arg→Gln mutation at amino acid 403 in one allele of the cardiac and slow skeletal muscle β-myosin heavy chain (MHC). Arg 403 is in a highly conserved actin binding loop of the myosin head and is likely to be important for function. It was previously shown that β-MHC isolated from these patients translocates actin, *in vitro*, more slowly than wild type (Cuda *et al., J. Clin. Invest.* 91:2861, 1993). Surprisingly, we found no significant difference in isometric tension/cross-sectional area, measured at slack length in 5 mM ATP, 200 mM ionic strength, pCa 4.5, pH 7.1, and 20 °C, with single fibers from normal controls (153 ± 12 kN/m^2, mean ± sem, n = 7) and affected individuals (144 ± 24 kN/m^2, n = 11). We defined slack length as the zero-force intercept of the passive length-tension curve (solution as above with pCa 8). Slack lengths, measured by white light diffraction (Goldman, *Biophys. J.* 52:57, 1987) ranged from 2.3 - 2.7 μm for normal (mean 2.4 ± 0.05 μm; n = 12) and 1.6 - 2.5 μm for abnormal fibers (2.15 ± 0.03 μm; n = 25). At sarcomere length (SL) 2.5 μm, resting tension was higher in abnormal (mean 4.1 ± 0.6 kN/m^2, n = 24) than in normal fibers (1.4 ± 0.5 kN/m^2, n = 11). To determine if the shorter sarcomeres in the abnormal fibers coincide with a decrease in thick filament lengths, some of the fibers used in the mechanical studies were stretched and fixed for electron microscopy. On average, we observed shorter A-band lengths in abnormal (1.21 ± 0.13 μm, mean ± sd, n = 174, SL range 1.3 - 2.3) *vs.* normal fibers (1.66 ± 0.04 μm, n = 160, SL range 2.0 - 3.2). This mutation in the actin-binding loop not only impedes shortening velocity, it also appears to alter thick filament structure, possibly contributing to the severity of this form of HCM.

Support: NIH grant HL15835 to P.M.I., PA Chapt. of the AHA and HHMI.

Tu-Pos155

X-RAY DIFFRACTION EVIDENCE THAT ATTACHMENT CONFORMATION OF WEAKLY BOUND CROSSBRIDGES IN MUSCLE IS HIGHLY VARIABLE (NONSTEREOSPECIFIC). ((S. Xu+, S. Malinchik+, T. Kraft+, B. Brenner+ and L. C. Yu+)) +NIAMS, NIH. ‾Hannover Medical School, Hannover, Germany.

Generation of *isometric* force, different from quick tension recovery, was proposed to result from a structural change in the actomyosin (cross-bridge) complex associated with the transition from a weakly bound configuration to a strongly bound configuration (Brenner, et al., 1995). Structurally, we proposed that the weak to strong transition is from nonstereospecific attachment to stereospecific attachment. Recently we have systematically obtained two dimensional X-ray diffraction patterns from skinned rabbit psoas fiber bundles, relaxed and in rigor, such that direct quantitative comparisons can be made. (Data obtained on EMBL beamline X-13 at DESY). For 4°C and 20°C, and ionic strength 50-150 mM, under relaxing condition, at least 6 orders of thick filament based layer lines are visible. Analysis of the axial centroid position of the inner region of the first layer line suggests that the layer line is a mixture of overlapping thick and thin filament based layer lines and their relative contribution varies with ionic strength, correlating with the fraction of weakly bound cross-bridges. The behavior of the mixed layer line could be explained by modelling attachment of myosin heads to specific sites on actin while the binding angle is variable. Another evidence of nonstereospecific binding is that the diffuse scattering is little affected by considerable change in the fraction of weakly bound cross-bridges as ionic strength is changed; i.e. the weakly bound cross-bridges are disordered. As a comparison, in transition from relaxed condition to rigor where the cross-bridge attachment is known to be stereospecific, the diffuse background decreases significantly. The results support the idea that the weakly attached cross-bridges assume nonstereospecific conformations.(NATO grant 930448; DFG Br 849/1-4).

Tu-Pos156

DOES LOWERING IONIC STRENGTH CHANGE WEAK CROSS-BRIDGE BINDING FROM A NON-STEREOSPECIFIC TO A STEREOSPECIFIC CONFORMATION? ((T.Kraft*, S.Xu+, B.Brenner‡, L.C.Yu+))*NIH, NIAMS, Bethesda, MD.; ‡Medical School, Hannover, FRG.

Previously it has been proposed (Holmes, BJ 68:2s, 1995) that in skeletal muscle the transition of the cross-bridges into a strong binding force generating conformation can occur only after initial non-stereospecific weak cross-bridge attachment has proceeded to a "stereospecific weak" interaction. Based on the concept of Geeves (BJ 68:194s, 1995) it was suggested that such a stereospecific weak interaction is possible only when the actin filament has changed from a 'blocked' to a 'closed' state, either by Ca^{++} or by lowering ionic strength (μ) to below 50mM.
In our previous work using ATPγS we had shown that binding kinetics of weak interactions become slower when Ca^{++} is raised, while binding affinity is almost unchanged, suggesting some change in the weak cross-bridge binding upon addition of Ca^{++} (Kraft et al. PNAS, 1992); yet 2D-x-ray diffraction failed to reveal changes that would have indicated a change to stereospecific binding.
Now we tested the second possibility that lowering μ to below 50mM induces a transition into a stereospecific weak binding conformation. We recorded 2D-x-ray-diffraction patterns for μ = 83mM and 33mM with MgATP, at 1°C and 20°C, conditions where a large number of cross-bridges is weakly attached. Again we found no evidence for changes towards stereospecific binding (e.g. no rigor-like increase of actin layer-line intensities, no loss of myosin layer-lines). Therefore we conclude that with adding Ca^{++} or with lowering μ to below 50mM there is no indication of the attachment mode being different from the weak attachment with MgATP at low [Ca^{++}] and μ > 50mM and there are no features indicating a change to a stereospecific (e.g. rigor-like) binding.

Tu-Pos157

THE EFFECT OF NTP BINDING, CLEAVAGE RATES, AND CLEAVAGE EQUILIBRIUM CONSTANTS ON MECHANICAL BEHAVIOR OF THE SINGLE RABBIT SKELETAL MUSCLE FIBER AT 10°C. ((M. Regnier* and E. Homsher.)) Physiology Dept. UCLA Medical School, UCLA, Los Angeles, CA 90024 and *Dept of Physiol. and Biophys., U. Washington, Seattle, WA 99195.

The ability of dATP, CTP, and UTP to support isometric force was 1.0, 0.9, 0.5 respectively when compared to that of ATP. Similarly the unloaded shortening velocity (V_u) at 6 mM was 1.3, 0.7, and 0.25. We have estimated the rate of NTP cleavage (using rate of S-1 fluorescence increase as an indicator of the sum of the forward (k_{+2}) and backward (k_{-2}) rate of cleavage), the equilibrium constant for cleavage, K_2, (using single turn-over experiments), and the steady state rate of actin-activated NTP hydrolysis to assess the role of NTP binding, NTP cleavage on mechanical behavior. The rate of NTP cleavage ($k_{+2}+k_{-2}$) was 50 s^{-1} for ATP, dATP, and CTP and 6 s^{-1} for UTP. The value of K_2 for ATP and dATP was 1.8 and that for CTP and UTP were 0.3 and 2.5 respectively. The second order rate constant for acto-HMM dissociation by ATP, dATP, CTP, and UTP were $1.5x10^6$ $M^{-1}s^{-1}$, $1.1x10^6$ $M^{-1}s^{-1}$, $7x10^4$ $M^{-1}s^{-1}$, and $1.4x10^5$ $M^{-1}s^{-1}$ respectively. Actin-activated NTPase V_{max} for dATP, CTP, and UTP (at 25°C) was 1.7, 0.9, and 0.3 relative to ATP. Since dATP binding, cleavage, AM dissociation are little affected compared to those for ATP, the increased V_u seen in dATP may be associated with an increased rate of dADP release from the strongly bound crossbridge. The reduced force and shortening velocity in CTP is probably related to the low K_2 for CTP cleavage and the reduced affinity of the crossbridge for the CTP. The depressed force and V_u seen in UTP may stem from the reduced rate of UTP binding and cleavage and an increased UDP release rate. (Supported NIH Grant AR-30988 [EH]).

Tu-Pos158

DIELECTRIC MEASUREMENT OF HYDRATION OF MYOSIN SUBFRAGMENT-1 ((M. Suzuki[1], J. Shigematsu[2], Y.Fukunishi[1] and T. Kodama[2])) [1]NAIR/MEL, AIST, Tsukuba, 305 Japan, [2]Kyushu Inst.Tech, Fukuoka 820, Japan

We studied the hydration state of myosin subfragment-1(SF-1) measuring microwave dielectric dispersion. Chymotryptic S1 was prepared from rabbit skeletal muscle myosin, concentrated to 20 - 40mg/ml, and dialyzed against 20mM KCl containing 5mM $MgCl_2$ and 10mM MOPS (pH7.0). The sample solution was placed in a glass cell controlled at 20.0±0.01°C. The measurement were made with an open-end coaxial probe connected to a microwave network analyzer. We first analyzed the dielectric spectra (0.2 -20GHz) by the method of Wei et al.[J. Phys. Chem, 98,6644(1994)], which assumes the hydration shell of protein to have a relaxation frequency much lower than sub-GHz and only gives the number of water molecules in a strongly restrained state around a protein molecule (N_{strong}). To estimate the number of weakly restrained water molecules(N_{weak}), we then took into account the infinite frequency limit of dielectric constant of solutes which should be positive and attributed to the electronic polarization of atoms and evaluated the total number of water molecules both in weakly and strongly restrained state ($N_{total}=N_{strong}+N_{weak}$). The N_{total} for SF-1 thus obtained was 2,200 and N_{strong} was 900; hence N_{weak}=1,300. The N_{total} values obtained by similar analysis for bovine serum albumin, cytochrome C, hemoglobin, myoglobin and ovalbumin were in good agreement with those obtained by calorimetry, NMR and vapor pressure analysis. The N_{weak}/N_{total} ratio were different for these proteins, however. We also studied hydrophobic amino acids. The result indicates that hydrophobic groups have restrained water shells having relaxation frequencies of 4~6 GHz. Molecular dynamics simulation of hydrophobic interaction between two octane molecules in water showed that the Helmholtz's free energy does not change with the intermolecular spacing until the octane pair come close together within 5 angstroms so that the thickness of hydrophobic hydration shell roughly corresponds to water diameter. Taken together, a large part of weakly restrained water is very likely attributed to hydrophobic hydration.

Tu-Pos159

KINETICS OF LOW FORCE CROSS-BRIDGES AT SUBMAXIMAL ACTIVATION IN SKINNED SKELETAL MUSCLE FIBERS DURING SHORTENING. ((H. Iwamoto)) Dept. Physiol., Sch. Med., Teikyo Univ., Tokyo 173 JAPAN.

Previous study (Iwamoto, 1995, Biophys. J., 68:243) suggested that the force generation in muscle is preceded by the formation of low force, slowly dissociating A•M•ADP•P_i cross-bridges. Lowering [Ca^{2+}] of bathing solution did not increase the population of these low force A•M•ADP•P_i cross-bridges. Since the formation of weak binding cross-bridges is not inhibited at low [Ca^{2+}], it is expected that the calcium-regulated step of the actomyosin ATPase cycle is the formation of the low force A•M•ADP•P_i cross-bridges. Calcium may activate the fiber by either increasing the forward rate constant (k_+) or reducing the reverse rate constant (k_-) of this step. To test which rate constant is calcium-sensitive, k_- was estimated in skinned rabbit skeletal muscle fibers isotonically shortening at low [Ca^{2+}], by measuring the negative strain of the low force A•M•ADP•P_i cross-bridges. The amount of negative strain is determined by the balance between the velocity of shortening and the rate of dissociation, k_- (Iwamoto, 1995, Biophys. J., 69:1022). The faster the dissociation (k_-), the smaller will be the negative strain. At low [Ca^{2+}] (pCa = 6.3; 50% of full isometric force is generated), a twofold increase of k_- would be expected if k_- were solely responsible for calcium regulation. However, the negative strain at low [Ca^{2+}] was ~1 nm *greater* than the value 2~3 nm at full activation (pCa = 4.4). The results supports the idea that calcium activation is achieved through an increase of k_+, not through a decrease of k_-.

Tu-Pos160

ATPase RATE IN CONTRACTING FIBERS FROM RABBIT PSOAS MUSCLE. ((Christopher S. Cook+, Hideo Higuchi* and Yale E. Goldman+)) +Pennsylvania Muscle Inst., Univ. of PA, Philadelphia, PA. 19104, *Biomotron Project, ERATO, JRDC, Osaka, Japan. (Spon. by E. Pugh)

The ATPase activity of contracting muscle provides an estimate of cross-bridge cycling rate. We present a novel method of determining the ATPase. In this protocol we load a rigor fiber with 5 mM caged ATP, 5 mg/ml of creatine phosphokinase (CPK) and a selected concentration of creatine phosphate (CP). The fiber is then transferred to silicone oil followed by laser flash photolysis releasing ATP (~1.7 mM, arrow in Fig.). During contraction, out-of-phase stiffness (viscous modulus, V) is 0.1 - 0.2 of in-phase stiffness. The CPK reaction buffers ATP concentration until CP runs out, at which point V declines. Lines are fit to the steady state and declining phases of V to determine the duration of the steady state (t_s). On the plot of t_s *vs.* [CP], 1/slope of the line = ATPase rate, which is constant from 0 - 20 mM CP. The mean ATPase rate was 0.355 ± 0.164 mM·s^{-1}, (mean ± sd, n = 16). Taking the concentration of myosin heads in a muscle fiber to be 154 μM (Ferenczi et al. *J. Physiol.* **352**:575, 1984), our value corresponds to a turnover rate of 2.3 s^{-1} at 10 °C, in agreement with Ferenczi et al. (1984). This technique can be used in conjunction with isotonic contractions to determine the amount of filament sliding per ATP utilized. Supported by NIH grant AR42333 and the MDA.

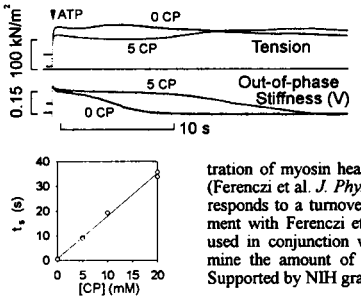

Tu-Pos161

REPRIMING OF TILTING IN THE MYOSIN LIGHT-CHAIN REGION FOLLOWING LENGTH STEPS IN MUSCLE FIBERS ((Seth C. Hopkins^, Cibele Sabido-David^B, Malcolm Irving^B, Yale E. Goldman^)) ^Pennsylvania Muscle Inst., Univ. of PA and ^BRandall Inst., King's Coll. London. (Spon. by F.A. Pepe)

In contracting muscle fibers, polarized fluorescence from the 6 isomer of acetamidotetramethyl rhodamine, covalently linked to Cys 108 of chicken gizzard regulatory light chain (RLC) exchanged into rabbit psoas muscle fibers, shows that the light-chain region tilts during a length step and during the quick tension recovery (Irving et al. *Nature* **375**:688, 1995). To study the slower kinetics of subsequent structural events following length changes, test length steps (ΔL_T, upward arrows in Fig.) were applied at various times after conditioning steps (ΔL_C, downward arrow). A 4 nm / half sarcomere release in isometric contraction causes a small decrease in Q_{II} which is reversed when the ΔL_T restretch occurs within 2 ms. Restretches at longer times produce larger increases in Q_{II} that eventually equal the deflection observed after a stretch in steady-state contraction. The half-time of this repriming process is ~16 ms, which is faster than the recovery of Q_{II} itself after ΔL_C. A repriming process with a similar timecourse is evident for the converse protocol (ΔL_C stretch, ΔL_T release). These data show the disappearance of a sub-population of cross-bridges whose RLC tilt upon ΔL_C can be reversed by a ΔL_T, and the appearance of a new sub-population whose RLC initiate their tilting from an orientation distribution closer to the steady-state. Supported by NIH grant AR26846, MDA, and the Wellcome Trust, UK. We thank J.S. Craik, B. Brandmeier, J. Kendrick-Jones, J.E.T.Corrie, and D.R. Trentham for the labeled RLC.

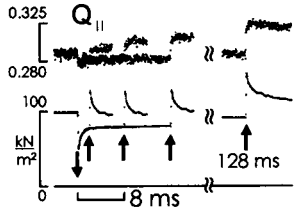

Tu-Pos162

RATE OF CROSS-BRIDGE DETACHMENT AND REATTACHMENT FOLLOWING A STEP STRETCH IMPOSED ON TETANICALLY STIMULATED SINGLE MUSCLE FIBERS. ((M. Reconditi, F. Vanzi, G. Piazzesi & V. Lombardi)) Dipartimento di Scienze Fisiologiche, University of Florence, Italy. (Spon. by Y.E. Goldman)

Time resolved structural and mechanical experiments (Lombardi et al., *Nature* **374**:553, 1995; *J. Physiol.*, abstract in press) indicate that the quick recovery of tension (phase 2) after a step stretch is only partly due to the reversal of the working stroke. The late component of phase 2 and phase 3 are related to complete detachment of the strained cross-bridges followed by fast reattachment and force generation. To obtain information on the kinetics of the detachment/reattachment process, a multiple exponential equation based on this concept of complete replacement of the original cross-bridges was fitted to the tension transient following a step stretch. Steps of different size were imposed, under sarcomere length control by a striation follower, on single fibers from *Tibialis anterior* muscle of frog (*Rana Esculenta*) at 4°C and 2.13 μm sarcomere length. According to the multiple exponential fit of the records, the late part of phase 2 and the ensuing transient potentiation in phase 3 are explained with a 2-4 ms time lag between detachment (rate constant, r_d, 120-150 s^{-1}) and reattachment and force generation (rate constant, r_3, 75-110 s^{-1}). The detachment rate is decreased by increasing strain between 1 and 5 nm/half sarcomere stretches.
Supported by: Telethon Italy (grant n. 625)

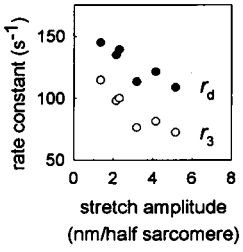

Tu-Pos163

MECHANISMS OF FORCE PRODUCTION DURING RAMP STRETCHES OF SKELETAL MUSCLE FIBERS. ((S. Lehman, E. Burmeister and R. Cooke)) Dept. of Human Biodynamics, Bioengineering Graduate Group, UCB, and Dept. of Biochem./Biophysics, UCSF.

We stretched single glycerinated rabbit psoas fibers at constant velocity under sarcomere length (SL) control by laser diffraction, and investigated mechanisms of the two phases of force response by imposing length perturbations. A linear rise in force occurs over the first 5.31 ± 0.27 nm per half sarcomere (HS) of stretch (Phase I). When SL is stepped back to initial length during Phase I, force falls below isometric force, then recovers over the next 10-40 ms. Fiber stiffness during Phase I is the same as stiffness before the stretch. These results are consistent with models in which viscoelastic cross bridges (CB's) remain attached during Phase I (e.g. Huxley and Simmons, 1971). After Phase I, force continues to rise during stretches at < 1 SL/s, but more slowly than in Phase I. To test the hypothesis that this rise (Phase II) is due to sarcomere inhomogeneity (Julian and Morgan, 1979), we imposed a second stretch 30 ms after the first. Force rise in Phase II is smaller during the second stretch, a result inconsistent with this hypothesis. Small (2.5 nm/HS) steps superimposed on ramp stretches during Phase II cause an abrupt rise in tension, lasting only a few ms. This result is inconsistent with an elastic force producing element in parallel with CB's, but is consistent with a mechanism in which CB's detach and reattach rapidly. Supported by UCB Graduate Opportunity Fellowship and HL32145.

Tu-Pos164

A MODEL OF CROSS-BRIDGE DYNAMICS: CROSS-BRIDGE INTERACTIONS WITH FILAMENT COMPLIANCE. ((T.L. Daniel, P.B. Chase, J.Sherman and A.C. Trimble)) Depts. of Zoology, Applied Math, Radiology, and Physiology and Biophysics. Univ. of Washington, Seattle, WA 98195. (Spon. by R.W. Wiseman)

Recent reports of significant filament compliance (Huxley *et al.*, 1994, Biophys J 67:2411) suggest that current models of cross-bridge dynamics must be re-evaluated. Mass-action kinetic models do not explicitly account for state transitions of cross-bridges when significant local deformations arise. Accordingly, we have formulated an alternative approach that explicitly accounts for forces borne by individual cross-bridges, thin filament binding sites, and thick filament attachments. The model is based on solutions to the matrix of binding site and attachment locations subject to local cross-bridge forces. Cross-bridge behavior is modeled as a simple three state process with strain-dependent rates: a detached state whose binding rate is maximum at 7.5 nm strain, a weakly bound state, and a strongly bound state. Each cross-bridge is exposed to random thermal fluctuations and the likelihood of state transition is computed from the rate equations. Thus we combine explicit mechanical calculations of forces and deformations with stochastic forcing. Two results emerge: (1) simple molecular kinetics, when immersed in a mechanically coupled system, yield predictions that capture published measures of ATPase activity (1 to 3 s^{-1}), tension transients, and force velocity behaviors and (2) there appears to be mechanical tuning in which physiological values for filament compliance and cross-bridge stiffness yield maximum forces with no effect on ATPase activity. A key feature of this model is that deformations affect cross-bridge state transitions by providing binding sites not normally available in undeformed filaments. Support: NSF IBN-9511681, NIH HL52558, SGI.

Tu-Pos165

ACTIVATED MYOFIBRILS STRETCHED TO LESS FILAMENT OVERLAP PRODUCE MORE TENSION. ((Dwayne L. Dunaway, Marc L. Bartoo, Rocco Huneke, Gerald H. Pollack)) University of Wash., Seattle, WA 98195

Experiments examining the relation between active tension and filament overlap using fibers or muscles have consistently yielded anomalous results: when specimens were ramp-stretched to less overlap, active tension was enhanced. This unexpected result -- higher tension with less overlap -- has had no easy interpretation, and it has been suggested that this behavior might arise out of "undetected" sarcomeres, whose dynamics may have differed from the bulk of the population in those preparations.
To follow up, we carried out similar experiments on rabbit psoas-single myofibrils. Any ambiguity that might arise from hidden, or undetected sarcomeres is averted in myofibrils because all sarcomeres are in series and bear the same tension, and the length of each sarcomere can be measured. Myofibrils were set at a series of lengths that exhibited negligible passive tension, and then activated. When steady - state tension was attained, the specimen was stretched by 5 - 10% of initial length. Tension rose steeply during stretch and then declined to a new, steady value. This steady value of active tension was always higher than the prestretch value, even though measurements showed that sarcomeres were stretched to less filament overlap. It appears that the level of active tension at any degree of overlap is dependent on the prior lengthening or shortening history. Active tension and filament overlap are neither uniquely, nor linearly, related.

Tu-Pos166

RECRUITMENT OF DAMPED ELASTIC ELEMENTS DURING FORCE ENHANCEMENT BY STRETCH IN FROG MUSCLE FIBERS

((K.A.P. Edman and T. Tsuchiya)) Dept. of Pharmacology, University of Lund, S-223 62 Lund, Sweden.

Striated muscle that is stretched during tetanic activity increases its force above the level attained during an isometric tetanus at the corresponding length. When the stretch is performed above slack length force does not fully return to the control level after the end of stretch but remains enhanced for the rest of the activity period ('residual force enhancement after stretch'). We here report that strain of damped elastic elements within the fiber during stretch plays an essential part in the mechanism underlying the residual force enhancement after stretch. Single fibers from the anterior tibialis muscle of *Rana temporaria* were released to shorten against a very small load at different times after stretch (load clamp). The shortening records derived after a preceding stretch had a larger initial transient (completed within 10-15 ms) than that recorded in an isometric tetanus without stretch. The excess length change (L_S, nm/half-sarcomere) recorded during the initial transient provides a measure of the elastic strain produced during the stretch ramp. L_S was linearly related to the force enhancement produced by stretch (F_E , % of tetanic force) according to the following regression: $L_S = 0.200\ F_E + 8.65$ ($P<0.001$). Measurements performed on whole fibers and marked segments along the fiber agreed well. The recruitment of elastic components is most likely due to non-uniform distribution of the length change during the stretch ramp leading to differences in filament overlap along the myofibrils and variable amounts of staggering of the thick filaments within myofibrillar sarcomeres. Regions that have acquired a greater amount of filament overlap will tend to increase the force above the control level forming the 'residual force enhancement after stretch'. The weaker regions in series, being supported by the strained elastic components, will be able to hold the tension produced by the stronger parts. In line with this view the residual force enhancement after stretch was found to be linearly related ($P<0.0001$) to the slow component of tension rise during the stretch ramp.

Tu-Pos167

CONTRACTION-INDUCED INJURY TO SINGLE FIBERS FROM MOUSE EDL AND TIBIALIS ANTERIOR MUSCLES. ((Gordon S. Lynch and John A. Faulkner)) Inst. of Gerontology, University of Michigan, Ann Arbor MI 48109-2007.

Studies have shown that the extensor digitorum longus (EDL) muscle is more susceptible to injury from pliometric or lengthening contractions than the tibialis anterior (TBA) muscle (van der Meulen & Faulkner, *FASEB J* A345, 1994; Lieber *et al., J. Appl. Physiol.* 77:1926-1934, 1994). The mechanism for this protective effect in the TBA muscle is not known. We tested the hypothesis that single muscle fibers from the EDL would exhibit a greater magnitude of injury than fibers from the TBA muscle. The injury was assessed by the deficit in force development immediately following a single pliometric contraction. Experiments were performed on permeabilized single fiber segments from the EDL and TBA muscles of adult, male C57BL/10 mice. Fibers were set at a sarcomere length of 2.7μm, maximally activated by Ca^{2+} (pCa 4.5) and then stretched with a 10% or 20% strain (% of fiber length, L_f), imposed at a velocity of 0.5 L_f/s. The force deficit was determined as the difference between the maximum force (P_o) immediately after the stretch expressed as a percentage of the P_o before the stretch. Following stretches of 10% strain, the force deficits of single fibers from EDL and TBA muscles were not different (EDL: 7.7±1.2%, n=9; TBA: 11.1±1.6%, n=7). Similarly, with stretches of 20% strain, the force deficits of the two muscles (EDL: 14.4±1.4%, n=15; TBA: 11.8±1.2%, n=15) did not differ. We conclude that following pliometric contraction protocols, the smaller force deficit and decreased morphological damage to intact TBA compared with EDL muscles, cannot be explained by differences in susceptibility at the level of the contractile proteins, but to differences in other aspects of structural integrity, possibly including the sarcolemma. GSL was supported by a CJ Martin Research Fellowship from the NH & MRC (Australia). Supported by NIA grant AG-06157

Tu-Pos168

RAPID RECOVERY OF EXTENSOR DIGITORUM LONGUS MUSCLES IN mdx MICE FROM CONTRACTION-INDUCED INJURY. **((Susan V. Brooks)) Institute. of Gerontology, Department of Physiology, University of Michigan, Ann Arbor, MI, 48109-2007.**

A number of investigators have proposed that the lack of dystrophin in muscle fibers of *mdx* mice makes the sarcolemma prone to damage during contractions. Consistent with this hypothesis is the observation that *in vitro* protocols of repeated contractions with stretch produced greater deficits in force and greater numbers of fibers with sarcolemmal disruptions for muscles of *mdx* mice than for muscles of control mice. I hypothesized that the increased susceptibility to contraction-induced injury of muscle fibers in muscles of *mdx* compared with control mice results from fragility of the sarcolemma, disruption of membrane integrity, influx of calcium into the cytosol, and activation of calcium-dependent degradative pathways. Extensor digitorum longus muscles in 8- to 10-week-old male C57BL/10 control and *mdx* mice were exposed to 10 stretches *in situ* from the plateau of a maximum isometric contraction, one contraction each 10 sec. Stretches were initiated at optimum length for force (L_f) and were of 20% strain relative to L_f at 0.5 L_f/s. The magnitude of the injury, as estimated by the deficit in maximum isometric force, was measured at 10, 30, and 45 minutes, and 1 and 12 hours. Direct and indirect calcium-dependent degradative processes are activated rapidly and increase the severity of injury in the hours immediately following a protocol of injurious contractions. In muscles of control mice, contraction-induced injury is initiated by mechanical disruption of the ultrastructure of small groups of sarcomeres, and damage to the sarcolemma is not a significant factor in the induction of injury *in situ*. The ten contractions produced a significantly greater force deficit (68%) for muscles in *mdx* mice than for muscles in control mice (49%). Contrary to the hypothesis, for muscles in both *mdx* and control of mice, the force deficit decreased steadily over the first 60 minutes. The force deficit decreased further for muscles in *mdx* mice for up to 12 hours. These results do not support a significant role for calcium-activated intracellular degradative processes in the muscles of *mdx* mice following injury induced when maximally activated muscles are stretched. Supported by AG-06157.

Tu-Pos169

BINDING OF CREATINE KINASE TO THE I-BAND OF SKINNED SKELETAL MUSCLE FIBERS IS MEDIATED BY GLYCOLYTIC ENZYMES: AN *IN SITU* BIOCHEMICAL APPROACH. ((Th. Kraft[#], V. Nier[#], B. Brenner[#], T. Wallimann[$]))
[#] Medical School, 30625 Hannover, Germany; [$] ETH, 8093 Zürich, Switzerland.

In intact skeletal muscle, muscle-type creatine kinase (MM-CK) is associated not only with the sarcomeric M-line but most of the "cytoplasmic" MM-CK is located in the I-band region outside the acto-myosin overlap (Wegmann et al. JMRCM 8, 1987). If skeletal muscle is subjected to chemical skinning, the I-band associated MM-CK is lost completely and with time, also part of the M-line MM-CK diffuses out. Incubation of skinned muscle fibers with purified, fluorescently labelled MM-CK, however, did only result in reattachment of MM-CK to its binding sites at the M-line, while no MM-CK was found within the I-band (Kraft et al., BJ 69, 1995).

In this study, using confocal laser fluorescence microscopy, we found that if muscle fibers were preincubated with either fructose-6-phosphate kinase (PFK) or aldolase, MM-CK could rebind to the sarcomeric I-band as in vivo, indicating a direct interaction of MM-CK with either of the two glycolytic enzymes. Binding of MM-CK to the I-band in the presence of PFK occured only at low pH (pH 6.5), which is consistent with findings that PFK-binding to F-actin is pH sensitive. Pyruvate kinase (PK) itself also binds to the I-band, but did not induce binding of MM-CK to this sarcomeric region, although evidence for a dia-enzyme complex between PK and MM-CK has been presented earlier (Dillon and Clark, J. Theor. Biol. 143, 1990). This indicates that in skeletal muscle, some glycolytic key enzymes seem to specifically mediate binding of MM-CK to the thin filament region of the I-band, where glycolytic enzymes are thought to form large multi-enzyme complexes. These findings support the idea of a close functional coupling between glycolysis and the CK/PCr circuit (Wallimann et al. Biochem. J. 281, 1992).

Tu-Pos170

ECTOPIC ENDPLATES ON MOUSE SOLEUS MUSCLE FIBERS INDUCE LOCAL CHANGES IN Z-LINE THICKNESS. ((D.L.Bishop and R.L.Milton)), Indiana University School of Medicine, Muncie Center for Medical Education, Ball State University, Muncie, IN 47306.

To produce new ectopic endplates on mouse soleus muscle fibers the extensor digitorum longus nerve in the hind limb was dissected free for several millimeters, cut distally, and transplanted on to the proximal dorsal surface of the soleus muscle. Two weeks after this initial surgery the limb was reopened and the soleus muscle denervated. The ectopic endplates produced by these surgical procedures exhibit morphological characteristics similar to those innervating fast twitch muscle fibers. Following the initial formation of these ectopic endplates the soleus nerve usually reinnervates its original endplate sites, thus producing dually innervated muscle fibers. Four months after the denervation surgery the soleus muscle was dissected out of the animal and fixed. The existence of ectopic endplates was confirmed by the use of a stain for acetylcholine esterase. Individual dually innervated fibers were then dissected out of the muscle, processed for electron microscopy, and viewed under the electron microscope. Measurements of Z-line thickness in these fibers revealed that Z-lines were significantly thinner near the ectopic endplates than in the region of the original endplates; 110±11nm (mean±SD) at the ectopic endplates versus 143±28nm (mean±SD) at the original endplates. These results suggest that motoneurons can exert local control over the morphological characteristics of the muscle fibers that they innervate.

Supported by NIH grant AR40801 to RLM.

Tu-Pos171

ALTERATIONS IN FLIGHT MUSCLE ULTRASTRUCTURE AND FUNCTION IN *DROSOPHILA* TROPOMYOSIN MUTANTS ((Andrew Kreuz[1], A. Simcox[2], G. Sleeper[3], W. Barnes[3], and D. Maughan[3])) [1]Dept. Biochem., Johns Hopkins U., Baltimore, MD 21205, [2]Dept. Mol. Genetics, Ohio State U., Columbus, OH 43210, [3]Dept. Mol. Physiol. & Biophys. U. Vermont, Burlington, VT 05405.

We investigated the structure and function of indirect flight muscle (IFM) using null mutants of the two fly tropomyosin genes, *TmI* and *TmII*. *TmI* encodes a standard 284 amino acid muscle tropomyosin, Ifm-TmI, while *TmII* encodes two 400+ amino acid tropomyosins, TnH-33 and TnH-34. Previously, we have shown that *TmI* mutations cause myofibrillar disruptions and flightless behavior. Here we find that, unlike *TmI*, haploidy of *TmII* cause neither flightless behavior nor disrupted myofibrils (which probably accounts for the absence of reported *TmII* mutations). Reduction of Ifm-TmI disrupts the peripheral structure of IFM myofibrils, thereby producing a proportional reduction of dynamic stiffness and power output by preventing the formation of power-generating crossbridges. Wing beat frequency and flight ability are reduced correspondingly. Reduction of TnH-33 and TnH-34, while not producing as great an effect as an equivalent reduction of Ifm-TmI, reduces power output to a greater extent than myofibrillar structure and dynamic stiffness, suggesting that these IFM-specific isoforms play an important role in the mechanism of power production (via "stretch activation") of the flight muscles. Supported by NIH R01 40234.

Tu-Pos172

EFFECT OF TRAINING ON MECHANICAL PROPERTIES OF SKELETAL MUSCLE ((Del Rio V. J. & Muñiz M. J.)) Centro Universitario de Investigaciones Biomédicas. Universidad de Colima. A.P. 199 ,28000 Colima, Col. México.

The elements from which depend passive mechanical properties of the muscles also support active tension developement and prevent the effects of mechanical stress. The skeletal muscles of mammalians are composed by fast and slow twitch fibers and variable amount of connective tissue. The aim of this study was to investigate the effects of endurance and sprint training on the passive mechanical properties of slow and fast skeletal muscles of rats. Eight week-old male Wistar rats were ramdomly assigned to three groups. Two groups were trained for endurance and sprint for 10 weeks. The third group served as a control. The experiments were conducted "in vivo". The proximal and distal insertion of muscles were tightly fixed to a rigid frame and to a mobil transducer load respectively. The muscles were stretched and unstretched cyclically at 1mm/3s with increments of 1mm in successive cycles until rupture. With maximum stress and maximum strain of each cycle, we constructed the stress-strain curves from which we obtained the elastic modulus, ultimate stress and ultimate strain. The results show a significant diferences (**) betwen control and trained muscles (see Table).

RESULTS (Elastic modulus mean ± s.e. in 10^7 dines/cm^2; others mean ± s.e.)

	SOLEUS (SLOW)			PLANTARIS (FAST)		
Groups	Elastic modulus	Ultimate stress	Ultimate strain	Elastic modulus	Ultimate stress	Ultimate strain
CONTROL	2.35 ± 0.03 n=6	7.82 ± 0.69 n=6	0.51 ± 0.00 n=6	2.50 ± 0.06 n=6	10.25 ± 0.53 n=6	0.54 ± 0.01 n=6
SPRINT	2.35 ± 0.29 n=6	7.75 ± 0.97 n=6	0.44 ± 0.04 ** n=6	3.92 ± 0.20 ** n=6	14.04 ± 0.83 ** n=6	0.50 ± 0.04 n=6
ENDURANCE	1.82 ± 0.20 ** n=5	6.00 ± 0.00 ** n=5	0.56 ± 0.00 n=5	2.91 ± 0.30 ** n=5	12.05 ± 0.67 ** n=5	0.55 ± 0.02 n=5

Tu-Pos173

Local differences in myotendinous junctions in axial muscle fibres of carp (Cyprinus carpio L.). ((I.L.Y. Spierts and H.A. Akster)) Experimental Animal Morphology and Cell Biology, Wageningen Agricultural University.

At the myotendinous junctions, the terminal part of the sarcolemma, the interfacial membrane shows extensive folding, resulting in a great increase of membrane area. We used stereology (Eisenberg and Milton, 1984, Am. J. Anat. 171, 273-284) to study the membrane amplification at myotendinous junctions of red and white axial muscle fibres, fibre types that differ in contraction velocity and frequency of use. We also investigated anteriorly and posteriorly situated fibres of each type. According to van Leeuwen et al. (1990, J. Zool. 220, 123-145) posterior axial muscle fibres have a longer phase of eccentric activity than anterior muscle fibres. This should result in higher stresses and in larger loads on the myotendinous junction in the posterior fibres. We found that membrane amplification differed significantly between red and white fibres and between anterior and posterior fibres; red fibres and posterior fibres having the larger interfacial areas. Tidball and Daniel (1986, Cell Tissue Res. 245, 315-322) propose that the membrane amplification at myotendinous junctions depends on the magnitude and on the duration of the load on the junction. The larger membrane amplification in posterior fibres is in accordance with the larger forces expected to occur in the posterior fibres.

Tu-Pos174

MYOSIN HEAD ARRANGEMENT IN SURFACE SUBUNITS OF RABBIT SKELETAL MUSCLE THICK FILAMENTS. ((Rhea J.C. Levine)) Med. Col. PA and Hahnemann U., Phila. PA 19129

In previous studies, crosslinking active sites of nearest-neighbor myosin heads with $bis_{22}ATP{\cdot}v_i$ (donated by Dr. R. Yount) prevented thick filaments separated from *Limulus*, scallop, frog and goldfish muscles from dissolving in 0.6M KCl (Levine et al., J. Cell Biol. **107**:1739, '88; Levine, J. Struct. Res. **110**:99, '93). This indicates that on relaxed filaments, the surface myosin heads overlap with those from axially sequential myosin molecules, within each helical strand. In identical experiments, insect flight muscle (IFM) thick filaments fell apart into 120nm segments with myosin heads at one end, suggesting that their heads overlap with those from adjacent myosins in a crown (Levine, Biophys J. **61**:A300, '92). A similar study on native thick filaments from rabbit psoas muscle is reported here. All procedures were done at 23°C, on filaments adsorbed onto carbon coated copper EM grids.

Relaxed thick filaments showed myosin-based, near-helical order, which disappeared after 15 min on rigor buffer and largely reappeared after 15 min on $bis_{22}ATP{\cdot}v_i$. Control filaments, including: (1) untreated, native ones, incubated on buffered 0.6M KCl; or (2) those exposed first to $bis_{22}ATP{\cdot}v_i$, then to buffer+DTT (to reduce the disulfide bond in the crosslinker, thus severing it), dissolved completely. After 15 min on 0.6M KCl, filaments with crosslinked active sites (not reduced) separated into long strands of myosin molecules, linked by their heads. Thus, although the rabbit filaments remain less "intact" after the experimental procedure, the organization of myosin heads within their surface subunits is likely to be similar to that on all other vertebrate and most other invertebrate striated muscle thick filaments.

STIMULUS-SECRETION COUPLING

Tu-Pos175

ATP-SENSITIVE K+ TRANPORT IN RAT PANCREATIC ZYMOGEN GRANULE MEMBRANES AND ACTIVTION BY PROTEIN KINASE A. ((K. Gasser, K. Lindley, and M. Smith)) Dept. Biological Sciences, Northern Illinois Univer., DeKalb, IL 60115 (Sponsored by G. Kresheck)

Pancreatic secretory granules contain electrolyte transport pathways for Cl- and K+ that may contribute to exocytotic membrane fusion or net fluid secretion following membrane fusion. Recently the granule K+ transport pathway was shown to exhibit characteristics of the ATP-sensitive K+ channels, including inhibition by ATP and sensitivity to sulfonylureas. K+ transport by the zymogen granule membrane was measured indirectly by following K+ dependent osmotic swelling and lysis of the granule while incubated in an isoosmotic solution, pH 7.0, at 37C. This lysis rate was cation dependent, ATP and tolbutamide inhibited, and activated by diazoxide. The results also show that this granule K+ transport pathway can be activated by cAMP-dependent protein kinase phosphorylation.. ATP reduced the K+ dependent rate in a dose dependent manner with 2 mM causing a reduction of approximately 68%. Subsequent incubation of the zymogen granules with 15 units/ml of the catalytic subunit of PK-A restored 74% of this granule K+ transport activity. The granules retained cation selectivity following PK-A phosphorylation but became less sensitive to tolbutamide and glyburide inhibition. These results support the assertion of ATP-sensitive K+ transport by secretory granules and suggest a mechanism for their regulation consistent with the known signaling mechanisms controlling stimulus-secretion coupling in pancreatic acinar cells. (Supported by NIH GM50952)

Tu-Pos176

ISLETS OF LANGERHANS GENERATE CYCLIC, PROPAGATING ELECTRIC SIGNALS MODULATED BY GLUCOSE. ((R. Schatzberger, Y. Shezifi, L. Tavron, R. Khawaled, E. Lachhov, H. Milman, M. Shalit & Y. Palti)) B. Rappaport Faculty of Medicine, Technion and Carmel Biotechnology, P.O.B. 9667, Haifa 31096, Israel.

The electric activity of isolated Islets of Langerhans, EIG, was measured by means of external electrodes. Measurements were made on an islet stretching across two electrically insulated compartments containing a pair of electrodes connected to a differential amplifier. The islets normally generate well structured, synchronized potential spikes at a stable frequency of 0.5 - 2 Hz and amplitude of up to 0.5 mV. In the physiological range firing rate is approximately a linear function of [glucose]. At higher [glucose] the firing rate tends to saturate while at low glucose concentrations it becomes intermittent. The EIG disappears at low [glucose], i.e. 1-3 mM, depending on the animal species. Simultaneous EIG measurements from two islet locations, indicate that the EIG represents the propagation of an excitation wave. The above, and the differential effects of blockers on the amplitude and firing rate, point towards signal generation by a Functional Pace Maker. The EIG is abolished by Ca channel blockers, is unaffected by TTX or removal of $[Ca]_o$, however, its amplitude is directly related to $[Na]_o$, suggesting sodium ion flow through calcium type channels.

Tu-Pos177

(See W-Pos46a)

Tu-Pos178

IDENTIFICATION OF TWO ISOFORMS OF THE SARCOENDOPLASMIC RETICULUM Ca^{2+}-ATPase IN ISLETS OF LANGERHANS. ((Y. Tokuyama, A. Mittal, and M. W. Roe)) University of Chicago, Chicago, IL 60637.

The exocytosis of insulin from pancreatic β-cells depends on rises in intracellular Ca^{2+} concentration produced by influx of Ca^{2+} through voltage-dependent Ca^{2+} channels and release of Ca^{2+} from intracellular Ca^{2+} stores. Regulation of intracellular Ca^{2+} is mediated in part by active transport of cytosolic Ca^{2+} into the endoplasmic reticulum (ER) by sarcoendoplasmic reticulum Ca^{2+}-ATPases (SERCA). Three homologous genes (SERCA1, SERCA2, and SERCA3) encoding five isoforms of SERCA have been identified in a wide variety of excitable and non-excitable cells, however little is known about SERCA isoforms expressed in insulin-secreting cells. Using reverse transcriptase-polymerase chain reaction, we identified two genes encoding distinct isoforms of SERCA in lean Zucker rat pancreatic islets of Langerhans: SERCA2b and SERCA3. Initial estimates of the relative amount of SERCA gene expression in islets indicated that SERCA3 transcript levels were approximately 3-fold higher than SERCA2b. Western immunohybridization analysis of rat islet protein extracts probed with C4, a rabbit polyclonal antibody that recognizes all isoforms of SERCA, revealed two prominent protein bands, 110 kDa and 116 kDa, respectively. The functional significance of the presence of two isoforms of SERCA in islets is unclear. Our findings suggest the possibility that SERCA2b and SERCA3 are associated with different sites of Ca^{2+} sequestration in islet cell ER.

Tu-Pos179

BURSTING ELECTRICAL ACTIVITY OF PANCREATIC β-CELLS IN THE ABSENCE OF FUNCTIONAL K_{ATP} CHANNELS: MODULATION BY GLUCOSE METABOLISM. ((R.M. Santos, C.M. Antunes, A.M. Silva, L.M. Rosário and R.M. Barbosa)) Biochemistry Dept. and Center for Neurosciences, University of Coimbra, P-3049 Coimbra, Portugal. (Spon. by M.C.P. Lima)

Glucose induces bursting electrical activity in pancreatic β-cells and increases the fractional time spent at the burst depolarized phase but the underlying mechanism is not well understood. We have recently shown that bursting can be evoked by raising extracellular Ca^{2+} concentration in the presence of sulphonylurea blockers of K_{ATP} channels and have now used this paradigm to investigate the intrinsic sensitivity of the bursting mechanism to glucose metabolism. The membrane potential was recorded from isolated mouse islets of Langerhans, either separately or in simultaneous with the recording of $[Ca^{2+}]_i$ by fura-2 microfluorometry. Glucose (3-30 mM) increased the duration of the burst plateau phase and reduced the inter-burst interval in a dose-dependent fashion in the continued presence of tolbutamide or glibenclamide and 13 mM Ca^{2+}. The glucose effect was mimicked by 3-30 mM 2-ketoisocaproic acid (KIC), a metabolic substrate that bipasses glycolysis and enters directly the mitochondrial Krebs' cycle. Neither Rp-cAMPS, a specific inhibitor of cAMP-dependent protein kinase, nor staurosporine, a non-specific inhibitor of serine/threonine protein kinases, affected significantly the glucose effect obtained in the presence of tolbutamide and high Ca^{2+}, although both strongly inhibited the stimulatory effect of the permeant cAMP analogue db-cAMP on the electrical activity. The non-selective cation channel blocker diphenylamine-2-carboxylate (DPC) did not affect significantly bursting electrical activity recorded in the presence of tolbutamide and high Ca^{2+}, but it strongly attenuated the Mn^{2+}- and Co^{2+}-evoked quenching of fura-2 fluorescence observed at the dye isosbestic point and inhibited the $[Ca^{2+}]_i$ transients evoked by raising external Ca^{2+} concentration in the presence of the L-type Ca^{2+} channel blocker nifedipine. It is concluded that the operation of the bursting mechanism of the β-cell does not require K_{ATP} channels and is intrinsically sensitive to glucose metabolism. While the DPC-sensitive cation channel may be essential to provide β-cells with Ca^{2+} in the absence of stimulatory levels of fuel secretagogues, it does not appear to be essential for the operation of the bursting cycle. A direct activating effect of mitochondrially generated ATP is likely to provide the link between glucose metabolism and the bursting mechanism.

Tu-Pos180

INOSITOL 1,4,5-TRISPHOSPHATE METABOLISM IN PAROTID AND LACRIMAL ACINAR CELLS. ((K. Tritsaris, B. Nauntofte, T. D. Jørgensen, J. Gromada and S. Dissing)). Dept. Med. Physiol., Panum Institute, University of Copenhagen DK-2200, Denmark.

We investigated the rate of synthesis and catabolism of the Ca^{2+}-releasing metabolite inositol 1,4,5-trisphosphate ($Ins(1,4,5)P_3$) in intact and permeabilized acinar cells isolated from rat parotid and lacrimal glands. Maximal acetylcholine (ACh) stimulation of parotid acinar cells caused a rapid rise in the synthesis of all inositol phosphates with a production rate constant of 0.007 s^{-1} and after atropine addition, $Ins(1,4,5)P_3$ was degraded with a rate constant of 0.37 s^{-1}. From these rate constants we calculated that the peak for the $Ins(1,4,5)P_3$ signal should occur about 2-3 s after stimulation, which is consistent with the observed ACh evoked $Ins(1,4,5)P_3$ and Ca^{2+} peaks in acinar cells. In both permeabilized parotid and lacrimal acinar cells pulsed with $[^3H]$-$Ins(1,4,5)P_3$, the rate of dephosphorylation by the 5-phosphatase, resulting in $Ins(1,4)P_2$ synthesis, occurred with a half maximal effect ($k_{1/2}$) at 8 μM $Ins(1,4,5)P_3$, and was independent on $[Ca^{2+}]_i$ above 150 nM. The rate of phosphorylation by the 3-kinase to $Ins(1,3,4,5)P_4$ was, in parotid acinar cells, dependent on $[Ca^{2+}]_i$ between 50 and 600 nM but had a much smaller Ca^{2+} dependency in lacrimal cells. In permeabilized cells, $Ins(1,4,5)P_3$ released Ca^{2+} from internal stores with a $k_{1/2}$ of 2 μM and maximal effect above 6 μM. These findings show that the $Ins(1,4,5)P_3$ affinity for the 5-phosphatase is close to its affinity for the Ca^{2+} releasing receptor. Thus, upon stimulation the 5-phosphatase, in a Ca^{2+}-independent manner, exerts a strong control of $[Ins(1,4,5)P_3]$ in the range where $Ins(1,4,5)P_3$ releases Ca^{2+} from internal stores.

Tu-Pos181

Ca^{2+} INFLUX VIA Ca^{2+} CHANNELS, NOT CYTOSOLIC Ca^{2+} ACTIVITY DIRECTLY CONTROLS ADRENERGIC SECRETION IN RAT CHROMAFFIN CELLS. ((J. Fan, L. Cleemann, and M. Morad)) Inst. For Cardiovascular Sci. and Dept. Pharmacology, Georgetown University Medical Center, Washington, DC 20007.

Single adrenal rat chromaffin cells, maintained in primary cultures up to a week, were examined using simultaneously, a) the whole-cell voltage clamp technique, b) intracellular fluorescent Ca^{2+} indicator dyes (fluo-3 and calcium green), and c) amperometric measurements of catecholamine secretion with a carbon fiber μ-electrode, and d) rapid (<50ms) exchange of external solutions. The magnitude and time course of secretion were quantified both by measuring the average oxidation current and by a computerized analysis which counted the current spikes produced by individual secretory events. Voltage clamp depolarizations which activated Ca^{2+}current (I_{Ca}), was accompanied by secretory events reaching maximum in 80ms (average current) or 50 ms (spikes) and was maintained for the duration of I_{Ca} and depolarization. The intracellular Ca^{2+} activity ($[Ca^{2+}]_i$), on the other hand, continued to rise for 200 to 400ms after depolarization. Following repolarization, secretion stopped within 100ms while $[Ca^{2+}]_i$ remained elevated for 5 to 20 sec. Secretion and $[Ca^{2+}]_i$-transients had the same voltage dependence as I_{Ca} and were reduced when I_{Ca} was suppressed by nifedipine, low extracellular $[Ca^{2+}]$, and replacement of Ca^{2+} by Ba^{2+}. The results show that secretion was under direct and continuous control of I_{Ca}, was only slightly sensitive to alteration of global $[Ca^{2+}]_i$ and, therefore, most likely controlled by μ-domains of Ca^{2+}. Supported by AHA Maine and NIH HL16152.

Tu-Pos182

NA^+-DEPENDENT CA^{2+}-TRANSPORT MODULATES THE SECRETORY RESPONSE TO AN IMMUNOLOGICAL STIMULUS IN MAST CELLS
((E.Rumpel[1], U.Pilatus[2,3], A.Mayer[1], I.Pecht[2])) [1]Dept. of Physics, University of Bremen, Bremen, Germany; [2]Dept. of Chem. Immunology, Weizmann Institute of Science, Rehovot, Israel; [3]present address: Johns-Hopkins-University, Baltimore, USA

Immunological stimulation of rat mucosal mast cells (line RBL-2H3) by clustering their type I Fc_ε receptors by IgE and antigen causes a rapid transient increase of free cytoplasmic $[Ca^{2+}]$ due to its release from intracellular stores. However, optimal secretory response requires a sustained elevated $[Ca^{2+}]_i$, which is attained by Ca^{2+}-influx. Since increased membrane permeability for Na^+ has also been observed, and secretion is at least partially inhibited in the absence of $[Na^+]_o$, the involvement of a Na^+-Ca^{2+}-exchanger has been considered.

We investigated the coupling of the Ca^{2+}-and Na^+-Gradients across the cell membrane employing ^{23}Na-NMR, ^{45}Ca- and ^{86}Sr-Tracer and the Ca-sensitive fluorescent probe Indo-1.

Since the reduction of $[Ca^{2+}]_o$ provokes an $[Na^+]_i$-increase, and the decrease of $[Na^+]_o$ effects a Ca^{2+}-influx as well as an increase of cytoplasmic free $[Ca^{2+}]_i$, the activity of a Na^+-Ca^{2+} exchanger could be further confirmed.

Secretion assays, monitoring the released β-hexosaminidase activity showed a sigmoidal dependence on $[Ca^{2+}]_o$ in the presence of extracellular sodium. At $[Na^+]_o$=0.4mM the secretion was not affected by $[Ca^{2+}]_o$, (while it was almost completely inhibited at $[Na^+]_o$=136mM and $[Ca^{2+}]_o$<0.05mM). With increasing $[Na^+]_o$, the secretion decreased to a minimum around $[Na^+]_o$=20mM, followed by a steady increase to its maximal value.

A parallel Na^+-dependence of the Ca^{2+}-transport could be observed: At $[Na^+]_o$=136mM antigen stimulation caused a pronounced Ca^{2+}-influx, at $[Na^+]_o$=17mM a slight Ca^{2+}-efflux was detected, whereas at $[Na^+]_o$=0.4mM no Ca^{2+}-transport across the cell membrane could be observed.

Our results clearly indicate that the Na^+-dependence of the secretory response to $Fc_\varepsilon R$ I stimulation is due to its influence on $[Ca^{2+}]_i$ mediated by a Na-dependent Ca^{2+} transport.

Tu-Pos183

ADRENERGIC INHIBITION OF Ca^{2+} CURRENT AND SECRETION MONITORED BY CAPACITANCE AND ^{3}H-5HT SECRETION IN RINm5F CELLS.
((J.E. Richmond, A. Codignola*, M. Rogers and E. Sher*)) Békésy Lab. of Neurobiology, Univ. of Hawaii, Honolulu, HI 96822; *CNR Center of Cytopharmacology, 20129 Milan, Italy. (Spon. by I.M. Cooke)

The adrenergic inhibition of secretion from pancreatic β cells has been attributed to inhibition of voltage-operated calcium channels (VOCCs) and direct effects on secretion. RINm5F cells, a rat insulinoma cell line model for β-cell physiology, secrete 5-hydroxytryptamine (5HT) with insulin, as do β cells. Increases of intracellular Ca^{2+} ($[Ca^{2+}]_i$) via entry through VOCCs and release from stores initiate secretion. Here we simultaneously monitored Ca^{2+} currents (ICa) and cell capacitance (Cm) in RINm5F cells to assess the effects of noradrenaline (NA) on VOCCs and secretion at the single cell level. In control cells, step depolarizations to +10 mV cause step increments in Cm (ΔCm). 20 μM NA produced a strong and reversible inhibition of ΔCm (2nd step, 51%), despite minimal reduction (6%) of integrated ICa. To examine direct effects of NA in the absence of VOCC activity, $[Ca^{2+}]_i$ was increased by ionomycin (1 μM). ΔCm gradually increased during this treatment. NA completely and reversibly inhibited the increase in ΔCm. NA effects were mediated by a pertussis-toxin (PTX)-sensitive G protein, as NA failed to inhibit ΔCm increases in cells that had been pretreated with PTX (100 ng/ml, 3 hr). Using ^{3}H-5HT-loaded cells, we confirmed that ^{3}H-5HT release is inhibited by NA in a dose-dependent manner (50% at 1 nM). The Ca^{2+}-store uptake inhibitor, thapsigargin (1 μM), induced ^{3}H-5HT release which was also potently inhibited by NA. We conclude that NA acts via a G-protein to inhibit exocytosis downstream of elevation of $[Ca^{2+}]_i$.
Support: NIH grant NS15453, U. HI Fund (IC), Telephon Italy Fellowship to ES.

Tu-Pos184

ACTION POTENTIAL WAVEFORM "TUNES" QUANTAL RELEASE FROM EXCITABLE ENDOCRINE CELLS.
((S. Misler and D. Barnett)) The Jewish Hospital, Washington Univ. Med. Ctr., St. Louis, MO. 63110

In catecholamine-secreting rat adrenal chromaffin cells and insulin-secreting canine pancreatic ß-cells, a single action potential (AP), through its underlying high-voltage-activated calcium current (I_{Ca}), often induces the release of one or more quanta of hormone (see amperometry measurements by Zhou and Misler, JBC 270:3498 and Abstr. Soc. Neurosci. 21:334). We have begun to study the relationship of I_{Ca} evoked during the AP to the magnitude and time course of release in these cells. Cells, subjected to perforated patch recording (Cs pipette) and bathed in a modified Ringers containing K channel blockers, were intermittently stimulated with voltage clamp waveforms resembling APs evoked in these cells by brief depolarizations or secretogogues. (I_{Ca} was recordable during the interval corresponding to AP repolarization.) Quantal release was measuring as increases in membrane capacitance (ΔC_m) (see Barnett and Misler, this volume) and, in selected cases, the occurrence of amperometric spikes (ASs) as well. In both cell types, lengthening the interval of the slow repolarization of the AP following the overshoot increases the total Ca entry, Q (= $\int I_{Ca}\,dt$), and as well as ΔC_m and the number of ASs per AP. AP waveform changes that double Q produce ≥ 4-fold increases in quantal release and often lengthen quantal release latency. Though precise quantitation is often limited by (a) use-dependent changes in Ca and K currents and (b) the steep frequency dependence of exocytosis, these results suggest that in excitable endocrine cells, as in neurons, small changes in the waveform of AP repolarization can efficiently "tune" quantal secretion.
Support: NIH DK37380

MOLECULAR RECOGNITION AND BINDING II

Tu-Pos185

RAMAN STUDIES OF FLAVINS AND THE FLAVOENZYMES TRYPANOTHIONE REDUCTASE AND GLUTATHIONE REDUCTASE.
((D.D. Eads, L.J. Juszczak, L.S. Bloom, and J.S. Blanchard)) Albert Einstein College of Medicine, Bronx, NY 10461

Resonance Raman data are reported from the wild-type flavo-enzymes trypanothione reductase and glutathione reductase. In addition, resonance Raman data of site-directed mutants of these enzymes are reported where mutations have been introduced at positions which form contacts with the flavin ring. The effect of these mutations on the vibrational spectrum and how the vibrational spectrum of flavins can be used to assay the protein-flavin interactions will be discussed. Further resonance Raman studies of isoalloxazine ring compounds in protic and aprotic solvents are reported and compared to the protein data.

Tu-Pos186

APPLICATION OF RESONANCE RAMAN SPECTROSCOPY TO RETINOL BINDING IN CELLULAR RETINOL-BINDING PROTEIN, TYPE I.
((Darla K. Graff, *David E. Ong, Franklyn G. Prendergast)) The Mayo Foundation, Rochester, MN 55905; *Vanderbilt School of Medicine, Nashville, TN 37232.

Vitamin A derivatives (retinoids) play an important role in cellular development and regulation of gene expression. Four different cellular retinoid binding proteins solubilize and transport retinoids within particular cells throughout the body. These proteins have been implicated as being major factors in retinoid function and metabolism but their exact role remains unclear. The optical properties of retinol make it an ideal probe for spectroscopic investigation of the protein binding site. Resonance Raman spectroscopy has been used to obtain the vibrational signatures of retinol in different solvent environments as well as in the binding pocket of cellular retinol-binding protein, type I (CRBP-I). Absorption and fluorescence spectra have also been interpreted in terms of the Raman vibrational information. Changes observed in Raman frequencies and intensities of retinol are a result of differences in conformation, polarity, and specific protein binding interactions. Our results indicate increased planarity of the ligand upon binding, in agreement with crystallographic data. D.K.G. is supported by training fellowship DK-07198. This work is supported in part by GM34847 (F.G.P.) and DK-32642 (D.E.O.).

Tu-Pos187

CIRCULAR DICHROISM SPECTROSCOPY OF MONOCLONAL ANTIBODIES THAT BIND A SUPERPOTENT GUANIDINIUM SWEETENER LIGAND
((Sergey Y. Tetin and D. Scott Linthicum)) College of Vet. Medicine, Texas A&M University, College Station, TX 77843

Three monoclonal antibodies (mAb) with nanomolar affinity to the superpotent trisubstituted guanidinium sweetener ligand, N-(*p*-cyanophenyl)-N'-(diphenylmethyl)guanidine acetic acid, were studied by circular dichroism (CD) spectroscopy. Two mAb, NC6.8 (IgG2b, k) and NC10.8 (IgG3, k) exhibited similar CD spectra, but mAb NC10.14 (IgG2b, l) had very different CD spectra in both far and near UV regions. Some of these differences may be due to effects of aromatic amino acid side chains, especially tryptophan and tyrosine, located at the immunoglobulin intradomain surfaces. Heavy and light chain dissociation of reduced Fab fragments in 1 M acetic acid minimized these effects. Ligand binding changed the sign and amplitudes of the near UV CD spectra of all three mAb. Calculation of the CD difference spectra (bound minus free) of stoichiometrically bound antibody-ligand complexes allowed us to visualize the net spectral changes. Based on three dimensional structures experimentally solved for NC6.8 and theoretical models of NC10.8 and NC10.14, we suggest that the *p*-cyanophenyl moiety of the sweetener ligand acts as a molecular pointer in the CD spectra and identifies contact aromatic residues L:96W or L:96Y in the different antibody binding pockets.

Tu-Pos188

THERMAL DENATURATION OF TWO MONOCLONAL ANTIBODIES: AN IR SPECTROSCOPIC AND DSC INVESTIGATION.
((D.M. Byler, D.L. Lee, T.D. Sokoloski, D.P. Nesta, M.A. Devaney, P.R. Dal Monte, D.A. Wall, & J.M. Baldoni)) Philadelphia College of Textiles & Science, Philadelphia, PA and SmithKline Beecham Pharmaceuticals, King of Prussia, PA

Many research and development groups have targeted monoclonal antibodies as therapeutic agents. In this study, we have examined two such genetically engineered proteins, each specific to a different antigen, with regard to their stability in the face of thermal stress. Infrared (IR) spectroscopy and differential scanning microcalorimetry (DSC) were used to observe the effect of increasing temperatures on the structure and thermodynamic properties of these two proteins in aqueous solution. In particular, we have measured mean temperatures (T_m) and enthalpy changes (ΔH) associated with the unfolding of the peptide backbone. As is typical for proteins with a large fraction of β-structure, the strongest band in the second derivative IR spectrum of D_2O solutions of these proteins appears about 1638 cm^{-1}. A weaker β-structure band also occurs near 1690 cm^{-1}. As these proteins are slowly heated, these two bands disappear and new absorptions appear near 1619 and 1685 cm^{-1}. The latter bands are associated with the formation of gel-like aggregates. The similarity in the amide I' regions of the IR spectra of these two proteins reflects a strong correspondence in their overall secondary structures. Although the primary structure of the light chains of the one macromolecule is very different from that of the other (only ~35% homology), their heavy chains exhibit about 80% homology. By contrast, the thermodynamic properties of these proteins, as revealed by IR and DSC, appear to differ significantly. The one antibody had a major endothermic event (T_m) of about 70 °C (by DSC) and 67 °C (by IR), with ΔH (DSC) = 4.4 MJ/mol. A smaller endotherm at about 84 °C with ΔH (DSC) = 0.84 MJ/mol was also observed. The other protein had a T_m of about 80 °C (by DSC) and 72 °C (by IR), with ΔH (DSC) = 7.7 MJ/mol. These studies underscore the utility of IR spectroscopy and DSC for probing thermodynamic events associated with changes in protein structure.

Tu-Pos189

PREFERENTIAL SOLVATION OF PROTEINS STUDIED BY MAGNETIC CROSS-RELAXATION. ((Denise P. Hinton and Robert G. Bryant)) Chemistry Department, University of Virginia, Charlottesville, VA 22901

Nuclear spin cross-relaxation provides a sensitive and short-range measure of molecular proximity. The effects of cross-relaxation may be conveniently exploited to study specific interactions between small molecules and proteins. Magnetic relaxation of solvent protons in protein solutions and cross-linked protein gels is now understood to be carried primarily by rapid chemical exchange of a few solvent molecules bound in specific protein binding sites. The cross-relaxation spectrum then provides a way to study these sites and the competition for them by different solvent molecules. A quantitative approach to the cross-relaxation process and results on water, dimethyl-sulfoxide, acetone, methanol and acetonitrile will be presented for serum albumin gels. Similar experiments on solutes in vivo and in situ will also be demonstrated.

Tu-Pos190

EFFECTS OF ELECTROSTATIC INTERACTIONS IN THE KINETICS OF CYTOCHROME C PEROXIDASE-CYTOCHROME C ASSOCIATION. ((Huan-Xiang Zhou)) Department of Biochemistry, Hong Kong University of Science and Technology, Clear Water Bay, Kowloon, Hong Kong.

The effects of electrostatic interactions between cytochrome *c* peroxidase and cytochrome *c* on their association kinetics are studied by using the dielectric continuum model and Brownian dynamics simulations. When electrostatic interactions are turned off, the association rate constant is rather small ($\sim 10^5\ M^{-1}\ s^{-1}$), resulting from the requirement of proper orientations for the two proteins. Electrostatic interactions are found to increase the rate constant five orders of magnitude. The calculated rate constant is found to exhibit an ionic-strength dependence that is consistent with experimental results. Detailed analysis of electrostatic interactions shows that both long-range and local effects are at work in the enhancement of the association rate constant.

Tu-Pos191

INTERACTIONS BETWEEN SUGARS AND THE WHOLE CASEINS, BOVINE AND CAPRINE, DETERMINED BY ^{17}O AND ^{13}C NMR. ((A. Mora-Gutierrez[1], T.F. Kumosinski[2], and H.M Farrell[2], Jr.)) [1]Prairie View A&M University, CARC, Prairie View, TX 77446 and [2]USDA, ARS, ERRC, Philadelphia, PA 19118.

Evidence is presented that hydrophobic interactions are the major forces contributing to the binding of bovine and caprine whole caseins to sugars. The decrease in protein-protein repulsive interactions with increasing sugar concentration suggest that there is an increased degree of hydrophobic interaction associated with the hydrophobic surfaces of the caseins and the hydrophobicity of the sugars. In addition, significant changes in segmental motion are present in the phenylalanine rings comprising the hydrophobic core of the caseins. There was not observed sugar-induced conformational changes for these milk proteins. The ^{17}O NMR data emphasize a sugar-induced effect on casein stabilization and hydration.

Tu-Pos192

STRUCTURE AND MOLECULAR BASIS OF FILIPIN-STEROL INTERACTION.
((Rajini B. Anachi 1⊥ , K.R.K. Easwaran 1 and B.P. Gaber 2)) 1 Mol. Biophysics, I. I. Sc., India 560012; 2 Naval Research Laboratory (Code 6930) Washington, DC 20375; ⊥present address: Dept. of Biophysics, Boston Univ. Sch. of Med., Boston, MA 02118.

Interactions of the polyene antibiotic, filipin III (aglycon macrolide), with sterol molecules (cholesterol and ergosterol) was investigated to understand the molecular basis of polyene macrolide structure in antimycotic action. Optical spectroscopy (fluorescence and circular dichroism), differential scanning calorimetric (DSC), high resolution nuclear magnetic resonance (NMR) and computational tools were employed to study the system in model membrane and solution environments. Our studies using model membrane system suggest, a strong affinity between filipin and sterol complexes manifests as a phase recovery thermogram during DSC measurement. We have used NMR data in conjunction with molecular modeling to characterize filipin-sterol complex structure in solution state. Molecular details by NMR analysis describe hydrogen bond formation between the 3β-OH of sterol and the keto carbonyl of filipin and also reveal how the steroid ring pucker is modulated to accommodate the polyene. Molecular modeling takes NMR analysis a step further to help clarify the differences between cholesterol and ergosterol during their complex formation with filipin, that dictates their affinities for filipin.

Tu-Pos193

ROLE OF HYDROPHILIC BRIDGES IN PROTEIN ASSOCIATIONS: A DIFFERENCE BETWEEN PROTEIN-PROTEIN INTERFACES AND THE INTERIOR OF PROTEINS. ((Dong Xu, Shuo L. Lin and Ruth Nussinov)) Lab. of Math. Biol., NCI/FCRDC, P. O. Box B, Frederick, MD 21702

The role of hydrophilic bridges (ion pairs and pairs of polar groups) in protein associations was examined from two different perspectives: (1) Statistical analysis was carried out for 21 data sets to determine the relationship between binding free energy and the structure of the protein complexes. The number of hydrophilic bridges across protein binding interfaces shows a significantly stronger correlation with free energy than the buried hydrophobic or hydrophilic surface area and is the dominant contribution to free energy; (2) Following the methodology used by Hendsch and Tidor (Protein Science, 3:211, 1994), who showed that salt bridges mostly electrostatistically destabilize protein folding, we found that salt bridges across protein binding interfaces stabilize protein binding by employing a continuum electrostatic calculation with the DelPhi package. We suggest that the different roles of hydrophilic bridges in folding and in binding are due to their different micro dielectric environments: The composition of surface residues tends to be more hydrophilic than those in the interior of protein, and hence, the effective dielectric constant between ion pairs at the binding interface is generally larger than that at the interior of protein. Our calculations suggest that mutation of salt bridges across the binding interfaces can substantially destabilize protein associations. The results also challenge the widely held assumption that protein-protein interfaces have the same properties as the interior of proteins.

Tu-Pos194

EVIDENCE FOR GUIDED PROTONS IN α-HELICAL PEPTIDES. ((D.W.Kupke, Mohamed H. Farah and Hoan N. Nguyen)) Dept. Biochem. Univ. of Virginia, Charlottesville, VA 22908

Calcium-ion binding often occurs in a nonrandom manner to multiple, calcium-binding loops in proteins; the flanking helices to these loops have been suspected to guide the ion. Hence, we have been testing whether helices might direct protons to common acceptors at specific locations. Using the volume-change approach, where the differential compression of water molecules reflects the uptake of ions, we observe a non-random volume profile upon addition of protons to the helical peptide, Ac-Y$(DAAAR)_3$A-NH_2, upon protonation of the 3 aspartyl residues (10^o). The volume changes attending helix breaking (H-bond rupture, macro-dipole loss) complicate an analysis of the stepwise changes observed in the volume profile. Nonetheless, it appears clear from companion experiments with a similar, nonhelical peptide (containing prolines) that the protonations are guided in the helical case. In the nonhelical peptide, all aspartyl residues accepted protons in an apparently random manner, the data not being complicated by helix breaking.

(Supported by NIH Grant, GM-34938. The above peptides and related ones were a gift from R.L.Baldwin & B.Huyghues-Despointes.)

Tu-Pos195

HIGH AFFINITY PROTEIN-LIGAND BIOPHYSICS

((Patrick S. Stayton, Lisa Klumb, and Vano Chu)) Center for Bioengineering, Box 357962, University of Washington, Seattle, WA 98195

Insight into the molecular mechanisms controlling high affinity protein-ligand interactions and slow dissociation kinetics are of key significance to the field of structure-based drug design, where these features generally represent the target goals for therapeutic development. It is interesting to note, however, how little is known about the "simple" protein-ligand dissociation reaction coordinate. As a starting point in efforts to better elucidate the dissociation reaction coordinate,we have used the streptavidin-biotin model system to elucidate the molecular origins of the record-setting high affinity and slow dissociation rate. We have gained considerable insight into the structure of the transition state and the structure-function relationships controlling the activation barrier through site-directed mutagenesis studies of the aromatic contacts, hydrogen bonding network, and flexible loop closure associated with biotin binding. These studies have provided a detailed molecular picture of the dissociation reaction coordinate, and have provided considerable insight into the structural mechanisms by which the protein generates the large activation barrier to dissociation.

Tu-Pos196

EFFECT OF EXCLUDED SURFACE AREA UPON THE ADSORPTION OF PROTEINS TO SURFACES. ((R.C. Chatelier and A.P. Minton)) CSIRO, DCP, Clayton, VIC 3168, Australia and NIDDK, NIH, Bethesda, MD 20892.

Previous treatments of the role of excluded volume (or, in the two-dimensional limit, excluded area) in protein adsorption have been limited to the case of proteins that can be modeled as lines or circular hard disks. We introduce a scaled particle theory for the adsorption of proteins to locally planar surfaces, in which the cross-section of a protein molecule in the plane of the surface may be described by an arbitrarily shaped two-dimensional hard convex particle. The calculated adsorption isotherm for hard circular disks, like the earlier Stankowski-Andrews isotherm, shows enormous deviations from the Langmuir (ideal) isotherm, but agrees much more closely with the exact hard disk isotherm, derived from the hard disk virial expansion, over the entire range of validity of the expansion. Calculated isotherms indicate that relatively small differences in protein shape can result in qualitative changes in the shape and position of the adorption isotherm.

The theory has been extended to the case of one arbitrarily shaped component (A) adsorbed at a limiting low level of fractional area occupancy together with a second arbitrarily shaped component (B) adsorbed at any fractional area occupancy. Simulations of competition experiments -- measurements of the binding of A at constant concentration of free A as a function of the concentration of free B -- indicate that excluded volume can profoundly affect the results, and if not properly taken into account may invalidate qualitative conclusions drawn from the data.

Tu-Pos197

Kinetic Imaging of A Single Molecule ((W.M. Yu, P.T.C.So, T. French, W. Mantulin and E. Gratton)) Laboratory for Fluorescence Dynamics, Department of Physics, University of Illinois at Urbana-Champaign, Urbana, IL 61801.

Imaging of a single molecule is a new technique to study biological functions and dynamics of a single protein or other biomolecules. Advances in fluorescence microscopy coupled with a high efficiency photon collection systems allow detection of individual fluorescent molecule by a diffraction limited laser beam. We have used a single photon counting scanning microscope in combination with two-photon excitation to image a single molecule immobilized on a microscope cover glass. The scanning rate at each pixel can attain 50 KHz. This allows us to detect protein kinetic events down to tens of microseconds. This system can be more versatile and flexible than using a cooled CCD camera (Funatsu et al., 1995 Nature Vol. 374) which only operates at the video-rate. Two-photon excitation probes a 100 attolite sampling volume. In addition to the advantage of high background rejection by two-photon excitation, which is crucial for efficient single molecule detection, this small probing volume permits us working at nanomolar sample concentration ranges but still detecting a single molecule. By allowing a freely diffusing fluorescent substrate to randomly bind a single protein molecule, successive events of fluorescence "blinking" on and off at a unique spatial location contains kinetic information about the protein's function. The off-rate is directly obtained by record the time a ligand stays bound to the protein. The time between two sequential "blinking" events is indirectly related to the on-rate of a ligand. The kinetic events can also studied as a function of time. This work was supported by NIH grant RR03155.

Tu-Pos198

MEASUREMENT OF INTERMOLECULAR FORCES USING AN OPTICAL FORCE MICROSCOPE. ((Andrea L. Stout, Neil Switz, and Watt W. Webb)) School of Applied and Engineering Physics, Cornell University, Ithaca, NY 14853.

A single-beam gradient optical trap can serve as a force transducer suitable for measurement of forces in the 0.1 to 50 pN range. We are using an instrument derived from the optical force microscope of Ghislain, Switz, and Webb (Rev. Sci. Instrum. **65**: 2762-2767, 1994) to study a model receptor-ligand system, namely, the interaction between *Staphylococcus aureus* protein A (SpA) and IgG. SpA is conjugated to 1-micron polystyrene spheres at low protein:bead ratios, and IgG is covalently coupled at low densities to glass coverslips. By monitoring the displacements of an optically trapped SpA-bead as it is scanned over a surface, we can detect binding-detachment events and apply force calibrations to determine the force required to rupture individual SpA-IgG bonds. Preliminary results indicate that this force is dependent on the species of IgG used. More than 50 pN is required to rupture the bond between rabbit-IgG and SpA, while the forces required to detach SpA from mouse IgG and goat IgG are smaller, 15 pN for mouse-IgG and 5 pN for goat IgG.

Supported by NIH (RR04224) and NSF (BIR9419978) at the Developmental Resource for Biophysical Imaging and Opto-electronics.

Tu-Pos199

HIGHLY EFFICIENT DOCKING AND MATCHING BY COMPUTER-VISION AND ROBOTICS BASED TECHNIQUES. Ruth Nussinov, Shuo L. Lin, Daniel Fischer, Raquel Norel and Haim Wolfson, NCI-FCRDC, Frederick, MD and Tel Aviv University, Tel Aviv, Israel

Recently we have developed a geometrically based docking routine. This approach fulfills the following goals: (1) no predefinition of the binding site. The sole information required for carrying out the docking is the atomic coordinates of the molecules. Binding site information is not a prerequisite. However, if this information is available, it can be naturally incorporated, resulting in a significant increase in performance. (2) Docking of receptors and ligands of variable sizes. Docking is successfully carried out for both small and large molecule ligands onto large receptors. (3) High speed; completes in minutes on a workstation. (4) Low root-mean-squared deviations of the correct solution. The quality of the solutions is very high. The RMSD's for most complexes are under 1A. (5) The number of potential, geometrically correct solutions is manageable, before any filtering or optimization is applied. (6) Solution filtering is available. (7) The correct solution is a low energy conformation. The combination of these advantages allows picking the geometrically few top binding conformations for further detailed studies. In parallel, we have developed a highly efficient docking routine designed for docking large (protein) molecules. The entire molecular surface of the immunoglobulins and their antigens, have been docked, in high efficiency and low RMSD.

The Geometric Hashing algorithm has also been developed and applied toward structural comparison of proteins, detecting sequence-order-independent structural motifs in seconds.

Tu-Pos200

MOLECULAR ELEVATION PLOTS ((Malcolm E. Davis)) Bristol-Myers Squibb, P.O.Box 4000, Princeton, NJ 08543-4000.

The identification of binding sites on proteins is an important quest from both an academic and a pharmaceutical development perspective. Identification and examination of these sites provides an opening for the understanding of the mechanics of binding and thus to an understanding of the specificity for various ligands. The process of identification given only the structure, however, is difficult at best.

The only real starting point is that binding sites on proteins are typically associated with "holes" and "clefts" in the protein surface. Unfortunately quantification of the concept of "hole" is not unambiguous. One of the best attempts has been the work of Nicholls, Sharp, and Honig (Proteins 11:281–296 (1991)). They present a theoretical basis for the importance of the radius of curvature of the protein surface as a measure of the hydrophobic component of binding. Hence they provide the capability within their program GRASP to calculate and display the radius of curvature of the molecular surface.

Radius of curvature, however, has some shortcomings. In particular, it is a local property. As a result, "deep" holes and "shallow" holes can have similar radii of curvature. So, a useful adjunct would be some measure of the depth of a hole: something akin to a topological map showing elevation. But what would represent "sea level" for an irregularly shaped protein? We have found that a large probe molecular surface serves quite well.

In this poster, we present two simple approaches for generating these types of plots. They are demonstrated with an application to antibody binding sites. The molecular elevation plots for HyHEL10 (which binds the protein lysozyme) and 26-10 (which binds the small molecule digoxin) are compared.

Tu-Pos201

MULTINUCLEAR NMR INVESTIGATIONS OF UNIVALENT CATION BINDING SITES ON AN OLIGOMERIC DNA QUADRUPLEX. ((Hong Deng and William H. Braunlin)) Department of Chemistry, University of Nebraska, Lincoln, NE 68588-0304

The univalent cation binding sites on an oligomeric DNA quadruplex structure have been investigated by ^{1}H and ^{15}N, and ^{23}Na NMR. In the presence of $^{15}NH_4^+$, the oligonucleotide $d(T_2G_4T)$ forms a tetrameric parallel-stranded quadruplex structure which is similar to that in KCl solution (Wang & Patel (1993) *J. Mol. Biol.* **234**, 1171-1183). In addition to the formation of four stable guanine quartets, the three thymines at both ends also form stable thymine quartets, that are readily observable under low pH conditions. Two distinct ammonium binding sites on the quadruplex structure have been identified by ^{1}H NOESY and ^{15}N NMR. Ammonium ions bind inside the two 5'-terminal T-quartets as well as outside the 3'-terminal thymine quartet. There is no evidence for $^{15}NH_4^+$ binding to the G-quartet inside the core of the quadruplex structure. Competitive binding experiments indicate that ammonium ions preferentially bind to the quadruplex structure compared to sodium ions. Chemical exchange between bound and free ammonium ions is slow on both ^{1}H and ^{15}N NMR timescales. Specifically bound ammonium ions can not be displaced by K^+ ions, which supports a tetrahedral coordination of ammonium protons to O4 of thymines. Our data suggests that the stable G-quadruplex structure can be formed in solution without univalent cation coordination to the O6 of guanines inside the G-quartets.

Tu-Pos202

NMR STUDIES OF CATION BINDING ENVIRONMENTS ON UNUSUAL DNA STRUCTURES. ((Shibaji Kar, Hong Deng, William H. Braunlin)) University of Nebraska-Lincoln. Department of Chemistry, Lincoln, NE 68588-0304.

G rich DNA oligomers readily form quadruplexes and higher order structures. G rich polypurine strands can also associate with complementary poly pyrimidine strands to form triplexes. The formation of all these higher order DNA structures is cation dependent. Here we analyze the involvement of specific cations in triplex and quadruplex DNA. Proton nmr confirms the formation of DNA multiplets. Cation nmr has been used to investigate the exchange rates, binding site heterogeneity and motional parameters of the cations bound to and stabilizing the multiplets. There is a small class of tightly bound Na^+ in the Na-quadruplex solution. The Na^+ ions bound to the quadruplex are in slow exchange with the Na^+ free in solution. On the other hand, $MgCl_2$ and not NaCl is known to favor DNA triplexes. ^{25}Mg nmr of the $MgCl_2$ induced triple helix shows an equilibrium distribution of ^{25}Mg in different environments. Mg^{2+} bound to DNA quadruplex is found to be in slow exchange with free Mg^{2+}, in contrast to the Mg^{2+} binding environment in triplexes.

Tu-Pos203

NANOSECOND MOLECULAR DYNAMICS TRAJECTORIES FOR B-DNA OLIGONUCLEOTIDES BASED ON THE AMBER 4.1 FORCE FIELD INCLUDING WATER AND COUNTERIONS ((M.A. Young, G. Ravishanker, D.L. Beveridge)). Chemistry Department and Molecular Biophysics Program, Wesleyan University, Middletown, CT 06459.

We report here on the results of several new and relatively lengthy molecular dynamics (MD) simulations on DNA duplexes containing 12 and 25 base pairs and including water and NA^+ counterions. The trajectories range in length from several hundred picoseconds (ps) to 1 nanosecond (ns), and employ the new version of the AMBER 4.1 force field. The results are analyzed using newly developed computer graphic representations of DNA structural morphology, i.e. axis bending and groove widths, as embodied in the latest version of the Molecular Dynamics Toolchest (MDTC 2.0). The simulations have been configured to characterize the AMBER 4.1 MD model of DNA, and to study the sensitivity of MD results to the choice of force field, selection of boundary conditions, and initial placement of solvent. These results provide leading evidence for the novel idea of ion solvation in the minor groove of the DNA duplex. The longer DNA sequence, a 25 base pair phased A-tract sequence, was simulated using what was determined to be the best simulation protocol from the earlier round of dodecamer simulations. The results from this simulation begin to explain the complex experimental data available on what has been determined to be a structurally significant class of DNA sequences.

Tu-Pos204

INTERACTIONS OF A CATIONIC LIPID WITH DNA.
C.H. Spink[#] & J.B. Chaires[*]
[*]Biochemistry Dept, University of Mississippi Medical Center
2500 N. State St., Jackson, MS 39216
[#]Chemistry Dept, State University of New York, Cortland, NY 13045.

Cationic lipids have been used to aid in the transvection of foreign DNA into cells. Little is known about the nature of the interactions between the cationic lipid and DNA. We report here basic physical measurements to characterize the stoichiometry and binding equilibria of a simple cationic lipid, cetyltrimethylammonium bromide (CTAB), and DNA derived from E. Coli. Sheared DNA of about 200 base pairs was reacted with CTAB at varying stoichiometric amounts, and the resulting solutions studied by several physical techniques, including light scattering, isothermal calorimetry, and circular dichroism. UV-melting curves for the DNA were also determined in CTAB media. The binding of CTAB to DNA was found to be very tight, as indicated by biphasic melting curves of the DNA and from the isothermal calorimetric experiments. At ratios of CTAB to DNA-phosphate near 0.9, condensation of the DNA aggregate occurs, leading to precipitation out of solution. Prior to precipitation the binding up to a ratio of 0.5 CTAB/phosphate is very strong ($K_{assoc} > 10^7$). Between ratios of 0.5 and 0.9, the association is not as tight with K_{assoc} near 10^5, as estimated from thermal titration curves.

Tu-Pos205

EQUILIBRIUM BINDING AND DYNAMICS OF IMIDAZOLES, PYRIDINES, AND OTHER HETEROCYCLES TO THE PROXIMAL LIGAND BINDING SITE OF THE SPERM WHALE MYOGLOBIN MUTANT HIS93->GLY. ((D. Barrick)) Institute of Molecular Biology, University of Oregon, Eugene, OR 97403. (Spon. by J.A. Schellman).

By replacement of the proximal histidine of sperm whale myoglobin with glycine (H93G Mb), I have created a protein that can bind small organic bases such as imidazole on the proximal side of the heme [Barrick D. *Biochemistry* 33, 6546 (1994)]. Here I have used this protein to investigate the effects of chemical substitution of the ligand on the thermodynamics and dynamics of ligand binding. Equilibrium, association, and dissociation constants for the binding of thirty ligands to cyanomet H93G Mb were determined from visible and ^{1}H-NMR spectroscopy. This collection of ligands exhibits a range of affinity of approximately one million fold (10 nM to 10 mM K_d). To determine the role of the heme macrocycle in modulating the affinity of these ligands for H93G, the association of these ligands with hemin monocyanide in dimethylsulfoxide was studied by ^{1}H-NMR. The protein enhances ligand affinity by between 10^3 to 10^6 fold, The high affinity of the protein for ligands compared to heme is primarily the result of a slowing of ligand dissociation. Association rates of ligand to protein are as fast as, or faster than those of ligand to heme, indicating that the protein not only poses no kinetic barrier for ligand association, it enhances it relative to an organic solution. With the exception of the well-studied α-substituted ligands , there is no correlation between ligand affinities for free heme versus H93G Mb, suggesting that affinity differences result from interactions between ligand and either protein or aqueous solvent. To assess the contribution of the latter, ligand hydrophobicities were determined using a water/octanol partition. For several homologous ligands affinity correlates well with hydrophobicity, although ligand-protein interactions are seen to be equally important. Association rates are found to correlate with hydrophobicity, while dissociation rates correlate with specific ligand-protein interactions, suggesting that in the transition state for binding, the ligand is desolvated but not yet participating in native interactions with the protein.

Tu-Pos206

BIOPHYSICAL CHARACTERIZATION OF A CYTOTOXIC, TOPOISOMERASE I-POISONING TERBENZIMIDAZOLE AND ITS INTERACTIONS WITH A NATURAL DNA DUPLEX. ((Daniel S. Pilch[1,2], Zhitao Xu[1], Qun Sun[3], Edmond J. LaVoie[3], Leroy F. Liu[2], Nicholas E. Geacintov[4], and Kenneth J. Breslauer[1]))
[1]Department of Chemistry, Rutgers University. [2]Department of Pharmacology, UMDNJ-Robert Wood Johnson Medical School. [3]Department of Medicinal Chemistry, Rutgers University. [4]Department of Chemistry, New York University.

Bisbenzimidazoles, such as the Hoechst dyes (33258 and 33342), are members of a family of DNA-binding drugs that express cytotoxic activity through the poisoning of topoisomerase I. Significantly, such topoisomerase I poisons are capable of killing cancer cells which exhibit resistance to widely used chemotherapeutic treatments. As part of an effort to develop bis- and terbenzimidazole drugs that can serve as effective anti-cancer chemotherapeutic agents, we have characterized the properties of these molecules when free in solution and upon binding to Salmon Testes (ST) DNA. Initial studies focused on a terbenzimidazole derivative (5PTB) that exhibits particularly high degrees of cytotoxicity and topoisomerase I-poisoning activity. Our results reveal the following: (i) At concentrations >11 μM, 5PTB multimerizes; (ii) At neutral pH, free 5PTB is uncharged, while DNA-bound 5PTB is positively charged; (iii) The drug binds to and thermally stabilizes ST DNA, with this binding exhibiting three optically-detectable events, as well as properties characteristic of minor groove binding (e.g. an angle of ≈50° relative to the helix axis); (iv) The drug binds to ST DNA with a substantially lower affinity than Hoechst 33342, yet exhibits similar degrees of cytotoxicity and topoisomerase I-poisoning activity. We comment on potential correlations between the physiochemical properties exhibited by 5PTB when free in solution and/or upon binding to DNA and the cytotoxicity it exhibits through inhibition of topoisomerase I activity. Ultimately, it may prove possible to establish empirical correlations between the biophysical binding properties of a drug and its biological activities, thereby providing a rational basis for drug screening and design.

Tu-Pos207

MOLECULAR RECOGNITION OF UNUSUAL DNA STRUCTURES.((S. A. Winkle, V. Ramsauer, R. Gonzalez, A. Lambidis, L. Moore, S. Reinhardt, R. Tigani, J. Liang & R. D. Sheardy)) Department of Chemistry, Florida International University, Miami, FL 33099 and Department of Chemistry, Seton Hall University, South Orange, NJ 07079.

Extensive efforts in our laboratories have indicated that the DNA sequences 5'-CGCGCGCG-3' and 5'-TCTTG-3' have distinctive structural and thermodynamic properties. Theses distinctive features lead to these sequences (or the junctions of theses sequences with flanking sequences) serving as preferential binding targets for carcinogens, drugs and proteins. Using restriction enzyme inhibition assays, restriction enzyme kinetic assays and spectroscopic studies, we have investigated the binding of the carcinogen 4-nitroquinoline-1-oxide, actinomycin D, ametatrone, ethidium, tris-(9,10-phenanthroline)ruthenium, T7 RNA polymerase and *Eco*RV restriction endonuclease to these sequences or in the vicinity of theses sequences both in 16-base pair oligomers and in longer DNA fragments. Actinomycin D and *Eco*RV appear to have binding targets in the vicinity of $(CG)_4$ segments in both oligomers and longer DNAs. The carcinogen targets the sequence TCTTG. T4 RNA polymerase binds in the vicinity of both sequences. On the other hand, ametatrone, ethidium and tris-(9,10-phenanthroline) show no binding preference for either sequence relative to control oligomers and DNA fragments. The possible relevance of these results to biological properties of the DNA molecules will be discussed. Supported by PHS MBRS GM08205 (SAW) and PHS GM51069-01 (RDS).

Tu-Pos208

CHEMICAL CROSSLINKING OF ETHIDIUM BROMIDE TO DNA BY GLYOXAL ((F. Leng & J. B. Chaires)) Dept. of Biochemistry, University of Mississippi Medical Center,Jackson, MS 39216

Ehtidium bromide was found to be efficiently crosslinked to DNA by glyoxal. Kinetic studies showed that the rate of crosslinking reaction is strongly dependent on the glyoxal concentration. Comparative crosslinking studies using a series of phenanthridines and acridines showed that NH_2 groups at both the 2 and 7 positions of the drugs are required for efficient crosslinking. Comparative crosslinking studies using synthetic polynucleotides showed that the 2 amino group of guanine is absolutely required for crosslinking. Fluorescence contact energy transfer and relative viscosity experiments showed that the crosslinked drug remains intercalated into DNA. Fluorescence polarization and quenching studies revealed, however, that the crosslinked ethidium bromide is more mobile and solvent accessible than is the noncovalently bound drug. These findings suggest that the structure of the crosslinked drug-DNA complex is slightly different from that of the noncovalently bound drug-DNA complex. Agarose gel electrophoresis and sedimentation equilibrium experiments using homogeneous 214 bp DNA fragment showed that crosslinked ethidium bromide does not dissociate double helix. Melting studies of the 214 bp DNA and sonicated herring sperm DNA showed that crosslinking ethidium bromide to DNA stabilized the double strands of DNA. *Supported by NCI Grant CA35635 and by a grant from the Elsa U. Pardee Foundation (J.B.C.).*

Tu-Pos209

Mapping the Bleomycin Binding Site Using the Minor-Groove Blocked DNA Oligomers

Dongchul Suh and Lawrence F. Povirk
Medical College of Virginia, Department of Pharmacology and Toxicology
P.O. Box 980-230, Richmond, Virginia 23298-0230

Bleomycin has clinically been used in cancer chemotherapy. The structural details of the bleomycin-DNA complex is, however, not much known. In order to map the binding site of bleomycin during double-strand cleavage, a series of DNA substrates were designed and synthesized in which the minor groove of DNA was blocked by isobutyl alkylation at N^2 of each guanine near the potential cleavage site. Each modified oligomer was 5'-^{32}P-end labeled and annealed to a complementary sequence. Both normal and modified DNA substrates were treated with bleomycin or pepleomycin, and cleavage products were separated on sequencing gels. The cleavage patterns were quantitatively analyzed using phosphor-imager. The results suggested that cleavage by either drug requires access to only a small (~2bp) segment of the minor groove. Thus, the results tend to disfavor models in which the bleomycin bithiazole is extended along the minor groove. (Supported by N.I.H. Grant CA 40615)

Tu-Pos210

LIGAND SPECIFIC, RECEPTOR-MEDIATED DELIVERY OF A NOVEL NEOGLYCOPEPTIDE-OLIGODEOXYNUCLEOSIDE METHYLPHOSPHONATE CONJUGATE TO THE LIVER: DEVELOPMENT OF A NOVEL ANTISENSE DELIVERY VEHICLE TO HEPATOCYTES ((Jon. J. Hangeland, Joel. T. Levis, Yuan C. Lee, J. James Frost, Paul O. P. Ts'o)) Department of Chemistry, Johns Hopkins University, Baltimore, MD 21205. (Spon. by P. Ts'o)

Development of oligodeoxynucleotides (oligo-dNs) and their analogs as therapeutic agents is complicated by their low rate of transport across cellular membranes to reach the internal complementary sequences, and the lack of tissue-specific delivery. To obviate this barrier, bioconjugates between cell-surface receptor ligands (e.g., neoglycopeptides and folic acid) and oligodeoxynucleoside methylphosphonates (oligo-MPs) have been constructed containing homogeneous, chemically defined, covalent linkages. Experiments have established that a model conjugate, [YEE(ah-GalNAc)$_3$]-SMCC-AET-pU^{m}pT$_7$, is delivered to Hep G2 cells in a ligand-specific manner, reaching a peak value of 26 pmol per 10^6 cells after 24 hours incubation at 37 °C. Furthermore, injection via tail vein of this conjugate shows it to rapidly associate with the liver of mice to the extent of 37% of the initial dose after 15 minutes, after which the conjugate and its metabolites are rapidly cleared via the kidney and urine. Experiments to further define the biodistribution, pharmacokinetics and metabolic fate of this conjugate, and related structures, are in progress. In conclusion, these data show that this novel, biodegradable delivery vehicle represents a viable approach for the delivery of antisense oligo-MPs and other oligo-dN analogs to hepatocytes for therapeutic and diagnostic applications.

Tu-Pos211

LIPOSOME COMPOSITION MODULATES THE HEMOLYTIC ACTIVITY OF EDELFOSINE AND THE RELEASE OF ENCAPSULATED CARBOXYFLUORESCEIN. ((E. Kaisheva, Y. Zha, E. Mayhew, I. Ahmad, J.C. Franklin, W.R. Perkins and A.S. Janoff)) The Liposome Company Inc., Princeton, NJ 08536. (Spon. by P. Ahl)

Edelfosine, an ether linked lyso-PC, was added to 30 mole % cholesterol, 10 mole % XXPE-glutaryl and 50 mole % of various lipids differing in head group and saturation. The acyl chains of XXPE-glutaryl were matched to the lipid component having the highest concentration. The liposomes made from the mixtures were incubated with human red blood cells and the percentage of hemolysis was measured spectrophotometrically. All liposomal formulations of Edelfosine were significantly less hemolytic than non-liposomal Edelfosine with hemolytic activity increasing in the following order: DSPC>EPC>DOPC>DOPE. Carboxyfluorescein was entrapped in liposomes and the nonencapsolated material removed by gel-filtration. The release of carboxyfluorescein from the different liposomal composition was measured in osmotically balanced saline or plasma by monitoring the increase of fluorescence. There was an excellent correlation between the hemolytic activity and fluorophore leakage. Likewise, differences in ascorbate reduction rates for an ESR spin-labeled lipid was included in mixtures ± Edelfosine, which revealed a chain saturation dependence in the same order as above. The results are believed to reflect the steric arrangement and packing of Edelfosine within the bilayer.

Tu-Pos212

LIPID BILAYER PARTITIONING AND STABILITY OF SEVERAL NEW CAMPTOTHECIN-CLASS TOPOISOMERASE INHIBITORS. ((T.G. Burke, M. Chen, M.E. Wall and M.C. Wani)) The Ohio State University College of Pharmacy, Columbus, OH 43210 and Research Triangle Institute, Research Triangle Park, NC 27709

The intense intrinsic fluorescence emissions from several new camptothecin analogues substituted at the 7- and 10- positions have been exploited in order to characterize their partitioning and stability in lipid bilayers. Using published methodologies [Burke *et al.* **Biochemistry** 32: 5352 (1993)], we determined: 1) the structural basis of drug binding to lipid bilayers; 2) the lipid bilayer stability of each drug's α-hydroxy lactone moiety, a pharmacophore which is essential for antitumor activity; and 3) the site of drug binding in the bilayer. Equilibrium affinities of camptothecin and related congeners for small unilamellar vesicles composed of electroneutral dimyristoyl phosphatidylcholine (DMPC) or negatively-charged dimyristoyl phosphatidylglycerol (DMPG) were determined using the method of fluorescence anisotropy titration. Experiments were conducted in phosphate buffered saline (PBS) at 37 °C and overall association constants (K values) were determined. Of the compounds studied, the newly-synthesized compound 7-butyl-10-hydroxy-(20S)-camptothecin was found to display the highest membrane affinity (K_{DMPC} = 2,100 M^{-1}). Lipid bilayer interactions were found to stabilize the lactone ring of camptothecins and thereby conserve the biologically active form of each medication. NIH CA 63653.

Tu-Pos213

ROLES OF FACTOR V_a HEAVY AND LIGHT CHAINS IN PROTEIN AND LIPID REARRANGEMENTS DURING FORMATION OF A FACTOR V_a-MEMBRANE COMPLEX. ((V. Koppaka*, W.F. Talbot and B.R. Lentz)) Dept. of Biochemistry & Biophysics, Univ. of North Carolina, Chapel Hill, NC 27599-7260.

Factor V_a is an essential protein cofactor of the enzyme factor X_a, which activates prothrombin to thrombin during blood coagulation. Peptides of apparent M_r=94,000 (heavy chain; HC) and M_r=74,000 or 72,000 (light chain; LC), interact in the presence of Ca^{+2} to form active V_a. The two forms of V_a-LC differ by a small C-terminal fragment. Using V_a reconstituted with either LC form, we examined the effects of the two LC species on binding. 1) The activity of bovine V_a varied somewhat with LC species, the difference being greatest at limiting X_a concentration. 2) V_a composed of the 72,000 LC bound somewhat tighter to membranes composed of a mixture of neutral and acidic lipids, the difference being greater at 2 than at 5 mM Ca^{2+}. 3) The two forms of V_a undergo seemingly different conformational changes when bound to the membrane. Using V_a containing a mixture of LC species, we addressed the role of the two V_a peptides and of lipid rearrangements in binding. 1) V_a binding favors increased lateral packing density in both fluid and solid phases of mixed neutral/acidic lipid membranes. In the solid phase, V_a-LC and whole V_a had similar effects: in the fluid phase, V_a-HC and whole V_a both altered membrane packing. 2) Binding of V_a or its peptide components did not alter the shape of membrane order-disorder phase diagrams and, therefore, did not induce thermodynamically discernable lateral membrane domains. 3) V_a binds to membranes composed of only neutral phospholipid (K_d = 4.5 μM; stoichiometry = 70 phospholipids/V_a), as does V_a-HC (K_d = 0.1 μM; stoichiometry = 160). We conclude that membrane "binding" of factor V_a is best viewed as formation of a "protein-lipid complex". The process involves both chains of V_a, changes in lipid packing, acidic lipid-binding sites on the protein, and acidic-lipid- and Ca^{2+}-dependent changes in protein structure. *Supported by USPHS grant HL45916.*

Tu-Pos214

CONFORMATIONAL DIFFERENCES BETWEEN SUBSTRATE AND INTERMEDIATE DURING PROTHROMBIN ACTIVATION ON PHOSPHATIDYLSERINE-CONTAINING MEMBRANES: A FLUORESCENCE RESONANCE ENERGY TRANSFER STUDY ((Q. Chen & B.R. Lentz)) Dept. of Biochemistry & Biophysics, Univ. of North Carolina, Chapel Hill, NC 27599-7260.

Prothrombin activation to thrombin is a key control reaction in blood coagulation. During the process, prothrombin is sequentially cleaved at two peptide bonds (R^{323}-I and R^{274}-T) by factor X_a to generate meizothrombin and then thrombin. Phosphatidylserine(PS)-containing membranes from platelets are believed to facilitate this two-step process. Using fluorescence energy transfer (FRET), we determined the distances of closest approach between the membrane surface and the C-terminus of a specifically fluorescein-labelled double mutant bovine prothrombin (P(SA, GC)-FM) and meizothrombin (M(SA, GC)-FM). We monitored FRET from P(SA, GC)-FM or M(SA, GC)-FM to phosphatidylethanolamine-N-rhodamine B (Rh-PE; 0-5mol%) contained in membranes composed of PS (25%) and phosphatidylcholine (70% -75%). Plots of the energy transfer efficiency as a function of membrane concentration at 5-7 acceptor (Rh-PE) surface densities were analyzed globally to obtain dissociation constant (K_d), binding stoichiometry (n), and limiting energy transfer efficiencies. K_d=0.32μM with n=44 lipid/protein for prothrombin and K_d=0.28μM with n= 42 lipid/protein for meizothrombin. The distance of closest approach was obtained from the dependence of the limiting energy transfer efficiency on the Rh-PE surface density. With the assumptions of $\kappa^2 = 2/3$ and η=1.4, the distances were 96±2Å for prothrombin and 114±3Å for meizothrombin. The presence of factor V_a or of active site blocked factor X_a (EGR-X_a) did not alter these distances significantly. These direct measurements indicate that binding to PS-containing membranes induced tighter folding of the prothrombin molecule but subsequent extension of the meizothrombin intermediate, consistent with our hypothesis that membrane binding sequentially alligns bond R^{323}-I in prothrombin and R^{274}-T in meizothrombin with the factor X_a active site in the two-step thrombin generating process. *Supported by USPHS grant HL45916.*

Tu-Pos215

FUNCTIONAL AND STRUCTURAL CONSEQUENCES OF WATER SOLUBLE PHOSPHATIDYLSERINE BINDING TO BOVINE FACTOR X_a ((Jianfang Wang* and Barry R. Lentz)) Department of Biochemistry & Biophysics, University of North Carolina at Chapel Hill, Chapel Hill, NC 27599-7260.

The effect of soluble phospholipids {C6PS: 1,2-dicaproyl-sn-glycero-3-phospho-L-serine; C6PG: 1,2-dicaproyl-sn-glycero-3-phospho-rac-1-glycerol; C6PC: 1,2-dicaproyl-sn-glycero-3-phosphocholine} and membrane-associated phospholipids {bovine PS (phosphatidylserine); DOPG: 1,2-dioleoyl-phosphatidylglycerol; POPC: 1,2-palmitoyl-2-oleoyl-3-sn-phosphatidylcholine} on the rate of bovine factor X_{aa} autolysis was measured by analysis of SDS-PAGE gels. The rate enhancement of factor X_{aa} autolysis was found to be PS-specific. Two different methods, fluorescence titration using DEGR-X_a (factor X_a modified with DEGR-CK) and differential scanning calorimetry were used to study the structural consequences of C6PS binding to factor X_a. Results indicated that C6PS: 1) binds to multiple and cooperative sites on factor X_a and 2) induces a factor X_a conformational change in a Ca^{2+} dependent manner. C6PS binding parameters were estimated from simulation of DEGR-X_a fluorescence titration curves and titration of the rate of factor X_{aa} autolysis. Similar fluorescence titration curves were observed for DEGR-X_{aa} and DEGR-X_{gg}, indicating that the two forms of factor X_a have similar phospholipid binding properties. The results indicate that PS-specific sites on factor X_a alter both the conformation and proteolytic function of this enzyme. Thus, PS exposed on activated platelet membranes probably serves as an allosteric effector of factor X_a assembled into the prothrombin complex. *Supported by USPHS grant HL 45916*

Tu-Pos216

A GENERAL TECHNIQUE FOR PATTERNING OF FUNCTIONAL PROTEINS WITH PHOTOLITHOGRAPHY OF SILANE MONOLAYERS ((J.F. Mooney, C.T. Rogers, A.J. Hunt, J.R. McIntosh)) University of Colorado, Boulder, CO 80302.

Self-assembled monolayers have been used to adhere proteins to surfaces in several studies recently. Some of the mechanisms rely on simple adsorption, while others involve stronger chemisorption. In this work, we have attached functional antibodies in a two-dimensional pattern on a silicon dioxide surface by using a combination of adsorption and biotin/avidin interactions. The substrate is initially coated with n-octadecyltrimethoxy silane(OTS), and the silane monolayer is selectively removed from the surface by UV exposure through a lithographic mask. Adsorption isotherms for bovine serum albumin(BSA) tagged with FITC fluorescence had shown that BSA adheres to OTS on the order of a single monolayer coverage over 3 decades of solution concentration. However, the isotherms for glass and silicon wafer with a furnace oxide, require larger solution concentrations before significant adsorption occurs. The adsorption differential between the two surfaces allows the creation of a two dimensional pattern of BSA coverage. If the BSA is tagged with biotin, the pattern can be duplicated in a second layer consisting of streptavidin which creates a strong bond to the biotin, but which does not adhere to exposed substrate. This in turn provides a surface for adsorption of a third layer consisting of functional biotinylated antibodies. By flowing a series of proteins solution across the patterned substrate several layers can be built up in a patterned array. The biotin/avidin affinity, as well as antibody selectivity provide a general method to adhere a pattern of functional proteins to a surface.
Supported by ONR grant N00014-94-1-0621.

Tu-Pos217

THE SELECTIVITY OF ADSORPTION OF AMPHOTERICIN B TO DOPC/ ERGOSTEROL *VS* DOPC/ CHOLESTEROL MONOLAYERS. ((J. Barwicz and P. Tancrède)) Dépt. Chimie-Biologie, Université du Québec, P. O. Box 500, Trois-Rivières (QC) Canada G9A 5H7.

Amphotericin B (AmB) is the most effective antibiotic used in the treatment of systemic fungal infections. It is generally thought that the activity of this drug results from its interactions with ergosterol, the main sterol of fungi membranes. However, AmB also interacts with cholesterol, the major sterol of mammal membranes, thus limiting the usefulness of this drug due to its relatively high toxicity. The aim of the present work is to study the molecular basis of the interactions of AmB with these sterols contained in a DOPC film by using the monolayer technique. Two different concentrations of the sterols in the film (13 % and 30 %) at an initial surface pressure of 30 $mN \cdot m^{-1}$ and various concentrations of AmB in the subphase, ranging from a molecularly dispersed to a highly aggregated state of the drug were studied. Our results show that the monomeric form of AmB interacts with the ergosterol containing film solely. On the other hand, when AmB is dispersed as a pre-micellar or as a highly aggregated state in the subphase, a very significant selectivity of its interactions between the two sterols is observed. We show that the activity of AmB is most likely related to the micellar form of the antibiotic. These results are discussed in terms of the molecular organization of the two sterols within the monolayer film as well as in terms of the molecular structure of the sterols. We show that they provide a better understanding of the action of AmB (activity/toxicity) at the membrane level.

Tu-Pos218

Purification of Membrane Proteins by Non-Ampholyte Isoelectric Focusing: Application to Cytochrome b_5 and NADPH Cytochrome P450 Reductase. ((A.D. Hausfeld, R. Lieberman, N.A. Rodionova, and W.R. Laws)) Dept. of Biochemistry, Mount Sinai Sch. of Med., New York, NY 10029.

Purification of membrane proteins in the quantities as well as with the necessary purities required by many biophysical studies is often an expensive endeavor due to the numerous/elaborate procedures, the poor yields, and the time involved. We report the application of a new technique, membrane isoelectric focusing (MIEF), toward the purification of membrane proteins. MIEF uses an ion-selective membrane and a simple buffer system to generate the pH gradient, and therefore eliminates the difficulties associated with ampholytes [*Anal. Biochem.* **212**, 237-246 (1993)]. In addition, the pH gradient is established in a gel matrix, allowing for high yield recoveries of the focused, purified protein for subsequent studies. To counter the hydrophobic nature of membrane proteins and maintain solubility with minimal aggregation, we employed octyl agarose as the gel matrix and the buffers contained glycerol (20 %) and a non-ionic detergent (0.5 %). For this initial study, the purification of functional cytochrome b_5 and active NADPH cytochrome P450 reductase extracted from rat liver endoplasmic reticulum microsomes was achieved in two steps. The first procedure is a hydrophobic column, which is then followed by focusing the desired protein by MIEF. Application of this preparative protocol to other membrane proteins, especially cytochrome P450s, will be discussed. Supported by NIH grant AA09953.

Tu-Pos219

SPERMIDINE RELEASE FROM XENOPUS OOCYTES: ELECTRODIFFUSION THROUGH A MEMBRANE CHANNEL. ((Sha, Q., Lopatin, A.N. and C.G. Nichols)) Department of Cell Biology and Physiology, Washington University School of Medicine, St. Louis, MO 63110

The release of ^{3}H-spermidine from *Xenopus* oocytes was examined under different ionic conditions, and under voltage-clamp. In normal solution (2 mM [K^+]), the efflux rate is less than 1% per hour, and is stimulated ~ 2-fold by inclusion of Ca^{2+} (1 mM) in the incubation medium. Spermidine efflux is stimulated ~10-fold in high [K^+] (100 mM K^+) solution. In high [K^+] solution, efflux is strongly inhibited by divalent cations (K_i for Ba^{2+} block of spermidine efflux is ~ 0.1 mM), but not by tetraethylammonium ions or verapamil. Spermidine efflux rates were not different between control oocytes and those expressing HRK1 or IRK1 inward rectifier K^+ (Kir) channels. When the membrane potential was clamped, either by changing external [K^+] in oocytes expressing HRK1, or by 2-microelectrode voltage-clamp, spermidine efflux was shown to be strongly dependent on voltage, as expected for a simple electrodiffusive process, where spermidine^{3+} is the effluxing species. This result argues against spermidine diffusing out as an uncharged species, or in exchange for similarly charged counterions, and is consistent with efflux occurring through a membrane channel. These results are the first conclusive demonstration of a simple electrodiffusive pathway for spermidine efflux from cells.

Tu-Pos220

A SIMPLE BARRIER MODEL IS SUFFICIENT TO EXPLAIN 'CROSSOVER' EFFECT AND CORRECT SHIFT OF INWARD RECTIFICATION INDUCED BY MULTIVALENT POLYAMINES. ((A.N. Lopatin, E.N. Makhina and C.G. Nichols)) Department of Cell Biology and Physiology, Washington University School of Medicine, St. Louis, MO 63110

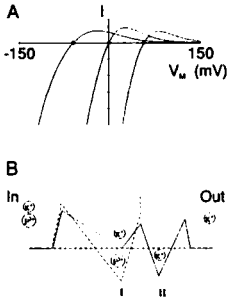

Fig. 1A. "Crossover" and shift of rectification for model in B in the presence of spermidine^{3+} at K_{OUT} = 15, 150 and 1500 mM, K_{IN} = 150 mM.

Inward rectification induced by multivalent polyamines (spermine^{4+}, spermidine^{3+}, putrescine^{2+}) is relieved by external [K^+], shifting strictly with E_K (Lopatin & Nichols, 1995, *J. Phys.* abstr.). We have sought to explain these results in terms of a single file pore containing multiple ion binding sites. It has been reported that the effects of 'crossover', and shift of rectification with E_K is not reproducible with blocking particles of valency > 1 (Hille & Schwartz, 1978, *J. Gen. Phys.* 72, 409-442). However, this is not an 'intrinsic" problem of the barrier model, and even a simple 2-site, 3-barrier scheme with a single polyamine binding site (Fig. 1) can reproduce the observed behavior if one assumes strong binding of K^+ ions in the selectivity filter, and electrostatic interaction between polyamines and K^+ ions inside the pore.

Tu-Pos221

A STOCHASTIC MODEL OF CELL-SUBSTRATE DETACHMENT VIA CENTRIFUGATION. ((C. Zhu, J.W. Piper, and R.A. Swerlick*)) School of Mechanical Engineering, Georgia Institute of Technology, Atlanta, GA, 30332; *Department of Dermatology, Emory School of Medicine, Atlanta, GA 30322

Cell-substrate adhesion and detachment are integral components of many physiological processes. A mathematical model has been developed to describe cell-substrate detachment in a commonly used centrifugation assay. The model treats the detachment of a cell as a stochastic event which is capable of occurring at any force with a certain probability. Using an exponential relationship between binding affinity and bond force, we explored different representations and determined that Bell's formulation (Bell, Science, vol. 200, p.618-627, 1978) described our data better than the formulation of Dembo et al. (Proc. R. Soc. Lond., vol. 234, p.55-83). Using this approach to determine bond formation and dissociation of the cell population, the fractions of the population adherent by any number of bonds in equilibrium were solved in closed form. The model was validated using an experimental system consisting of sialyl-Lewis X expressing colon carcinoma (Colo-205) cells adherent to a plastic surface coated with a construct of E-selectin. By comparing the model prediction with the experimentally measured percentage of adherent cells for both a range of coating densities and various levels of imposed relative centrifugal force, we can estimate the two-dimensional, no load affinity (K_a) for binding reaction between surface bound receptors and ligands as well as the ligand density on the carcinoma cells. We have also estimated the maximum bond stretch (γ) of the E-selectin - sLe^x bond. This sub-angstrom value is in agreement with a previous estimation (Alon et al., Nature, vol. 374, p.539-542, 1995). We are also able to predict the behavior of such a simplified binding system in response to changes in receptor-ligand binding characteristics such as K_a and γ. (Supported by a grant from the Whitaker Foundation and NIH training grant No. GM08433)

Tu-Pos222

A MECHANICAL ANALYSIS OF A MICROPIPET ASPIRATED RED BLOOD CELL LOADED BY A POINT FORCE. ((C. ZHU and S. CHESLA)) School of Mechanical Engineering, Georgia Institute of Technology, Atlanta, GA 30332

The micropipet technique is one of several experimental methods recently employed to measure single bond detachment forces in cellular adhesion. This method utilizes a micropipet aspirated red blood cell (RBC) as a force transducer. Using a finite difference computational method, Evans et. al. (Biophys. J., vol. 59, p838-848, April 1991) analyzed this problem and clearly showed that the technique was sensitive enough to make it attractive for measuring molecular detachment strengths. However, the issue of accuracy was not addressed. The determination of the transducer accuracy and how it depends on experimental parameters is a non-trivial problem and requires rigorous mechanical analysis concerning cell deformation under a point load. We describe an analytical approach based on a boundary layer analysis in which the singularity at the pole (where the point load is applied) is handled by rescaling the thin shell equilibrium equations to obtain an inner solution near the pole. This is then matched to an outer solution valid for the remaining cell membrane. A perturbation technique was used to decouple the governing equations of the stress field from those of the strain field, allowing the stress field to be statically determined and the deformed shape of the cell resolved. With this approach, a sensitivity evaluation of the experimental parameters important to an accurate force measurement is simplified, as well as the solution for the RBC force-deformation relationship itself. The presented solution is also compared and evaluated versus our own finite difference derived solution and shows good agreement. (Supported by NSF grant No. BCS-935037, NIH grant No. R29A138282 and NIH training grant No. GM 08433)

FOLDING AND SELF-ASSEMBLY II

Tu-Pos223

PROTEIN FOLDING AND ENZYMATIC ACTIVATION OF *PSEUDOMONAS AERUGINOSA* EXOTOXIN A. ((B.K. Beattie & A.R. Merrill)), Guelph-Waterloo Centre for Graduate Work in Chemistry, Dept. of Chem. and Biochem., Univ. of Guelph, Guelph, ON, Canada, N1G 2W1. (Spon. by Joan Boggs).

Pseudomonas aeruginosa Exotoxin A (ETA) and its C-terminal peptide that includes the catalytic domain responsible for its ADP-ribosyl-transferase (ADPRT) activity were studied by high performance size-exclusion liquid chromatography (HPLC), fluorescence spectroscopy, and circular dichroism (CD) spectroscopy. The enzymatic function of ETA can be activated *in vitro* by incubation with reducing agent (10 mM DTT) and denaturant (4 M urea) and the effect of various activation conditions (pH, urea, and DTT) on enzymatic activity was studied. Upon enzymatic activation, structural changes induced within both proteins' structures were monitored by HPLC and CD spectroscopy. These changes were correlated with concomitant alterations in the enzymatic activity of the proteins. The pH optimum of ADPRT activity for both ETA and PE40 was between 7.0 - 8.0 decreasing to nearly zero at acidic (pH 5.0) and basic (pH 11-12) values. Analysis of the pH titration data revealed the presence of two clearly separate pK, values which implicate a His residue (likely His 440 and 426) and a Tyr or Lys residue (possibly Tyr 481). The identity and possible role of an active site Lys residue is not known. Additionally, a significant increase in the Stokes' radii of both proteins was detected when the pH was lowered from 8.0 to 6.0. The enzymatic activity of PE40 was not affected by urea or DTT and its Stokes' radius decreased monotonically with increasing urea concentration. Also, the ΔG_N values for the folding of ETA (-18 kJ/mol) and PE40 (-33 kJ/mol) were determined by fluorescence methods using urea as the chemical denaturant [supported by the Medical Research Council of Canada, ARM].

Tu-Pos224

Low-Temperature Time-Resolved and Steady-State Fluorescence Spectroscopy Studies of Five Single-Tryptophan Mutants of *E. coli* Adenylate Kinase. ((T. Fulmer*[1], P. T. C. So*, M.Glaser[1], W. W. Mantulin*[1])) *Laboratory of Fluorescence Dynamics, Department of Physics, University of Illinois at Urbana-Champaign, [1]Department of Biochemistry, University of Illinois at Urbana-Champaign, Urbana, IL 61801.

The enzyme adenylate kinase (AK) from *E. coli* catalyzes the reaction ATP + AMP <==> 2ADP in the presence of magnesium. Based on the comparison of several high-resolution x-ray crystal structures, it is thought that the enzyme undergoes large domain movements upon substrate binding. Because the wild type AK is devoid of tryptophans, it is reasonable to construct a library of single-tryptophan mutants, with the tryptophans placed in various functionally and structurally important locations. These single-tryptophan mutants can then be used as probes of the protein dynamics of the wild-type enzyme and extensively characterized using a variety of fluorescence spectroscopic techniques. The present study attempts to address the dynamics of the native state of the enzyme (see accompanying poster for unfolding studies). In order to slow the rate of interconversion between the native AK's conformational states, it was necessary to do studies of the native-state dynamics at reduced temperatures. AK was placed in a solution of 80% glycerol, and changes in time-resolved fluorescence parameters were monitored over the temperature range from 25C to -70C. The lifetimes were analyzed as distributions, where the width of the distribution was assumed to be a sensitive indicator of local heterogeneity and interconversion between conformations. By this analysis, the five single-tryptophan mutants divided up into two groups, presumably depending on whether the tryptophan environment was buried and nonpolar or fully solvent-exposed. The differences could be attributed to protein substates or to substates of the glycerol. The ability of the five mutants to bind substrates was also studied in 80% glycerol using the bisubstrate analog Ap5A. It was found that the glycerol effectively closed shut the ATP binding flap, in this way preventing the Ap5A from occupying the ATP site. Control studies using steady-state methods confirmed this conclusion. [*Supported by NIH grant RR03155.]